Representative MS/MS spectra of identified lipids

Glycerophosphoserines

(Neutral loss-triggered MS^3 – 185 Da)

Low mass measurement accuracy MS/MS utilizing LTQ

Positive ESI: LPS 18:2; $C_{24}H_{44}NO_9P$; theoretical *m/z* 522.3, $(M+H)^+$

Neutral loss-trigged MS^3

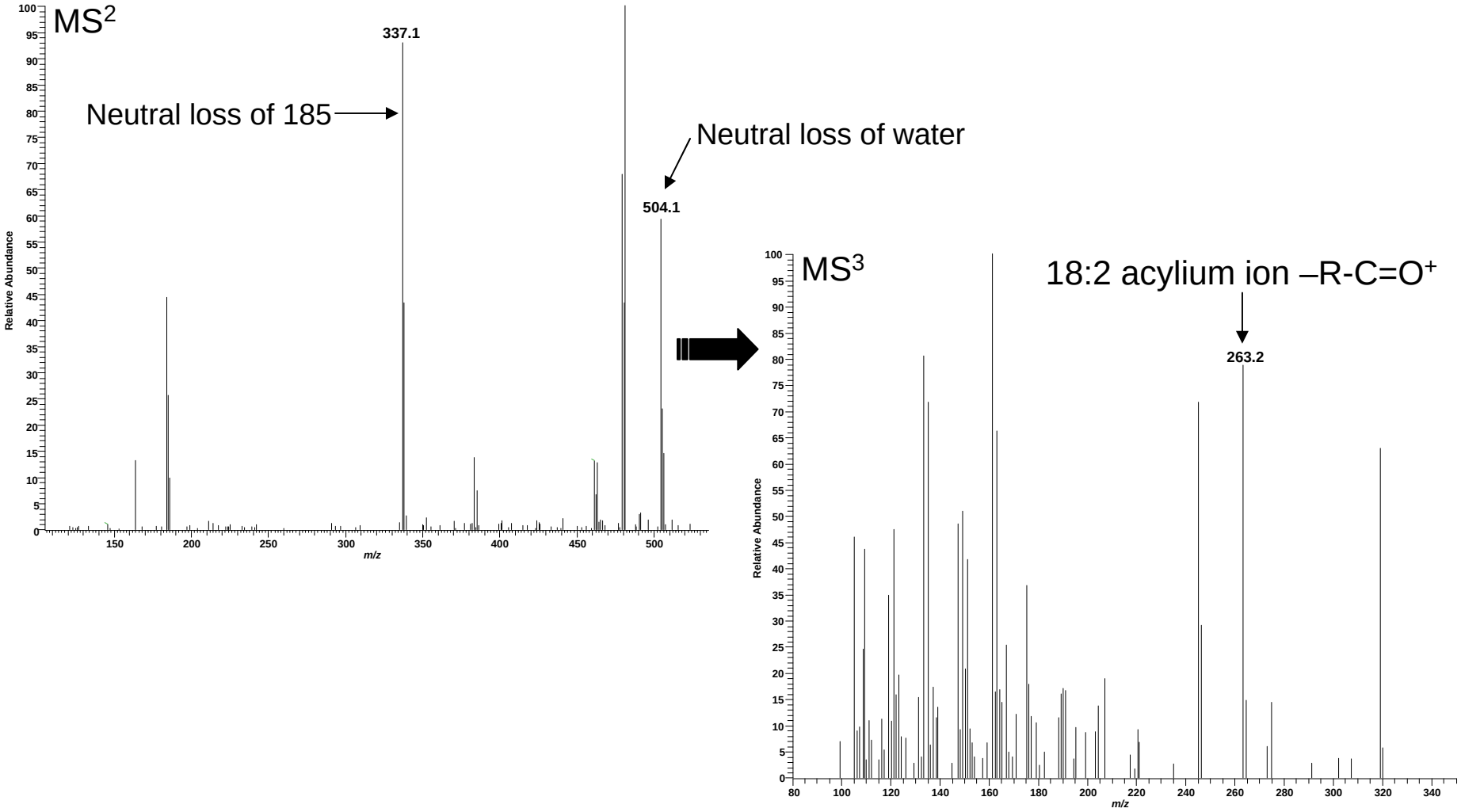

Low mass measurement accuracy MS/MS utilizing LTQ

Positive ESI: LPS 18:1; $C_{24}H_{46}NO_9P$; theoretical *m/z* 524.3, $(M+H)^+$

Neutral loss-trigged MS^3

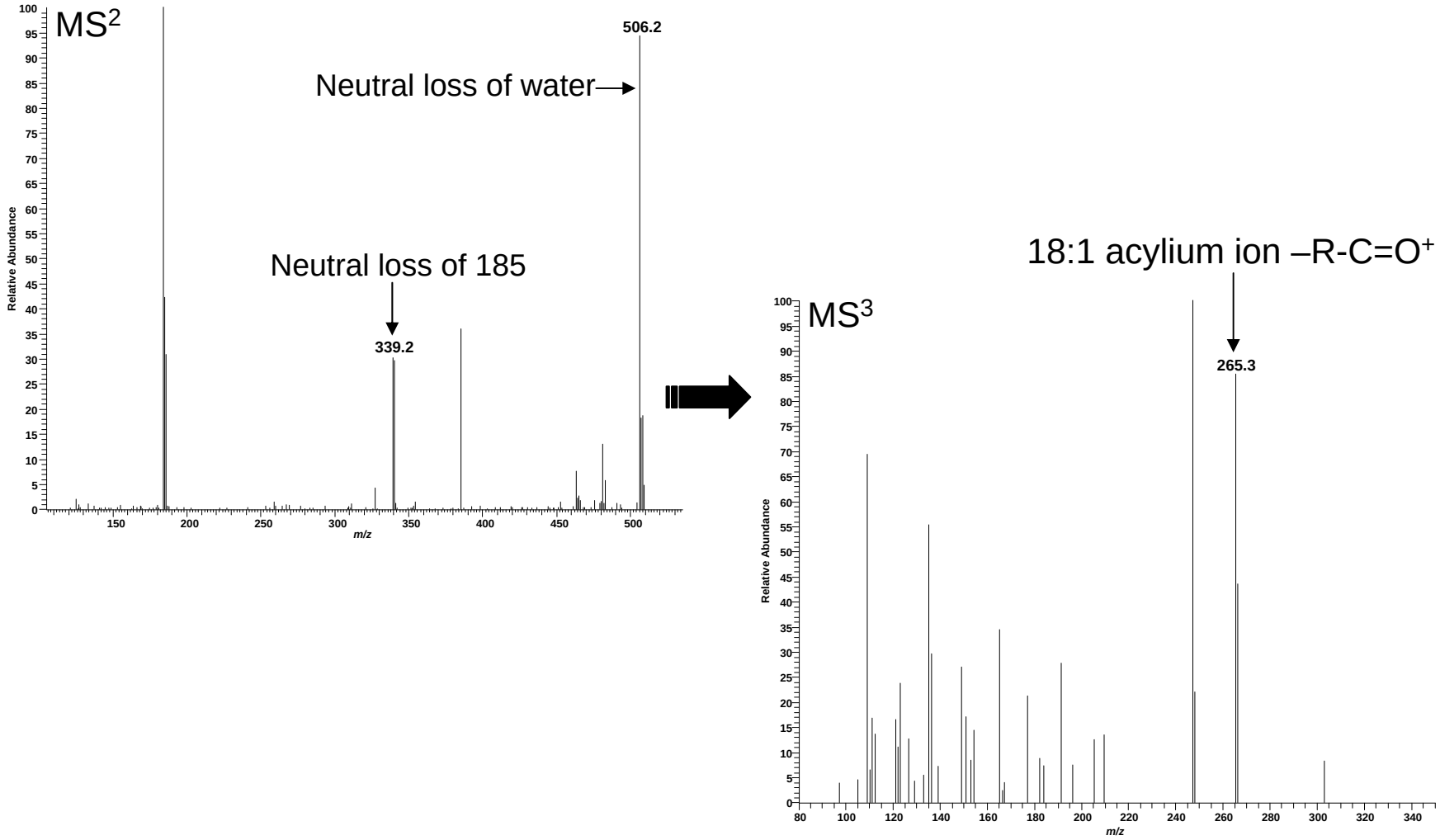

Glycerophosphoethanolamines

High mass measurement accuracy MS/MS utilizing LTQ-FT

Positive ESI: LPE 20:5; $C_{25}H_{42}NO_7P$; theoretical *m/z* 500.2777, $(M+H)^+$

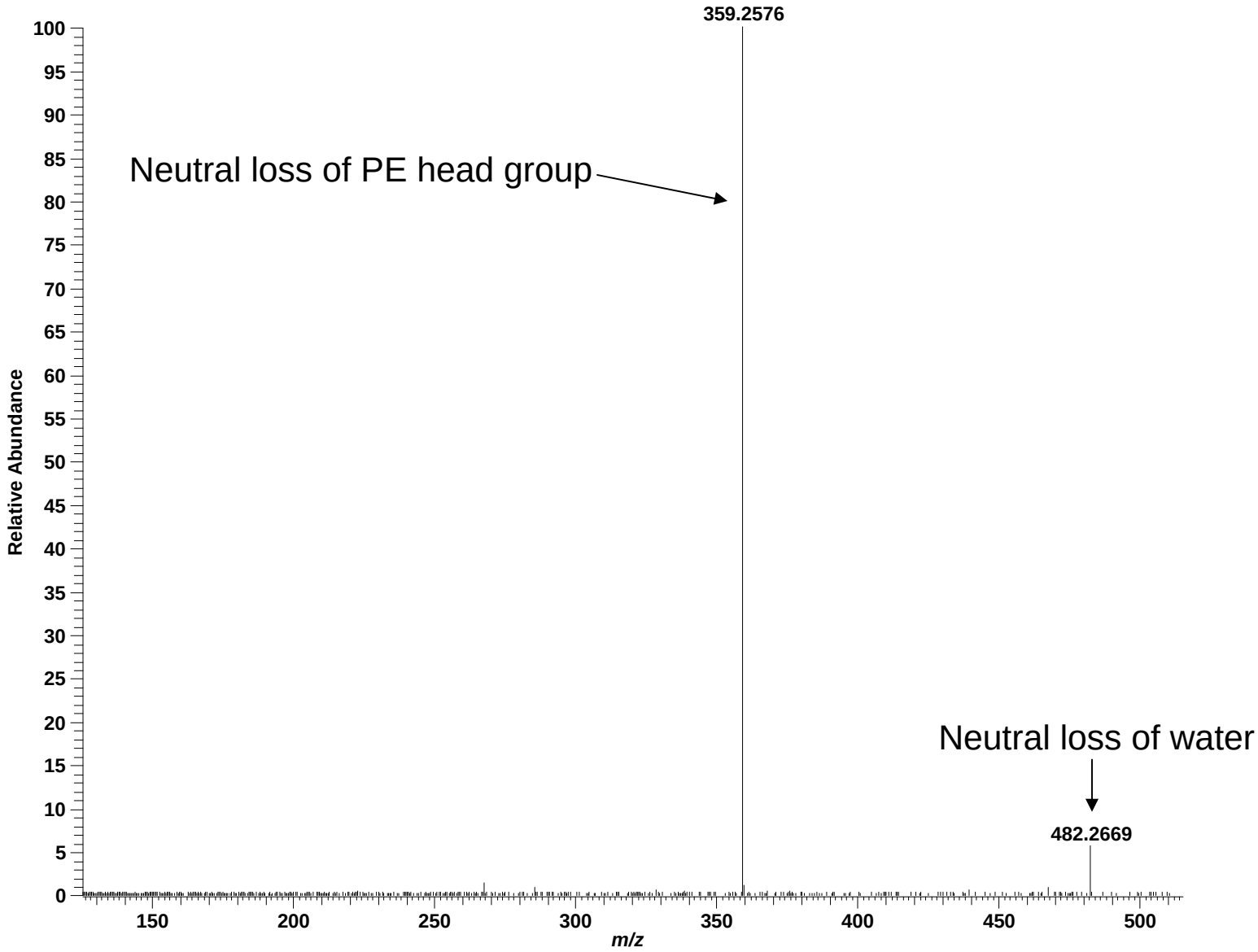

High mass measurement accuracy MS/MS utilizing LTQ-FT

Negative ESI: LPE 20:5; $C_{25}H_{42}NO_7P$; theoretical *m/z* 498.2621, $(M-H)^-$

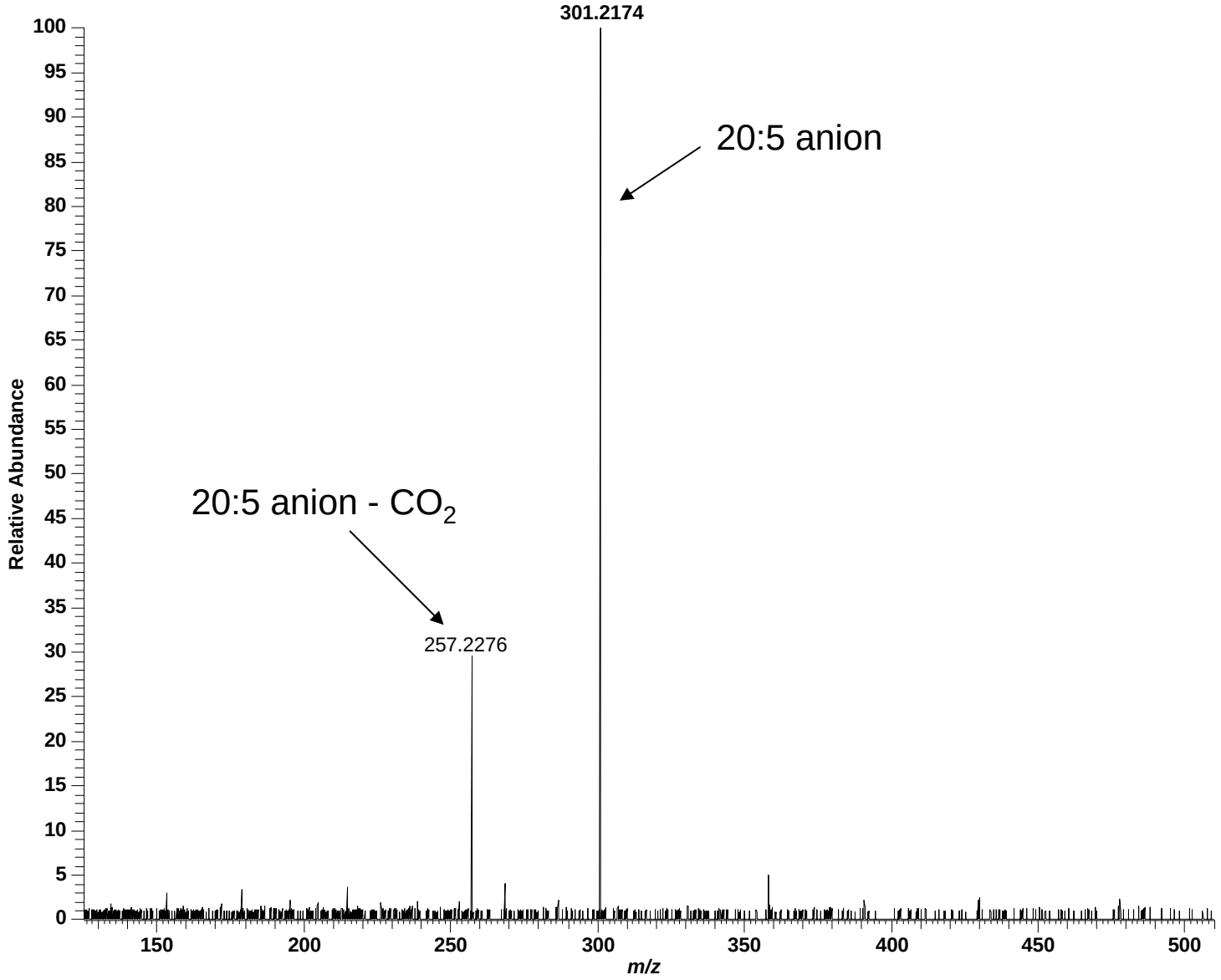

High mass measurement accuracy MS/MS utilizing LTQ-FT

Positive ESI: LPE 20:4; $C_{25}H_{44}NO_7P$; theoretical *m/z* 502.2933, $(M+H)^+$

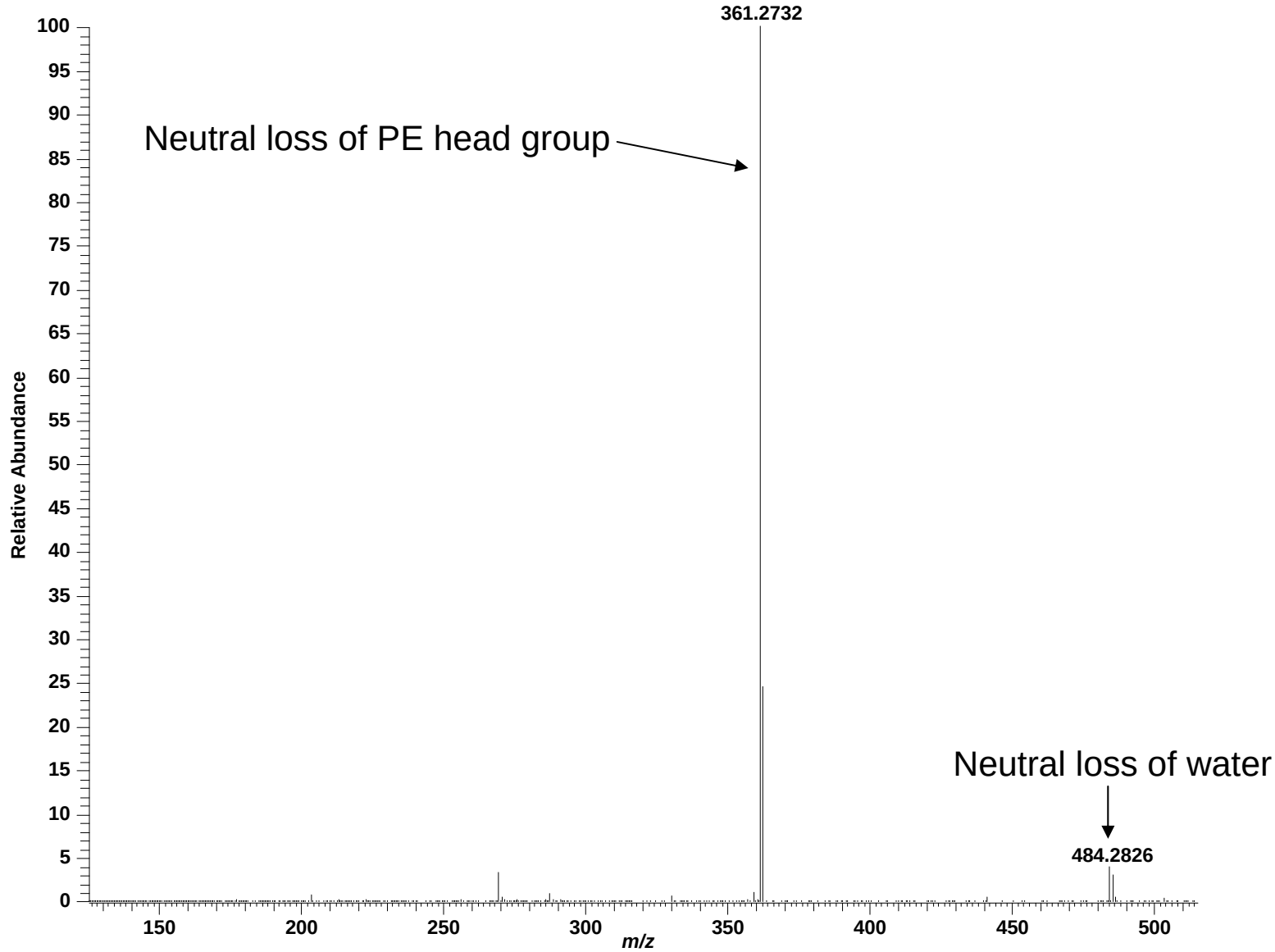

High mass measurement accuracy MS/MS utilizing LTQ-FT

Negative ESI: LPE 20:4; $C_{25}H_{44}NO_7P$; theoretical *m/z* 500.2777, $(M-H)^-$

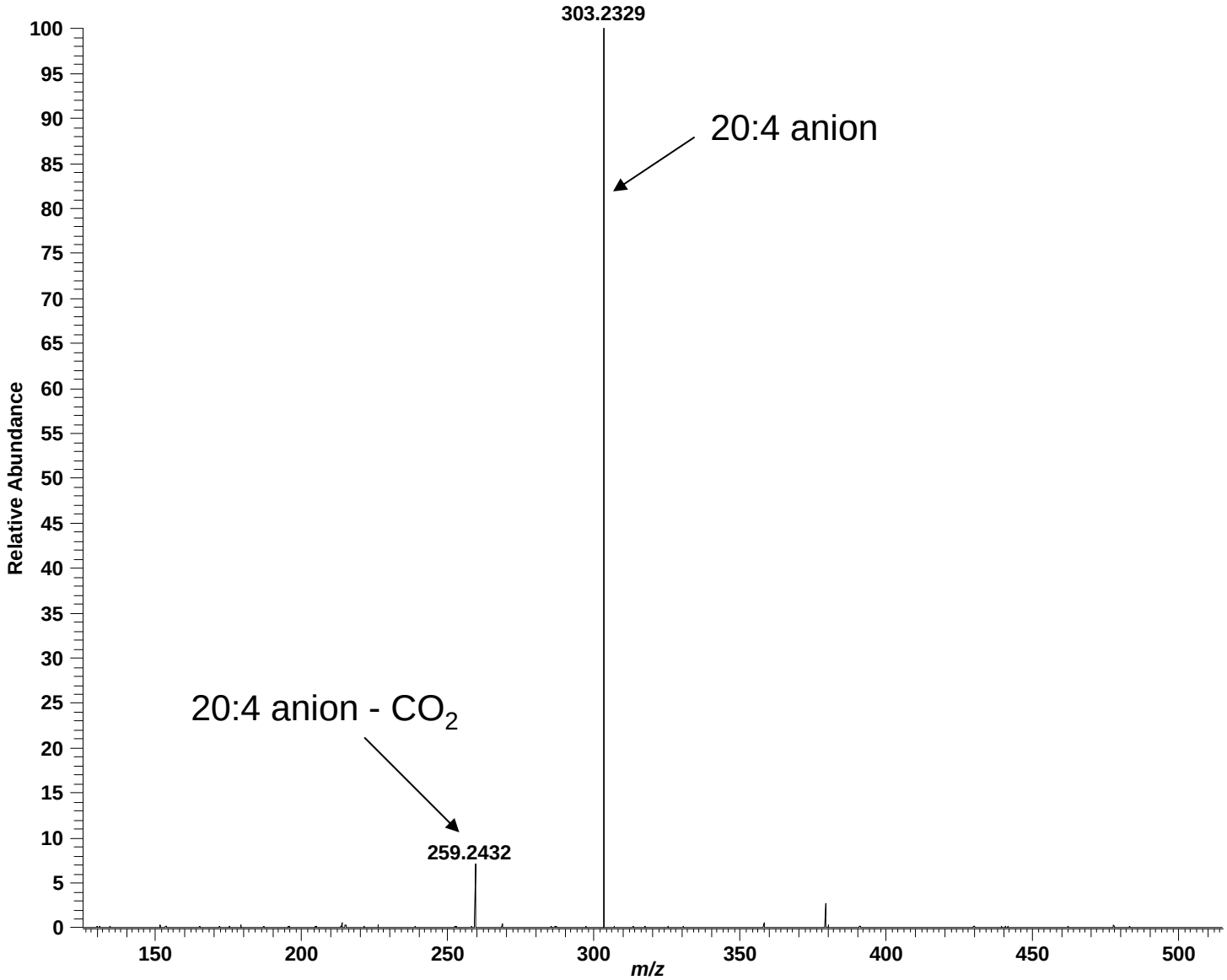

High mass measurement accuracy MS/MS utilizing LTQ-FT

Positive ESI: LPE 22:6; $C_{27}H_{44}NO_7P$; theoretical *m/z* 526.2933, $(M+H)^+$

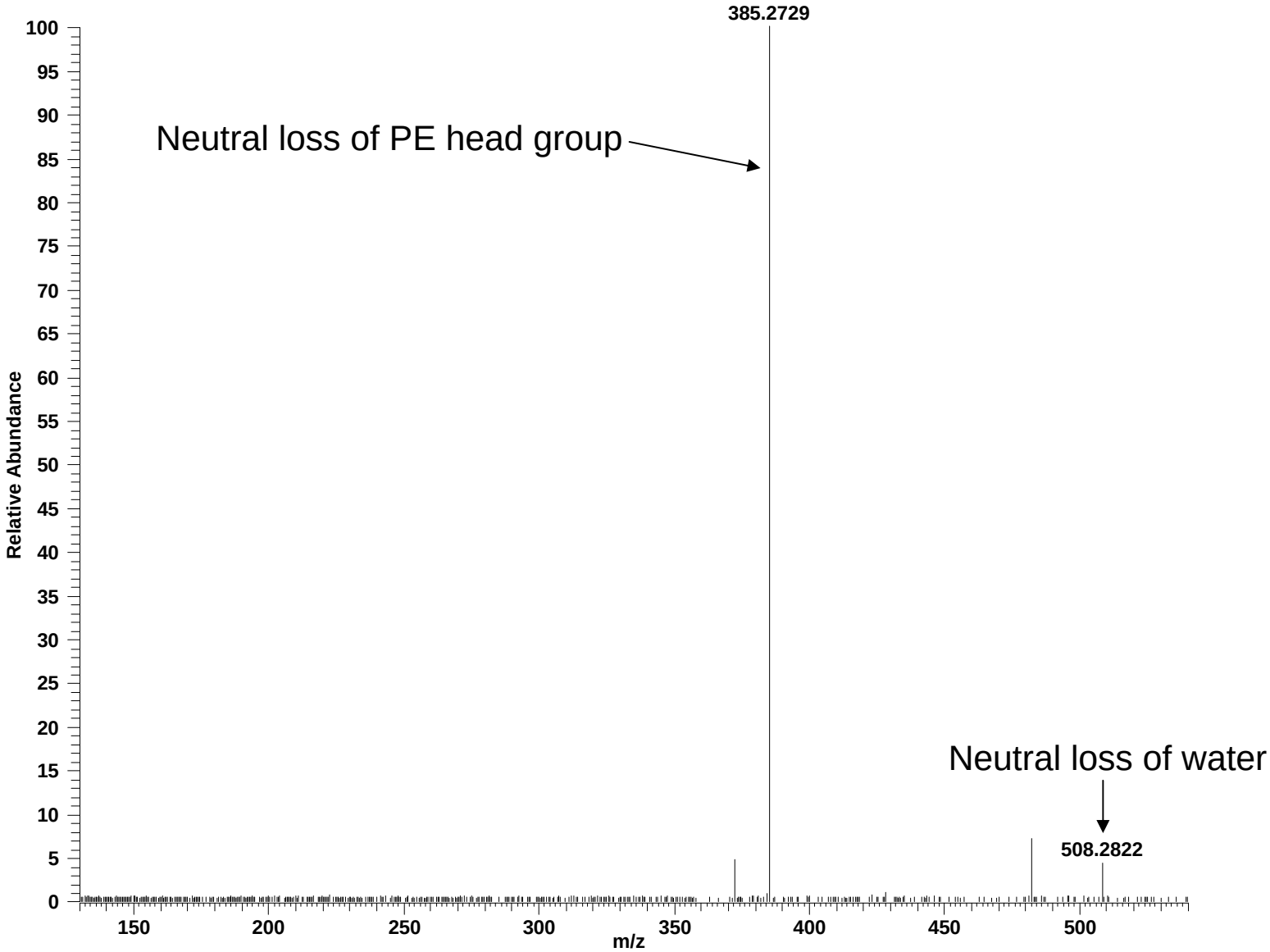

High mass measurement accuracy MS/MS utilizing LTQ-FT

Negative ESI: LPE 22:6; $C_{27}H_{44}NO_7P$; theoretical *m/z* 524.2777, $(M-H)^-$

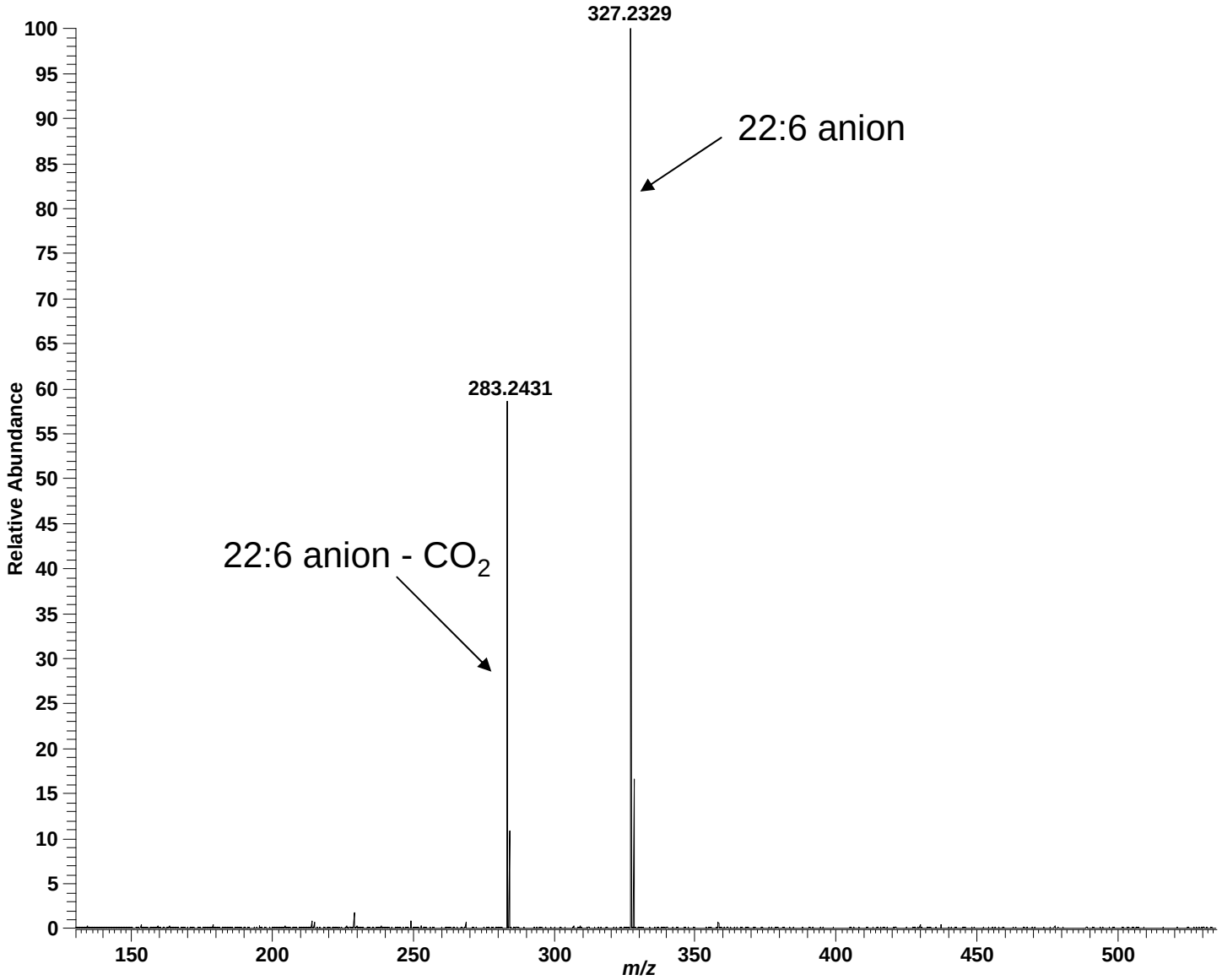

High mass measurement accuracy MS/MS utilizing LTQ-FT

Positive ESI: LPE 22:5; $C_{27}H_{46}NO_7P$; theoretical *m/z* 528.3090, $(M+H)^+$

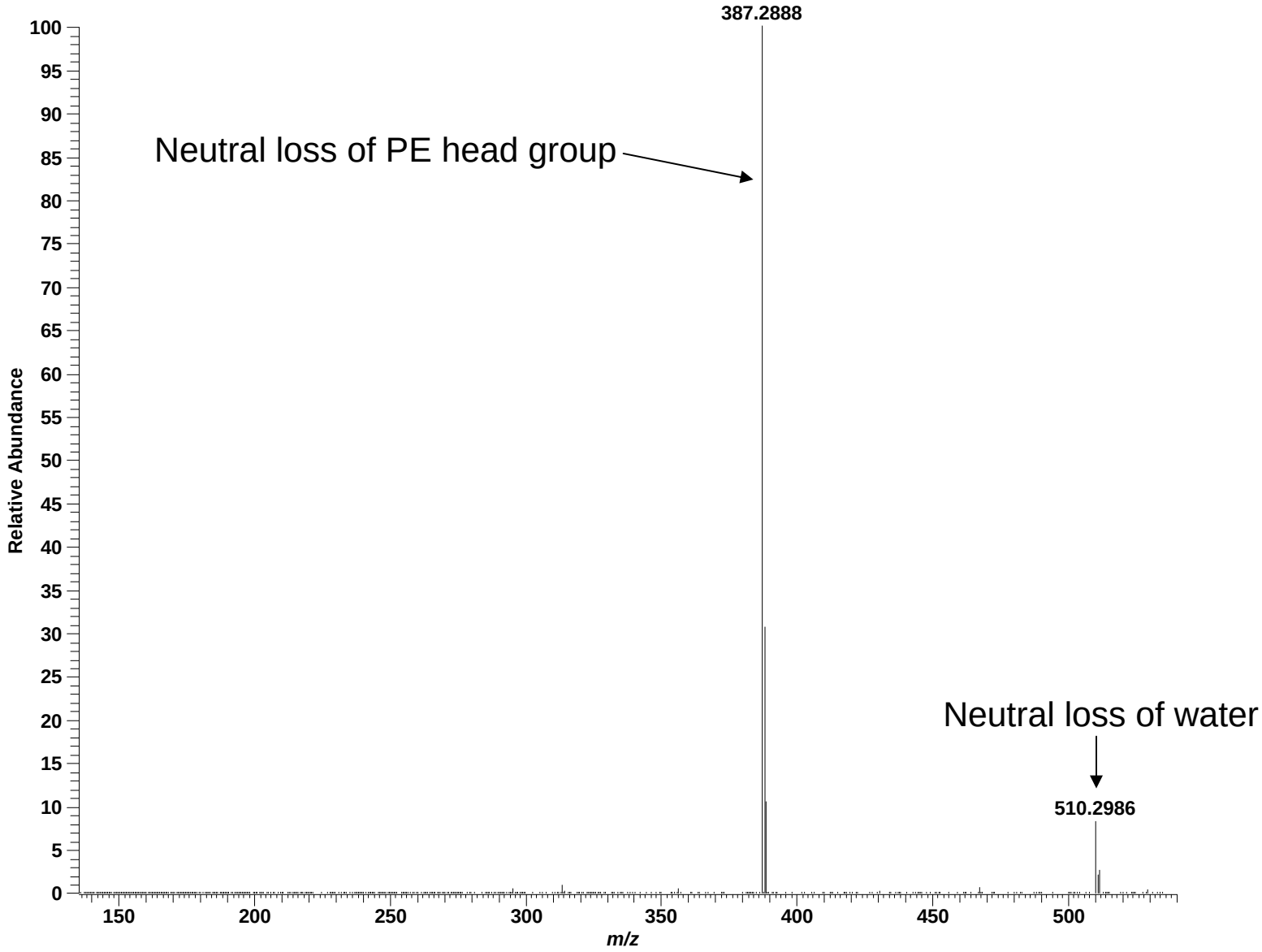

High mass measurement accuracy MS/MS utilizing LTQ-FT

Negative ESI: LPE 22:5; $C_{27}H_{46}NO_7P$; theoretical *m/z* 526.2933, $(M-H)^-$

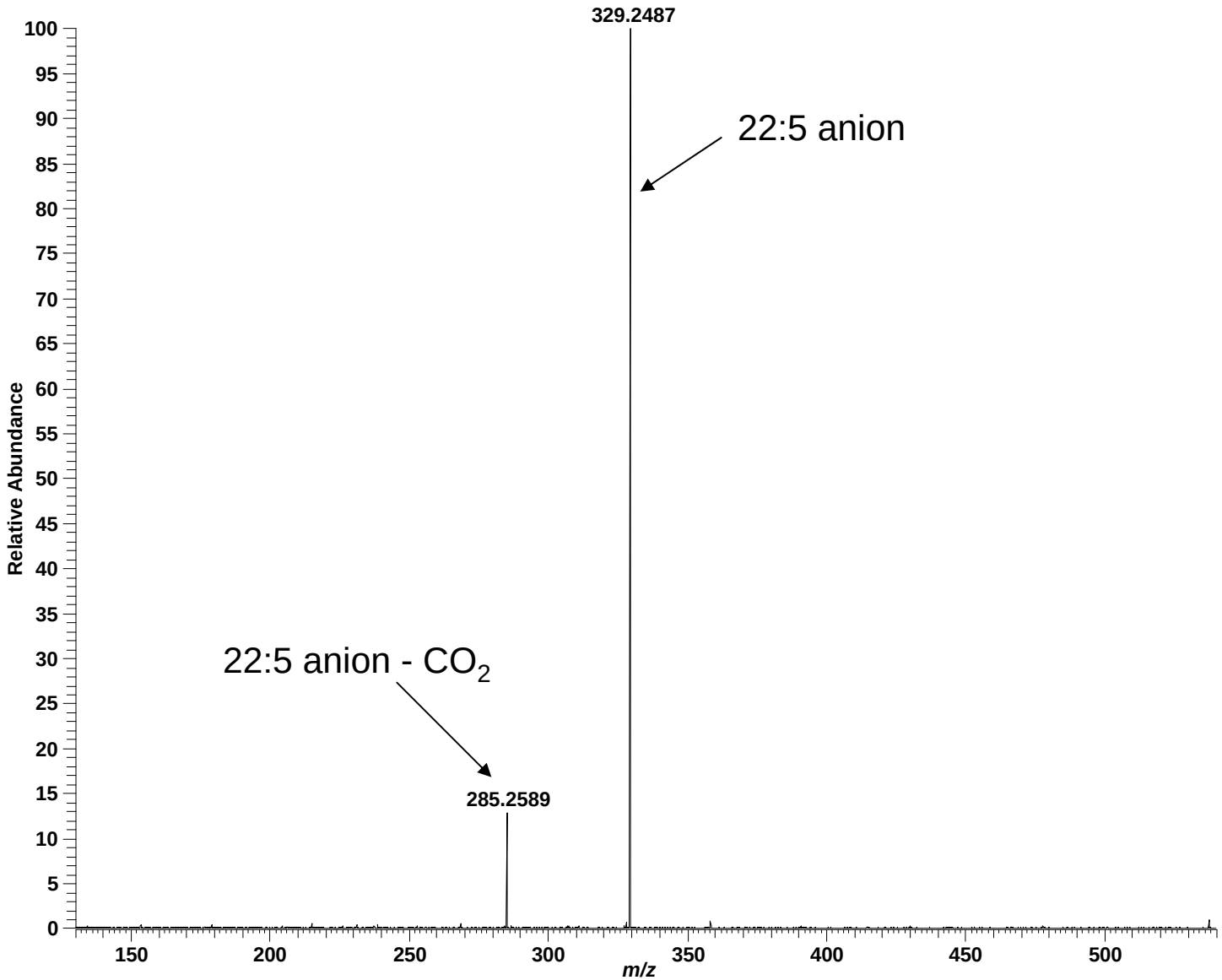

High mass measurement accuracy MS/MS utilizing LTQ-FT

Positive ESI: LPE 22:4; $C_{27}H_{48}NO_7P$; theoretical *m/z* 530.3246, $(M+H)^+$

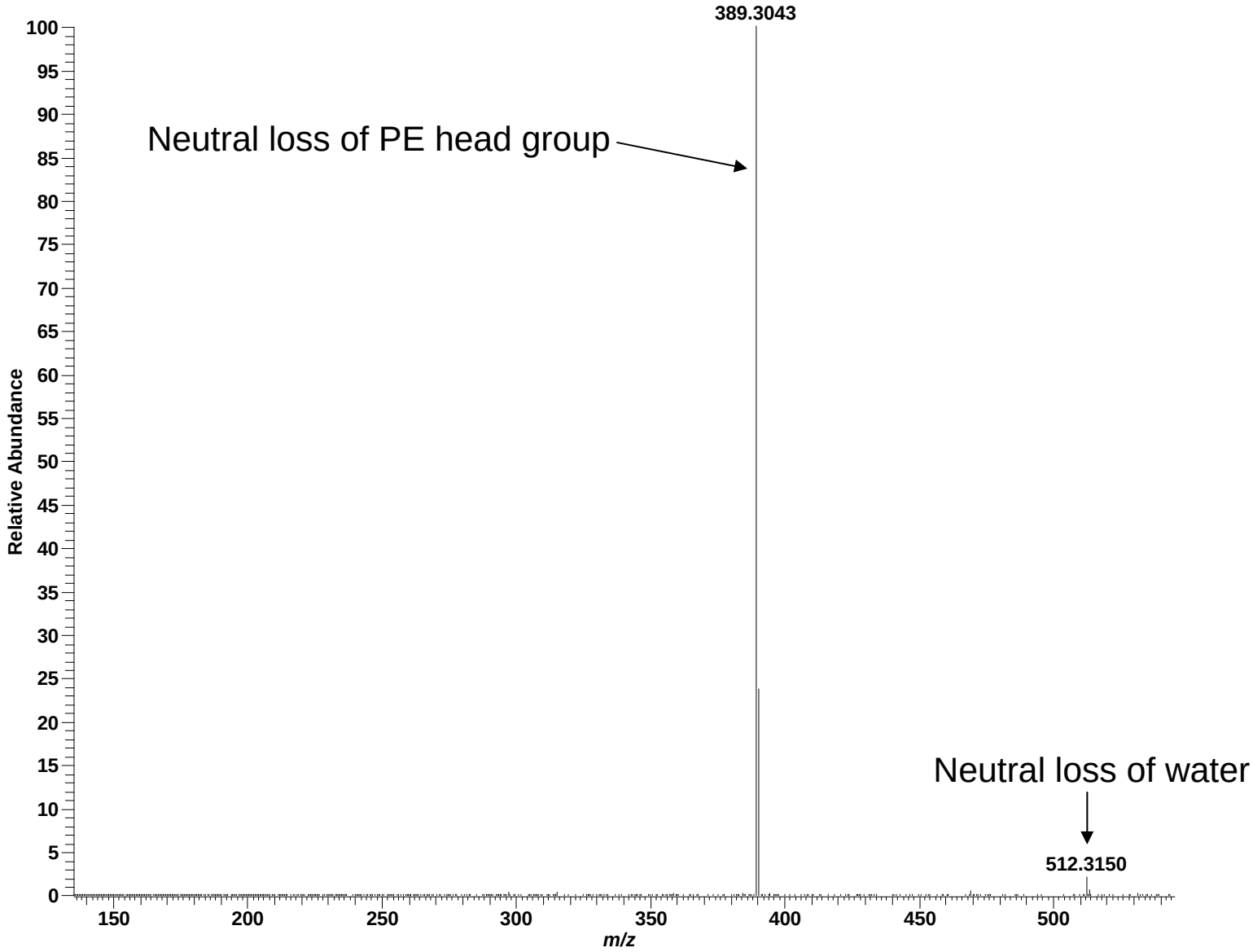

High mass measurement accuracy MS/MS utilizing LTQ-FT

Negative ESI: LPE 22:4; $C_{27}H_{48}NO_7P$; theoretical *m/z* 528.3090, $(M-H)^-$

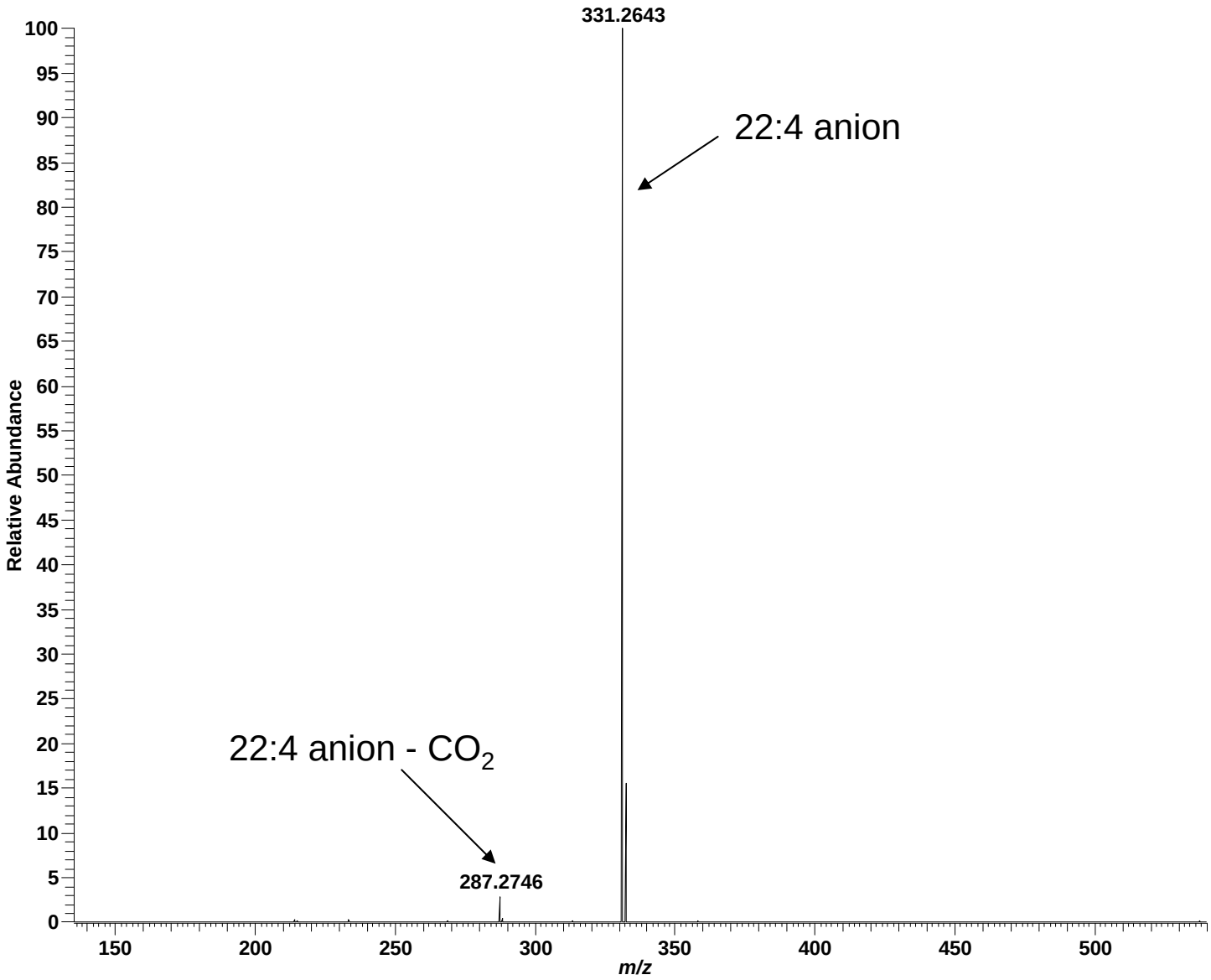

High mass measurement accuracy MS/MS utilizing LTQ-FT

Negative ESI: LPE 16:1; $C_{21}H_{42}NO_7P$; theoretical *m/z* 450.2621, $(M-H)^-$

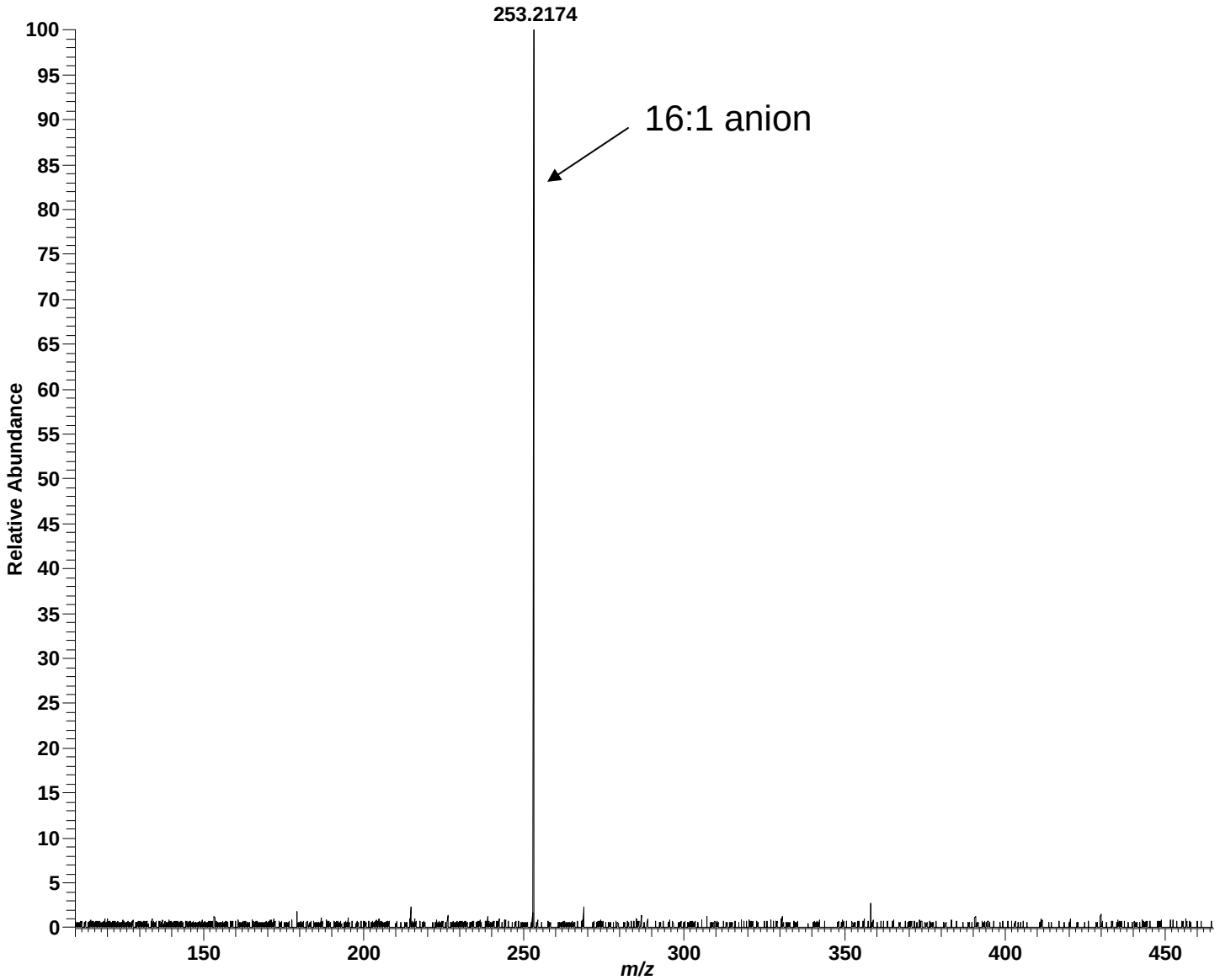

High mass measurement accuracy MS/MS utilizing LTQ-FT

Positive ESI: LPE 16:0; $C_{21}H_{44}NO_7P$; theoretical *m/z* 454.2934, $(M+H)^+$

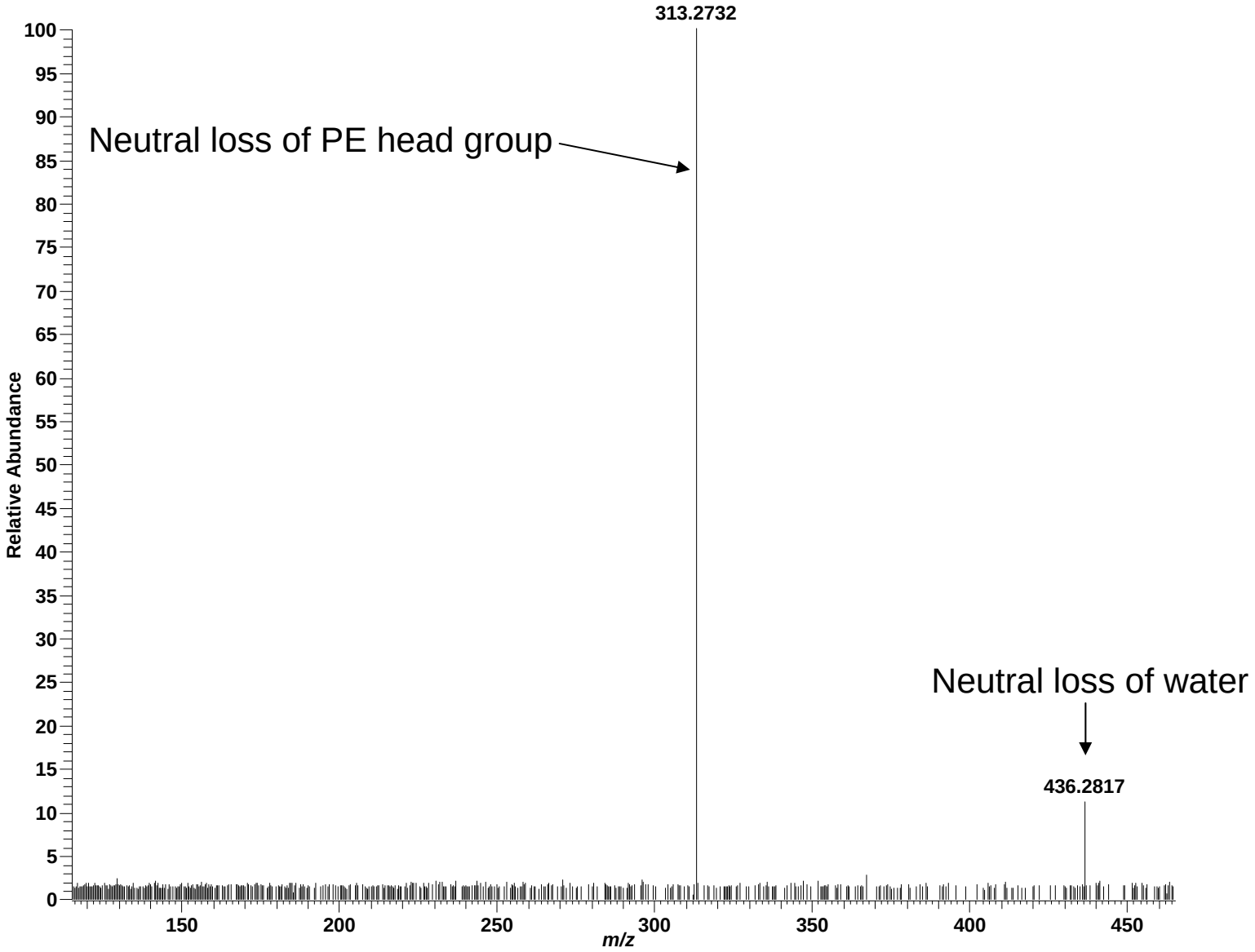

High mass measurement accuracy MS/MS utilizing LTQ-FT

Negative ESI: LPE 16:0; $C_{21}H_{44}NO_7P$; theoretical *m/z* 452.2777, $(M-H)^-$

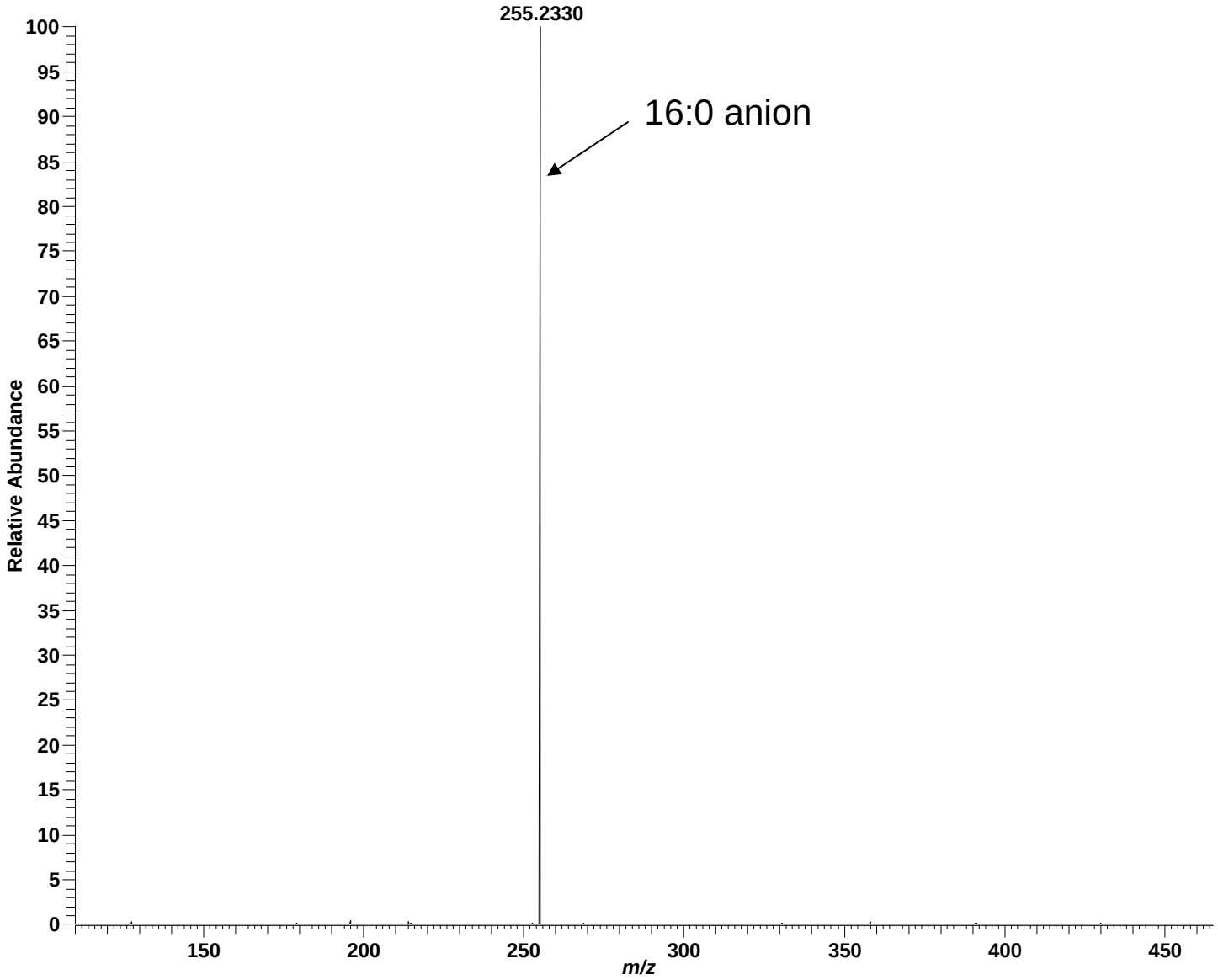

High mass measurement accuracy MS/MS utilizing LTQ-FT

Positive ESI: LPE 18:2; $C_{23}H_{44}NO_7P$; theoretical *m/z* 478.2933, $(M+H)^+$

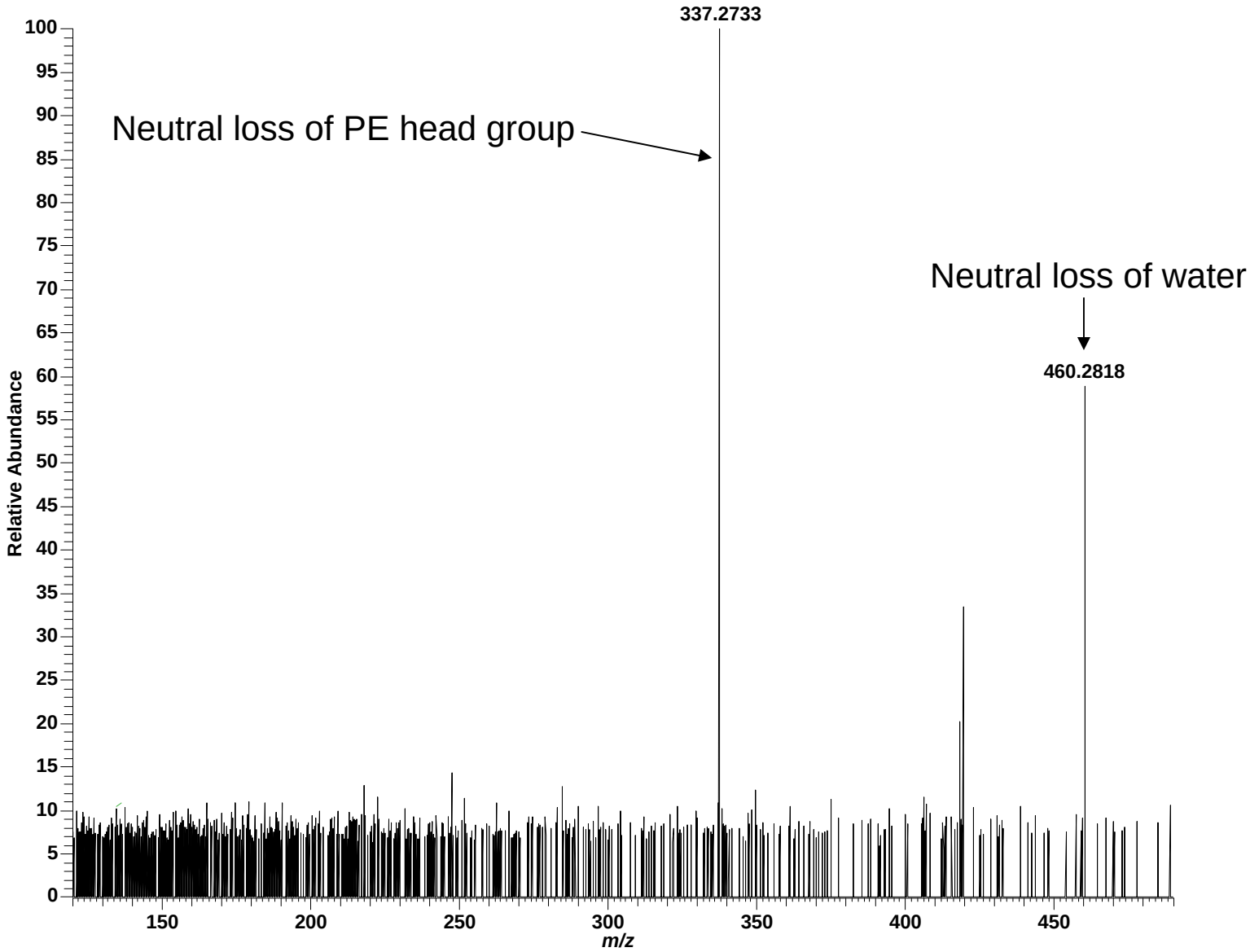

High mass measurement accuracy MS/MS utilizing LTQ-FT

Negative ESI: LPE 18:2; $C_{23}H_{44}NO_7P$; theoretical *m/z* 476.2777, $(M-H)^-$

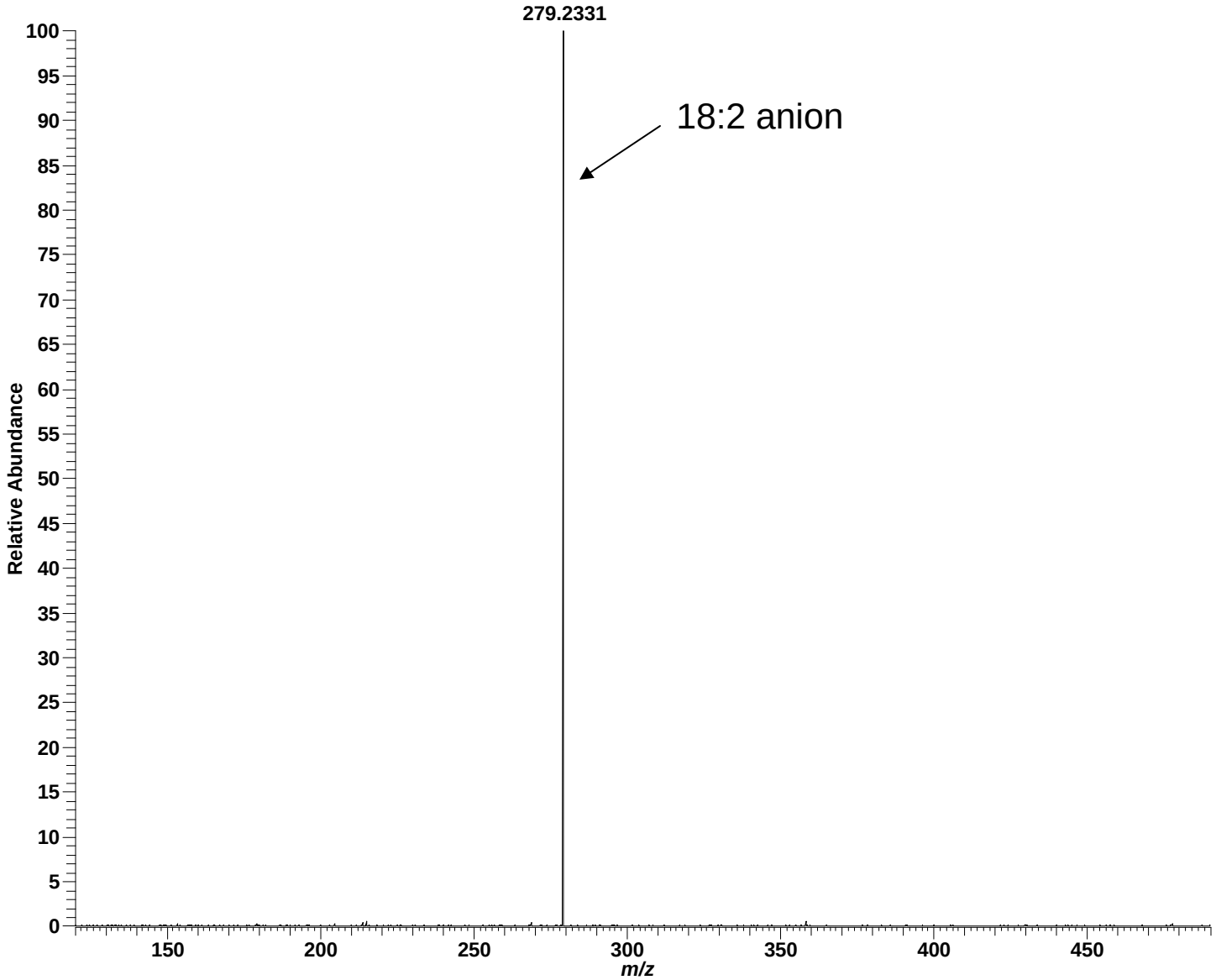

High mass measurement accuracy MS/MS utilizing LTQ-FT

Positive ESI: LPE 18:1; $C_{23}H_{46}NO_7P$; theoretical *m/z* 480.3090, $(M+H)^+$

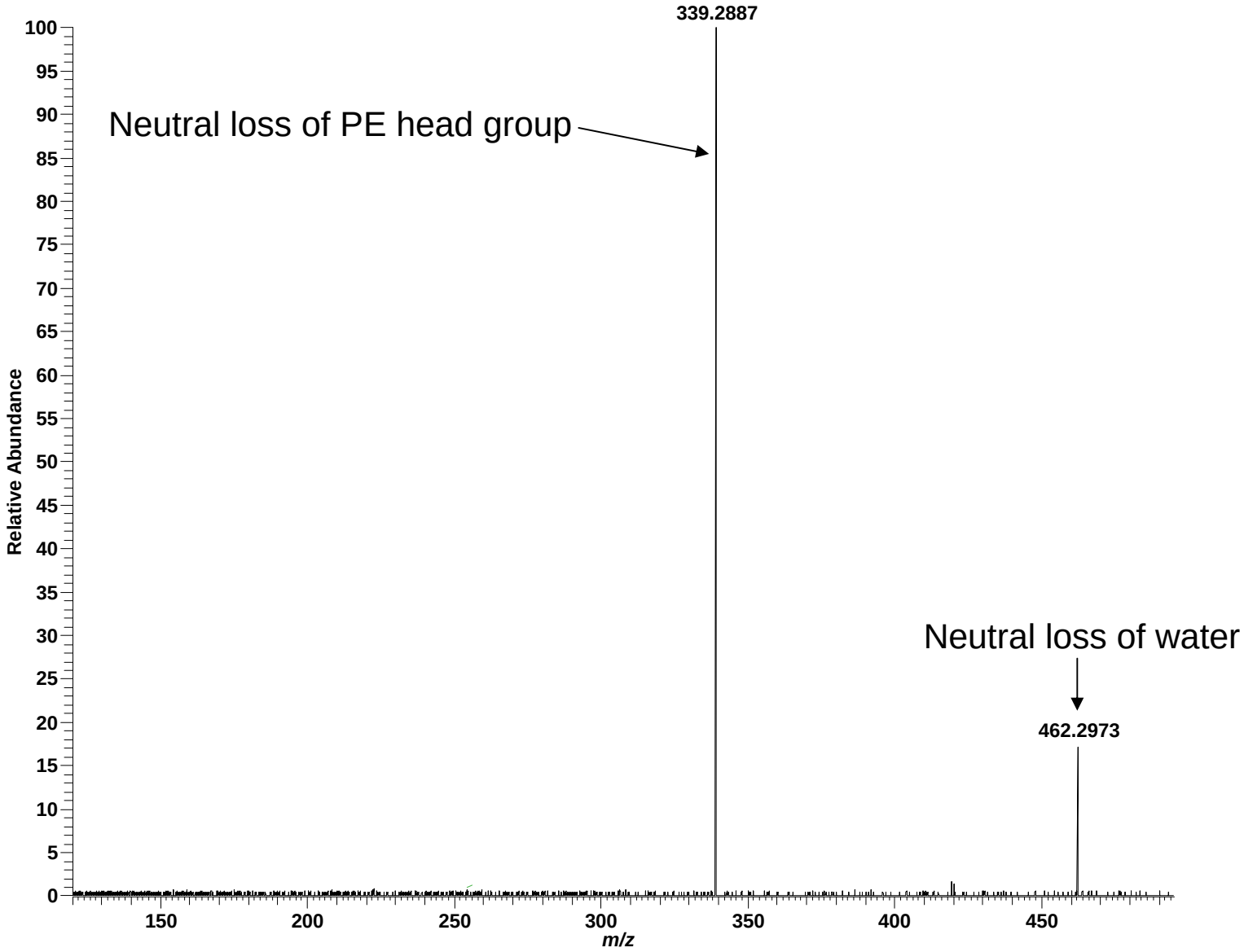

High mass measurement accuracy MS/MS utilizing LTQ-FT

Negative ESI: LPE 18:1; $C_{23}H_{46}NO_7P$; theoretical *m/z* 478.2933, $(M-H)^-$

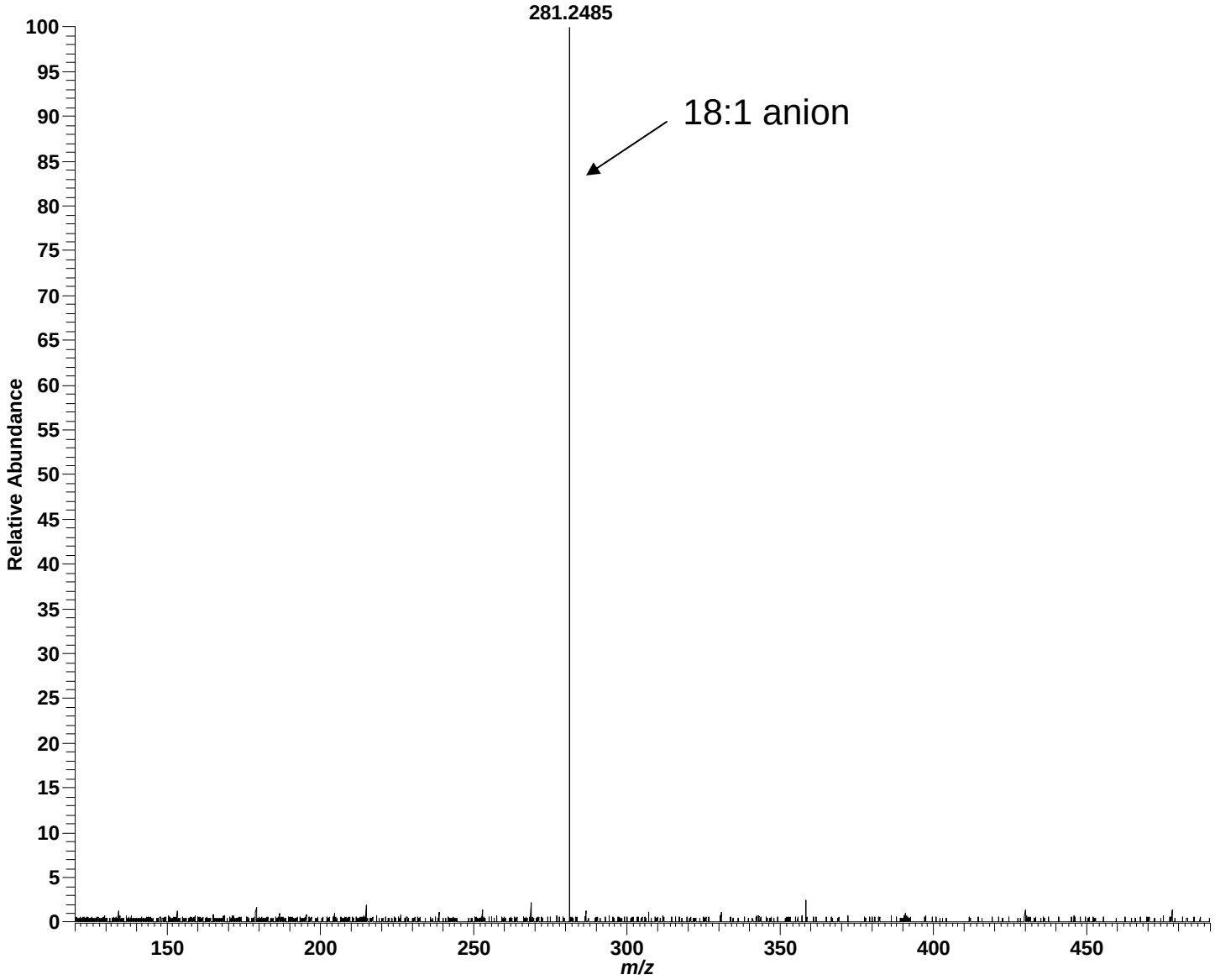

High mass measurement accuracy MS/MS utilizing LTQ-FT

Positive ESI: LPE 18:0; $C_{23}H_{48}NO_7P$; theoretical *m/z* 482.3246, $(M+H)^+$

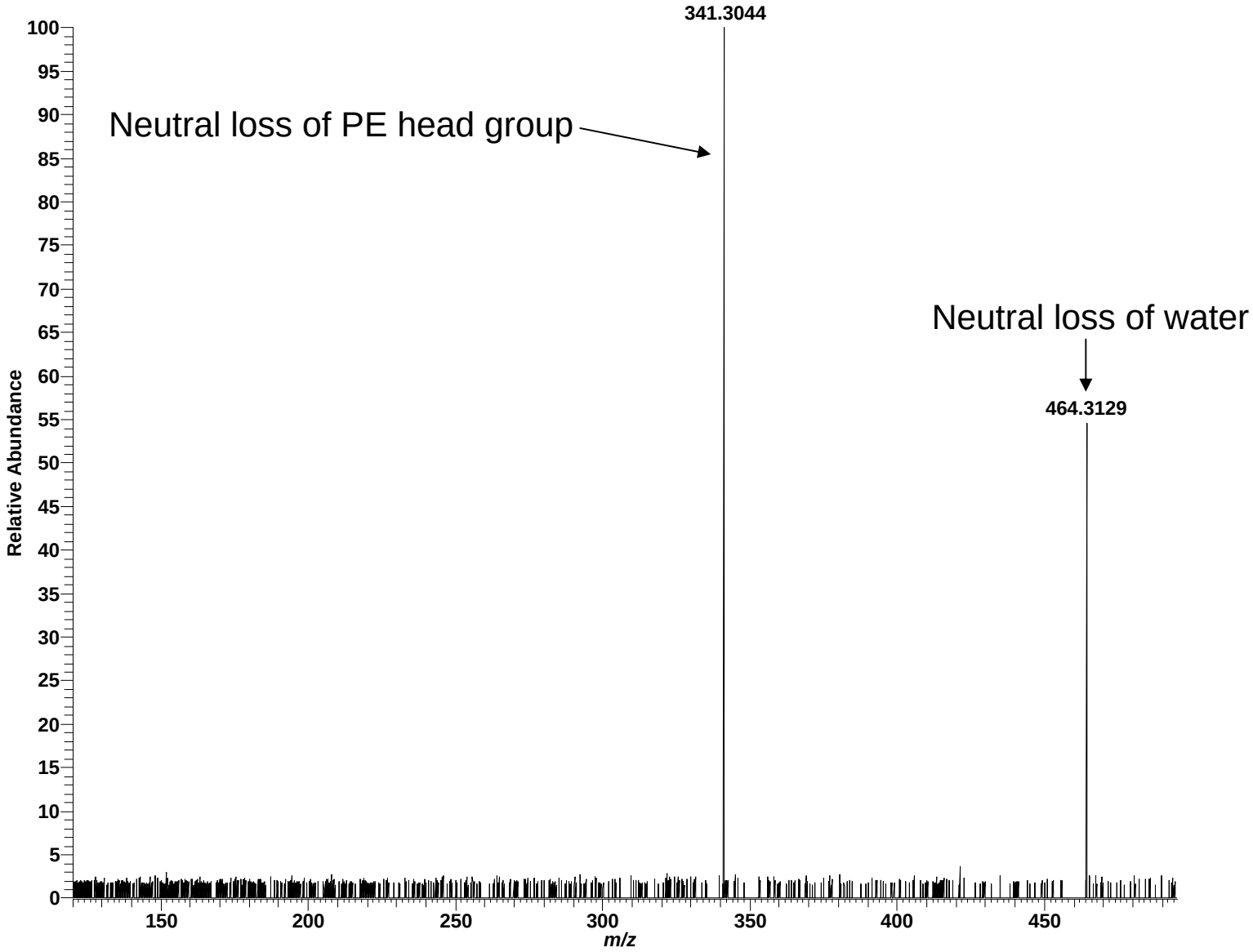

High mass measurement accuracy MS/MS utilizing LTQ-FT

Negative ESI: LPE 18:0; $C_{23}H_{48}NO_7P$; theoretical *m/z* 480.3090, $(M-H)^-$

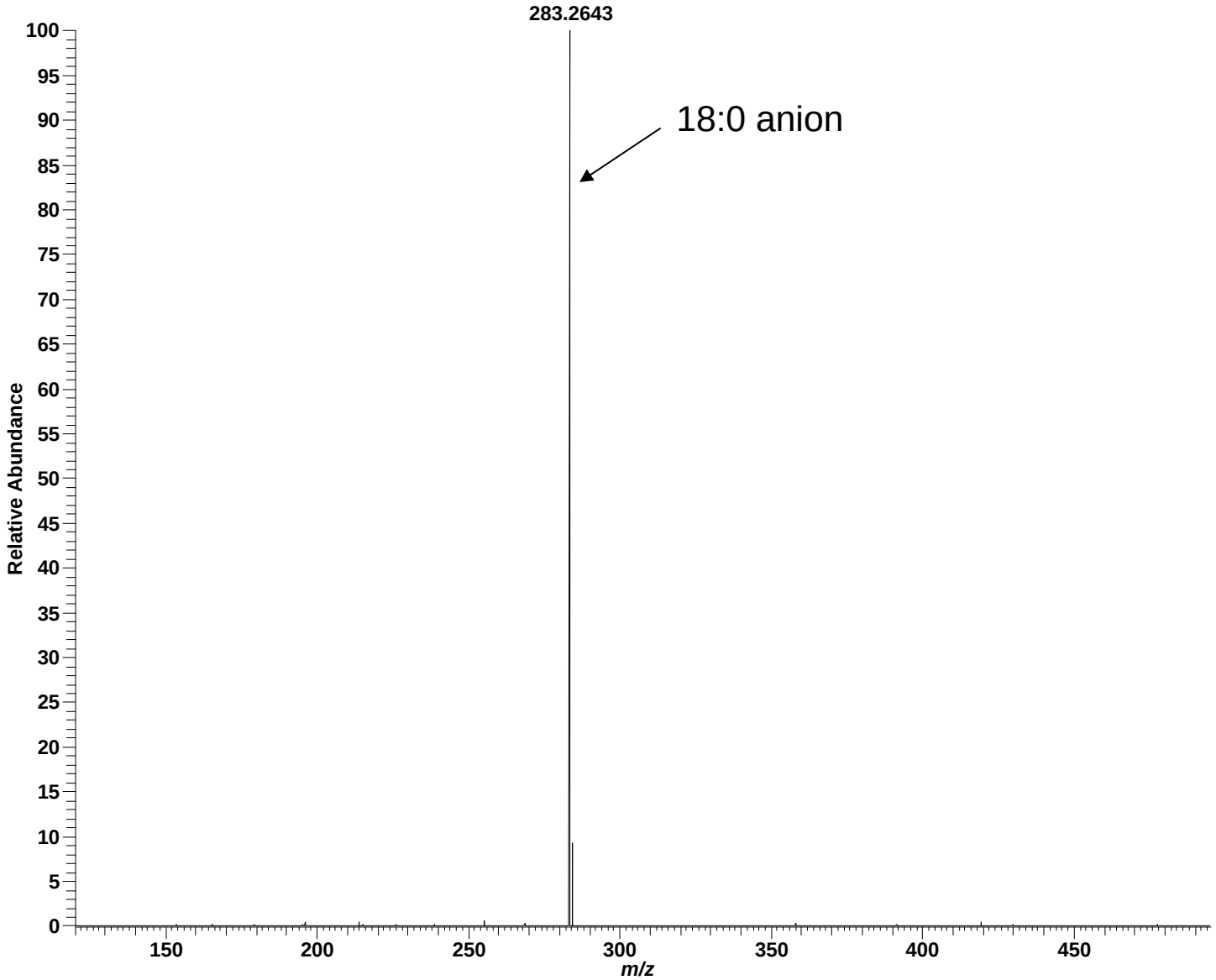

High mass measurement accuracy MS/MS utilizing LTQ-FT

Positive ESI: PE 16:0/20:4; $C_{41}H_{74}NO_8P$; theoretical *m/z* 740.5230, $(M+H)^+$

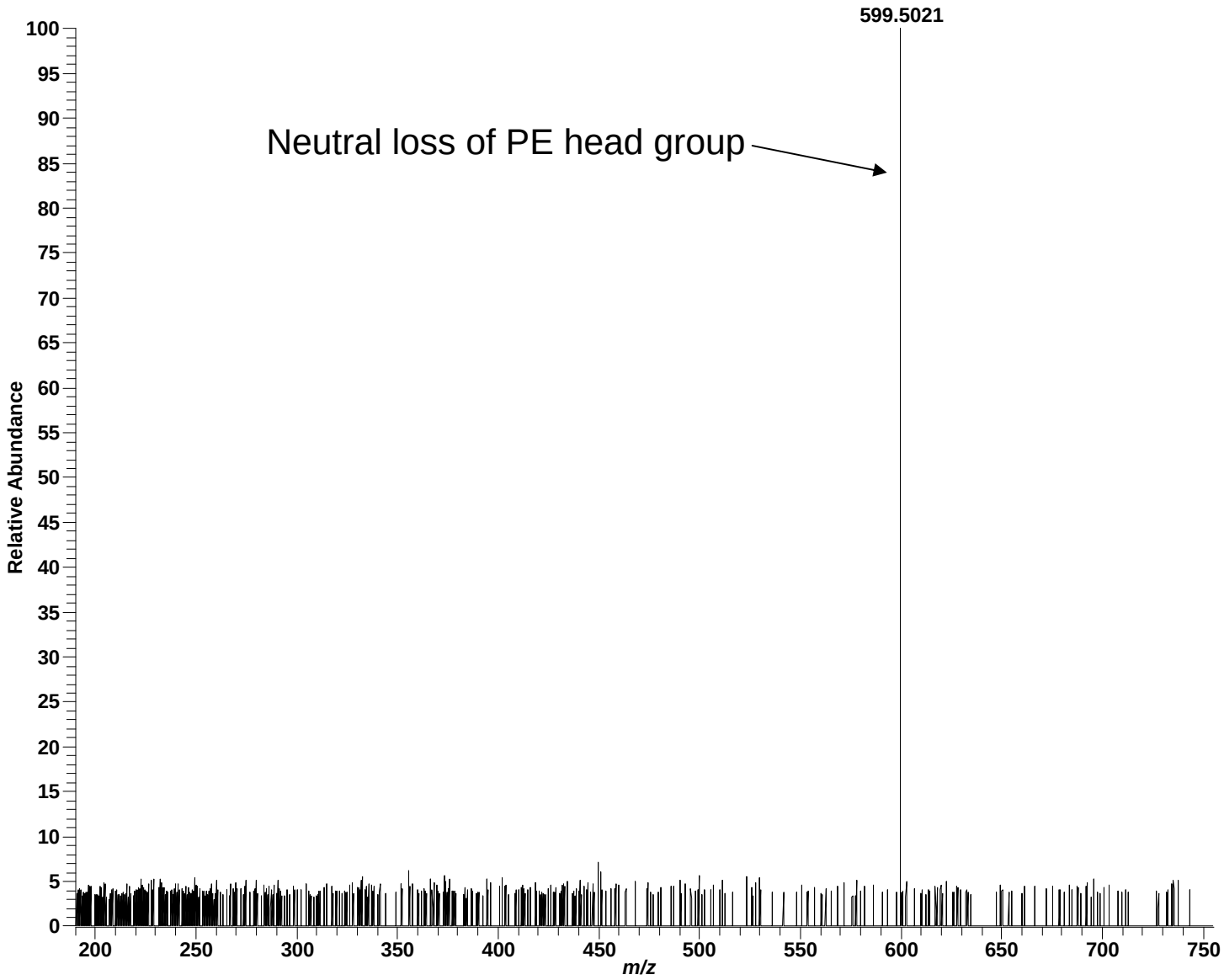

Low mass measurement accuracy MS/MS utilizing LTQ

Negative ESI: PE 16:0/20:4; $C_{41}H_{74}NO_8P$; theoretical *m/z* 738.5, $(M-H)^-$

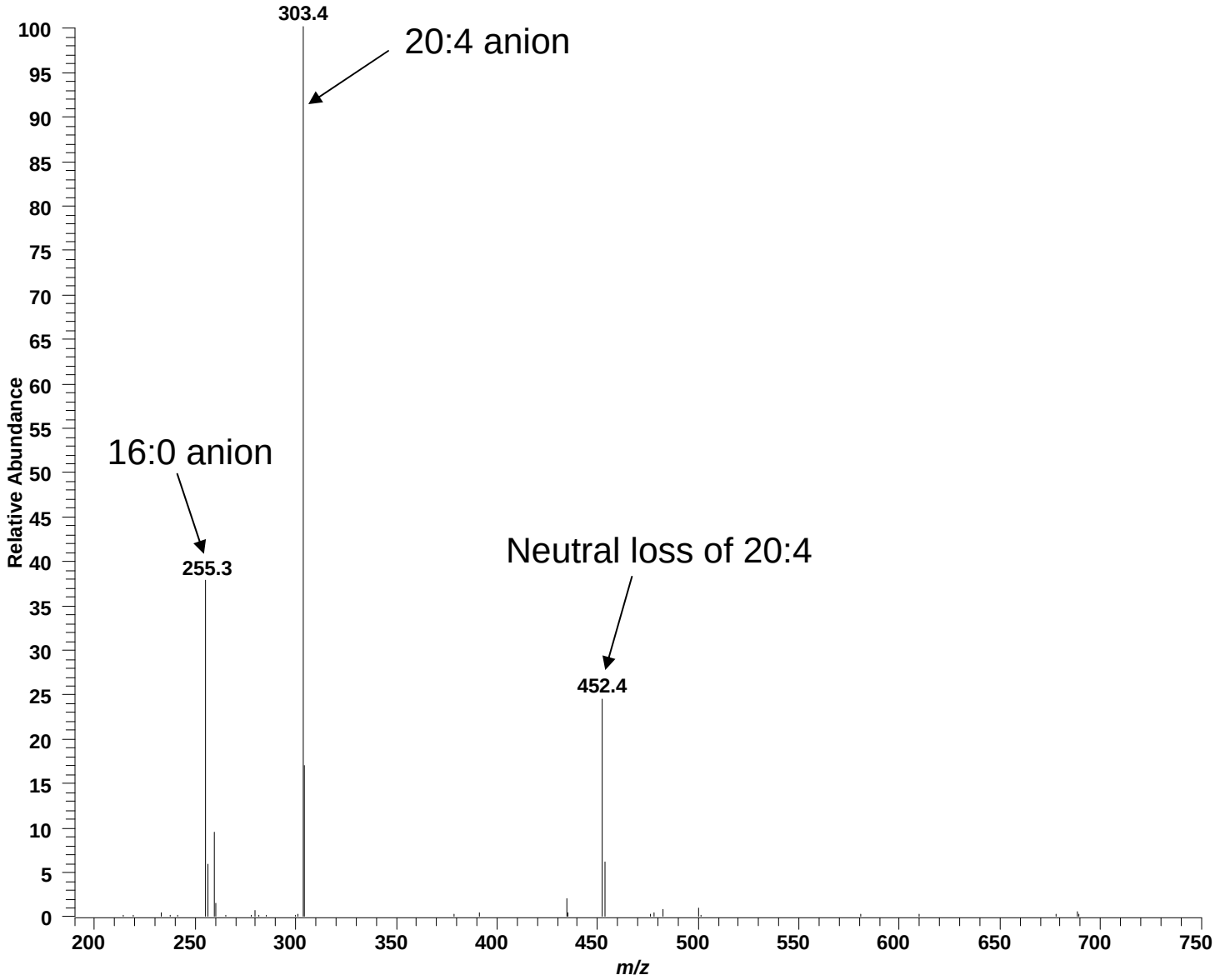

High mass measurement accuracy MS/MS utilizing LTQ-FT

Positive ESI: PE 16:0/20:3 or 18:2/18:1; $C_{41}H_{76}NO_8P$; theoretical *m/z* 742.5387, $(M+H)^+$

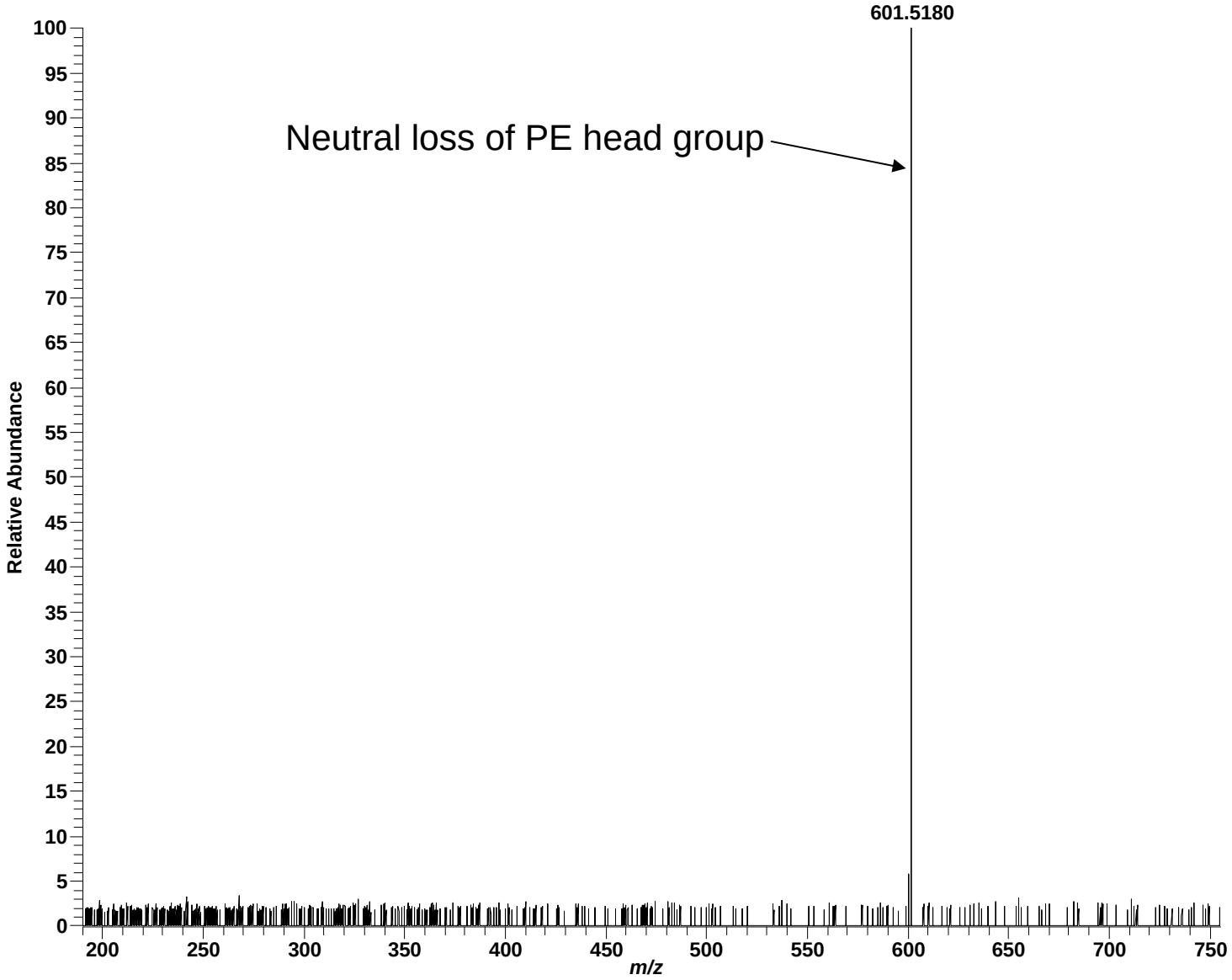

Low mass measurement accuracy MS/MS utilizing LTQ

Negative ESI: PE 16:0/20:3 or 18:2/18:1; $C_{41}H_{76}NO_8P$; theoretical *m/z* 740.5, $(M-H)^-$

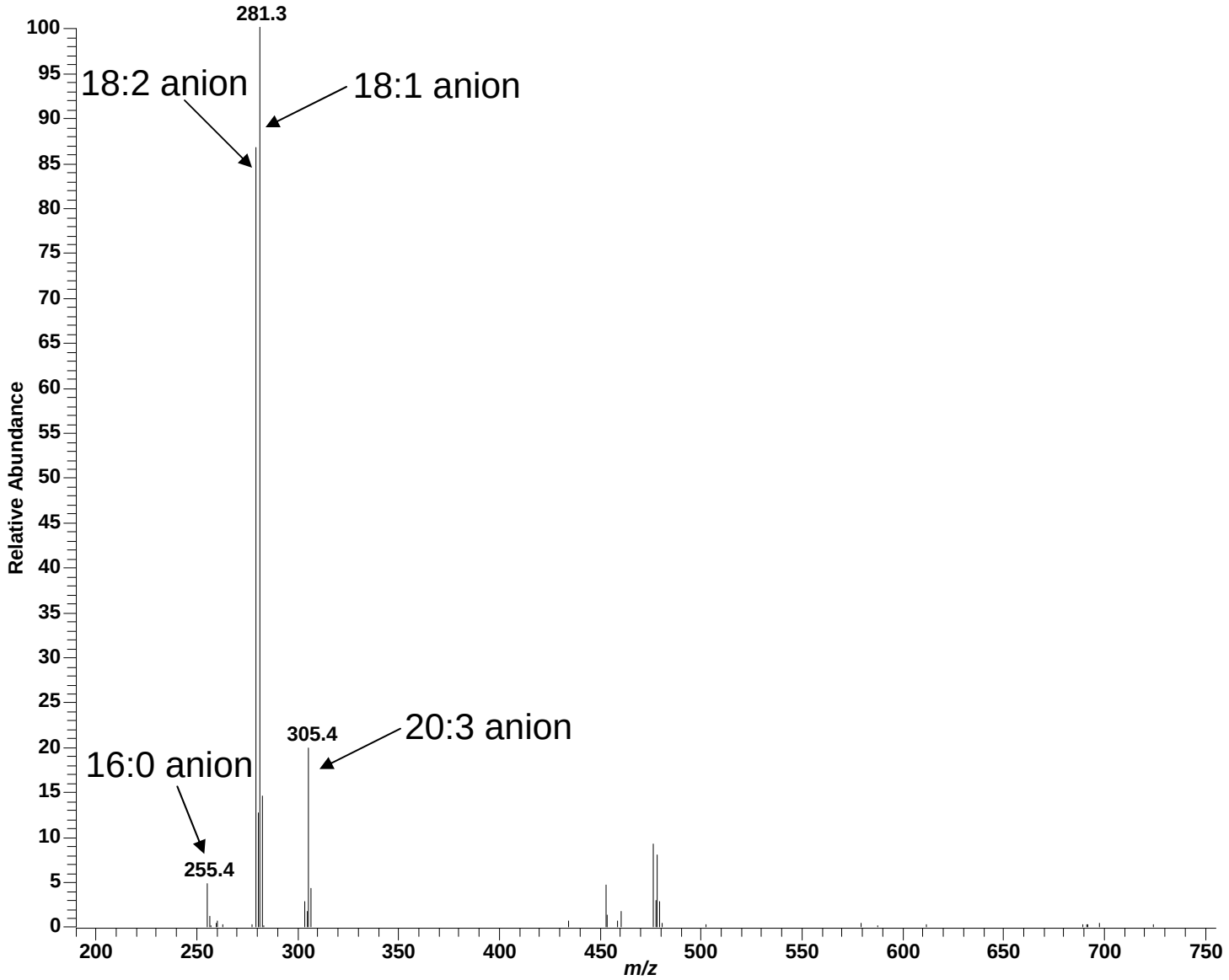

High mass measurement accuracy MS/MS utilizing LTQ-FT

Positive ESI: LPE 16:0/20:2 or 18:1/18:1; $C_{41}H_{78}NO_8P$; theoretical *m/z* 744.5543, $(M+H)^+$

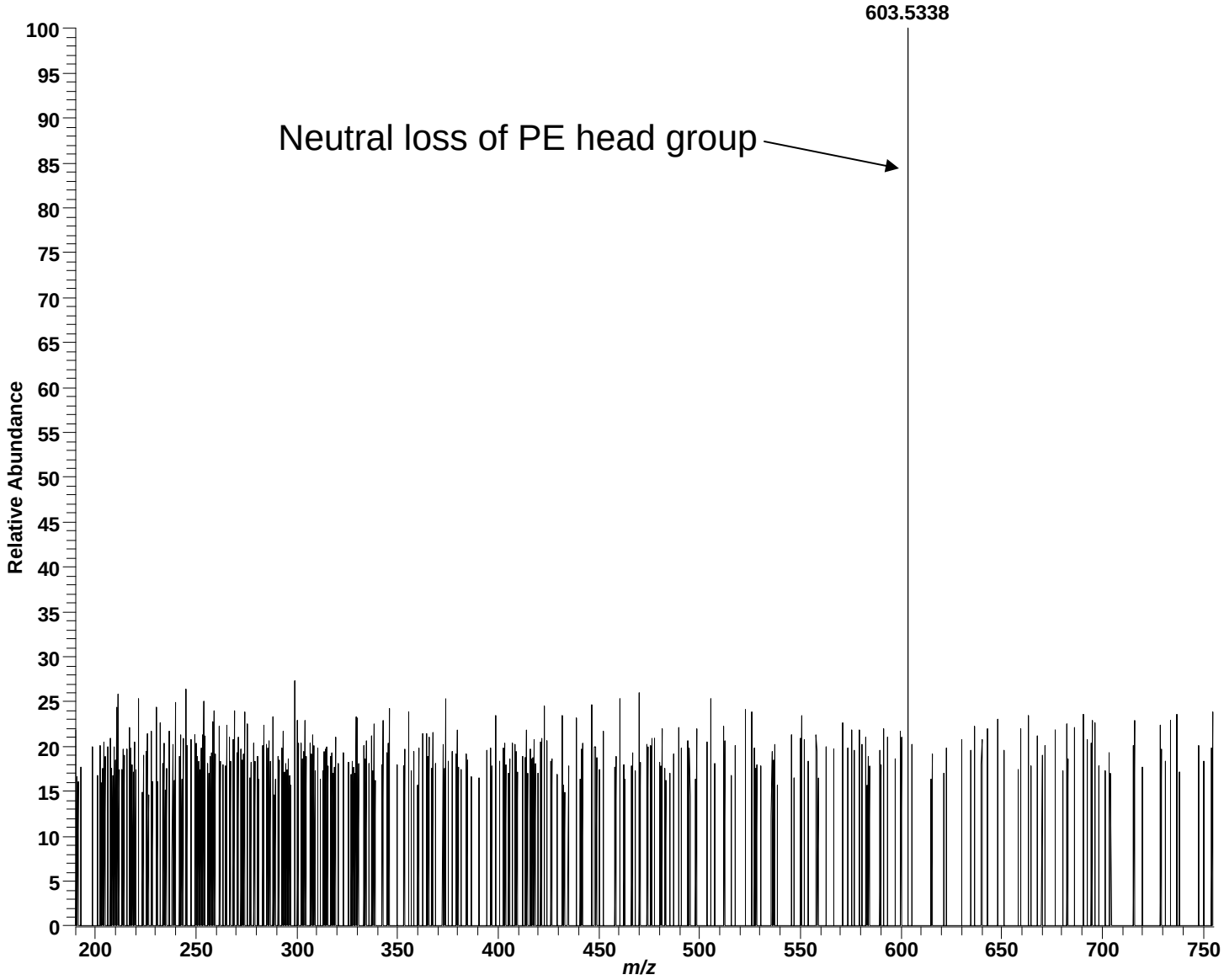

Low mass measurement accuracy MS/MS utilizing LTQ

Negative ESI: PE 16:0/20:2 or 18:1/18:1; $C_{41}H_{78}NO_8P$; theoretical *m/z* 742.5, $(M-H)^-$

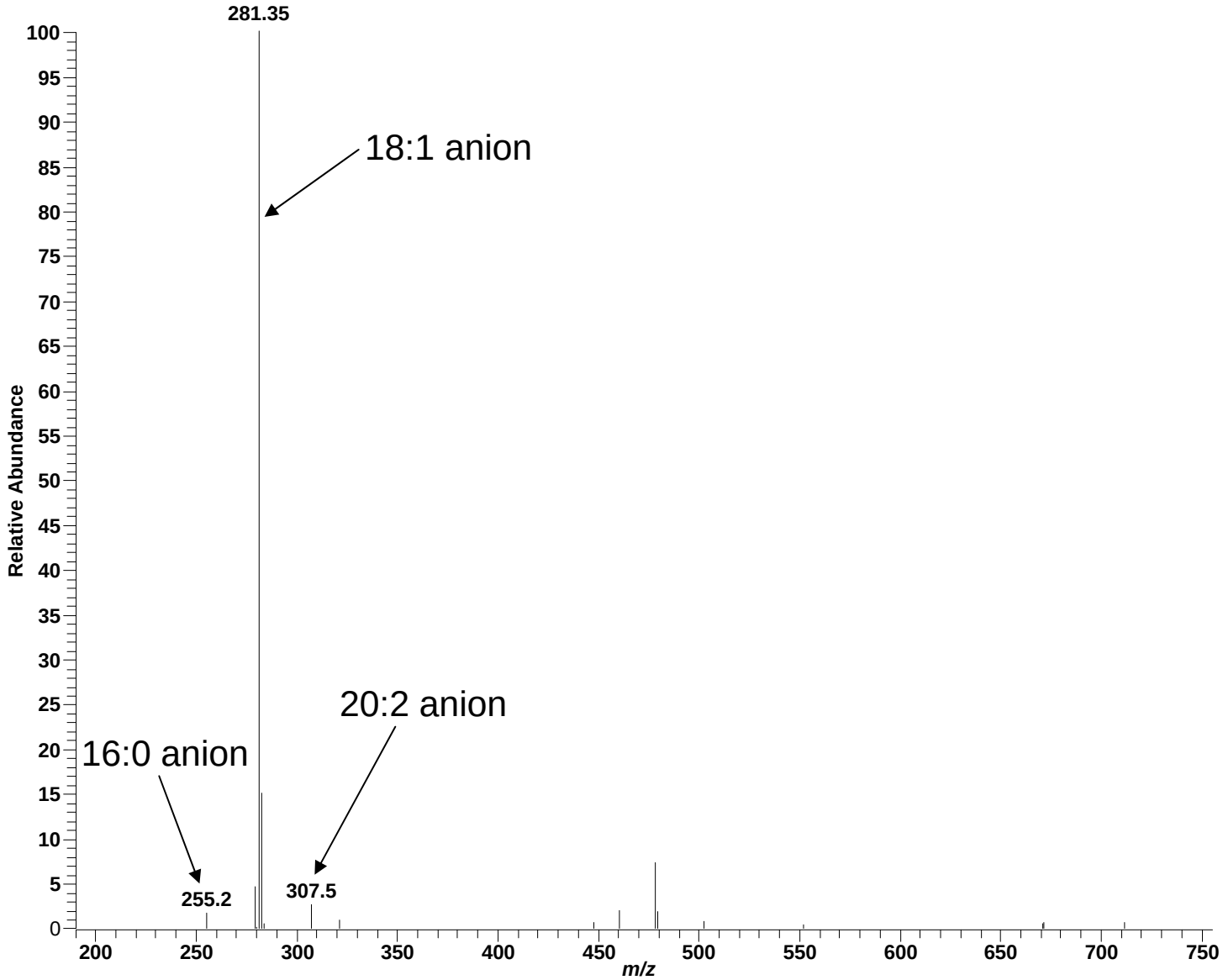

Low mass measurement accuracy MS/MS utilizing LTQ

Negative ESI: PE 18:1/20:4 or 16:0/22:5; $C_{43}H_{76}NO_8P$; theoretical *m/z* 764.5, $(M-H)^-$

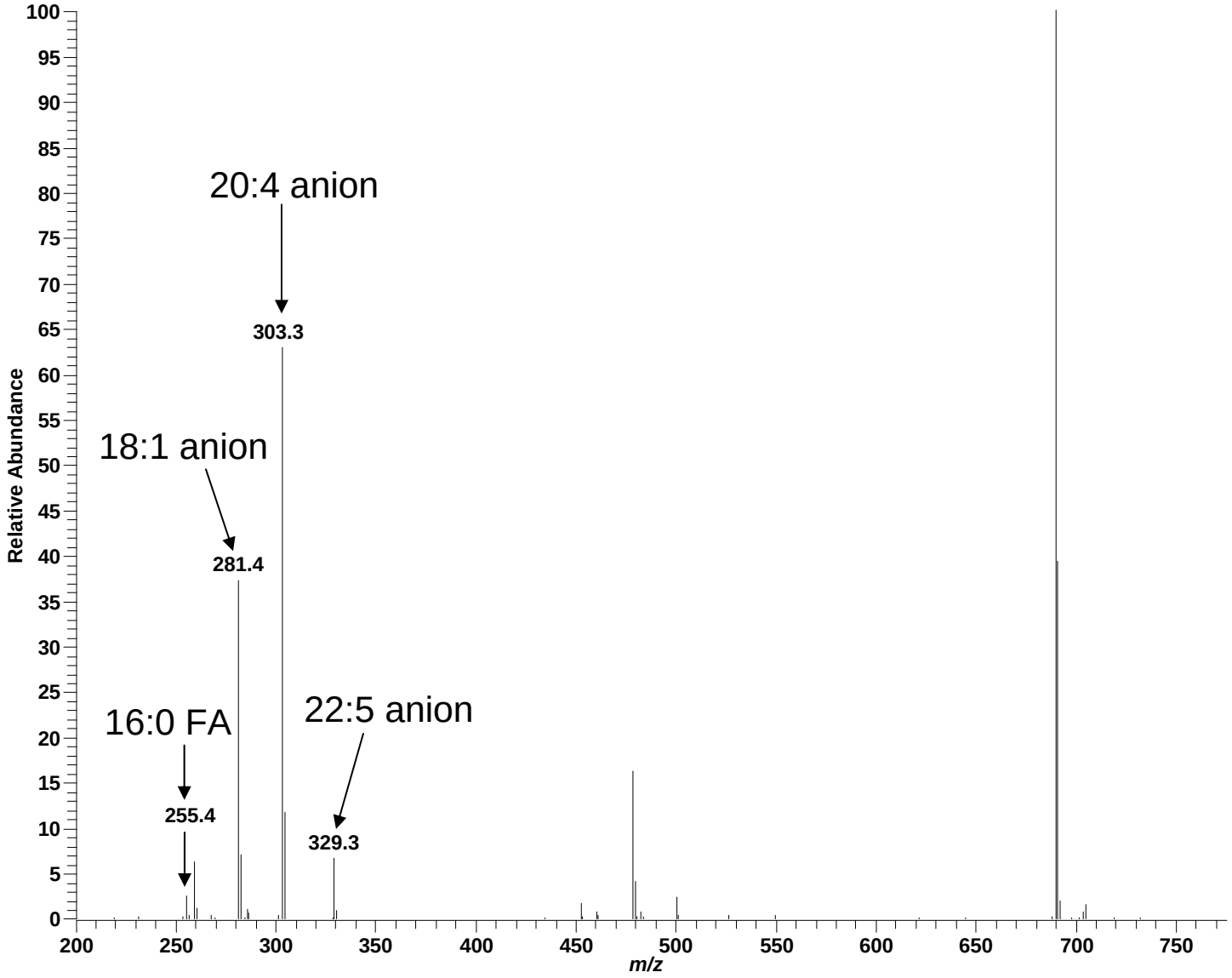

High mass measurement accuracy MS/MS utilizing LTQ-FT

Positive ESI: PE 18:1/20:3 or 16:0/22:4; $C_{43}H_{78}NO_8P$; theoretical *m/z* 768.5543, $(M+H)^+$

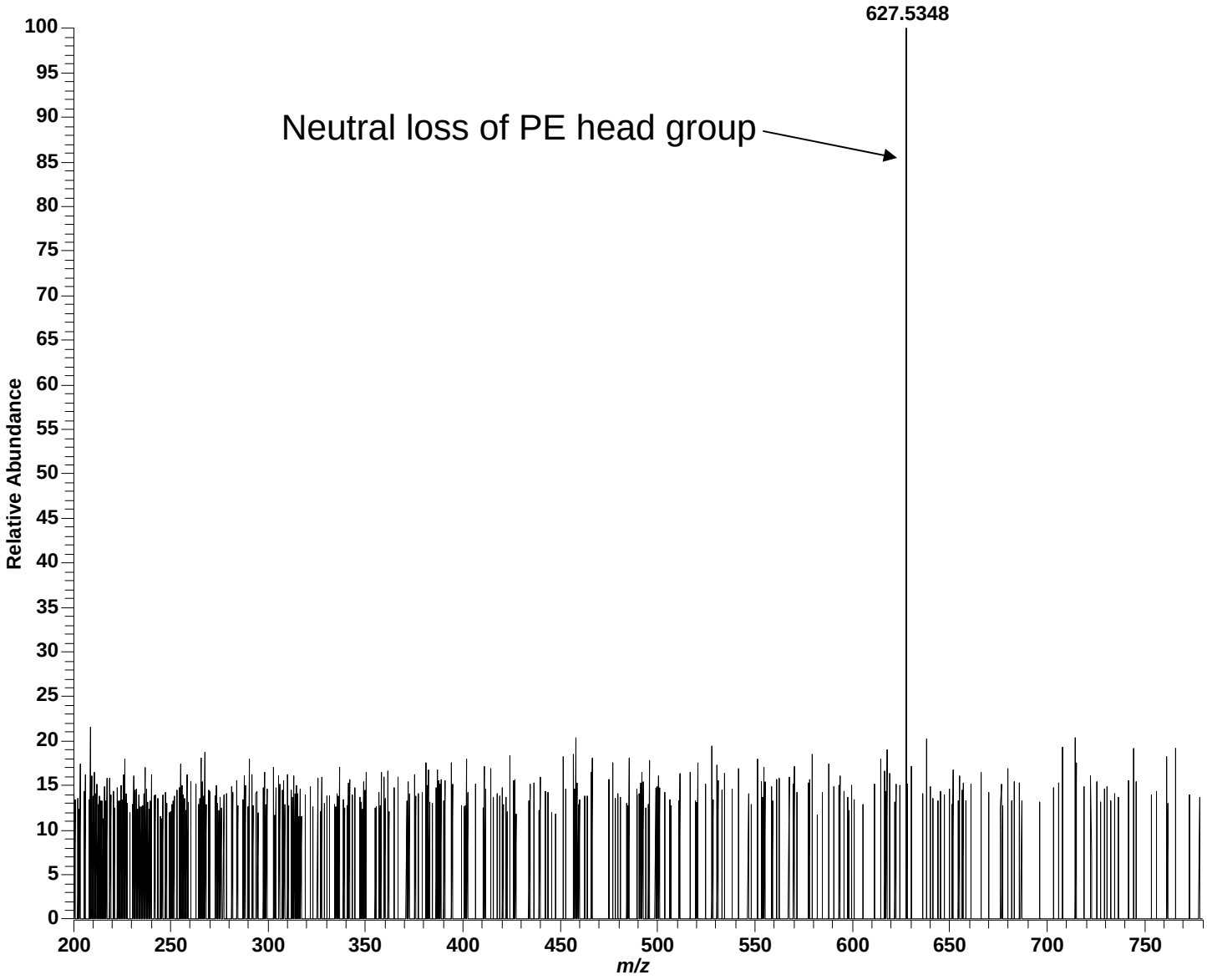

Low mass measurement accuracy MS/MS utilizing LTQ

Negative ESI: PE 18:1/20:3 or 16:0/22:4; $C_{43}H_{78}NO_8P$; theoretical *m/z* 766.5, $(M-H)^-$

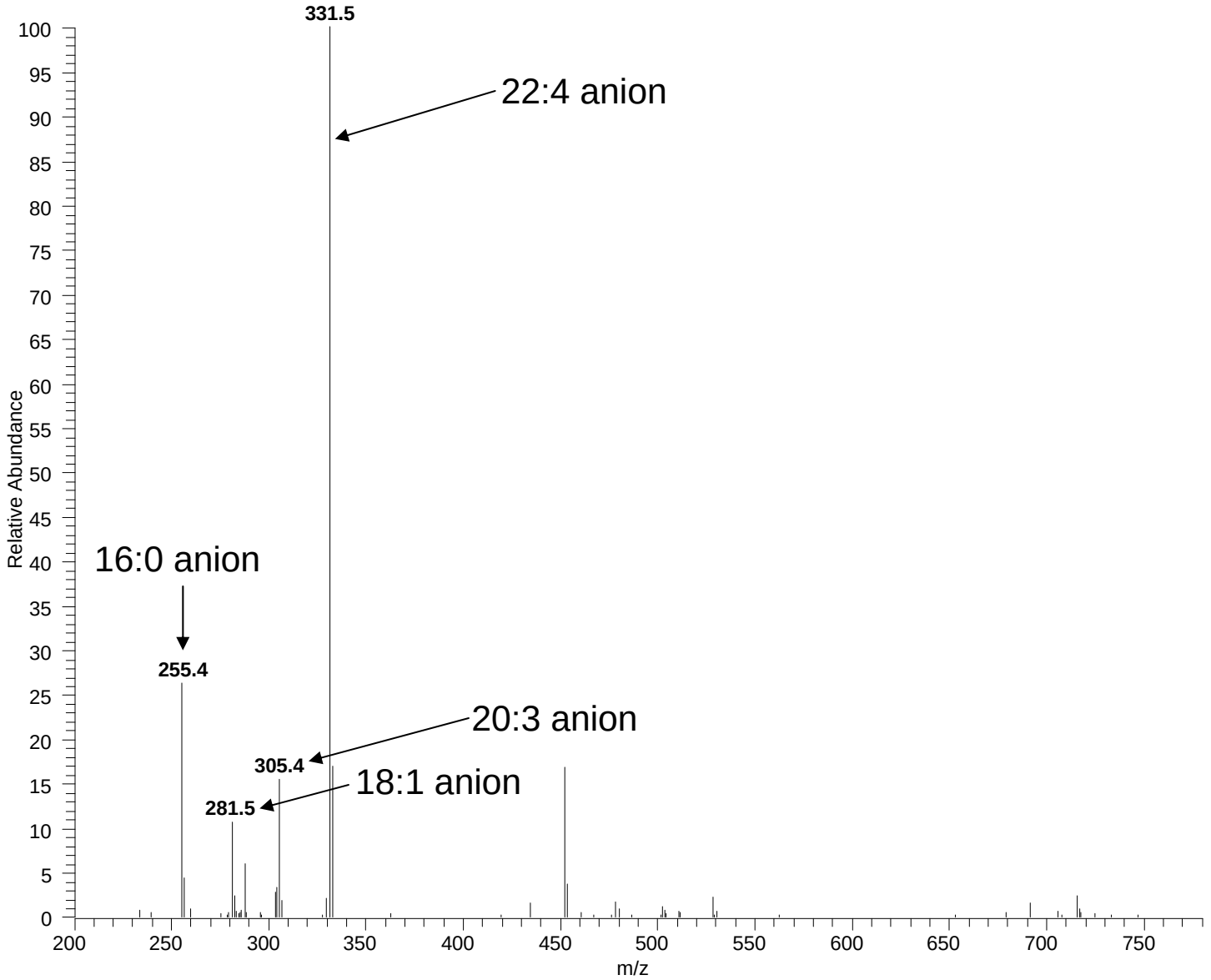

Low mass measurement accuracy MS/MS utilizing LTQ

Negative ESI: PE 16:0/18:2; $C_{39}H_{74}NO_8P$; theoretical *m/z* 714.5, $(M-H)^-$

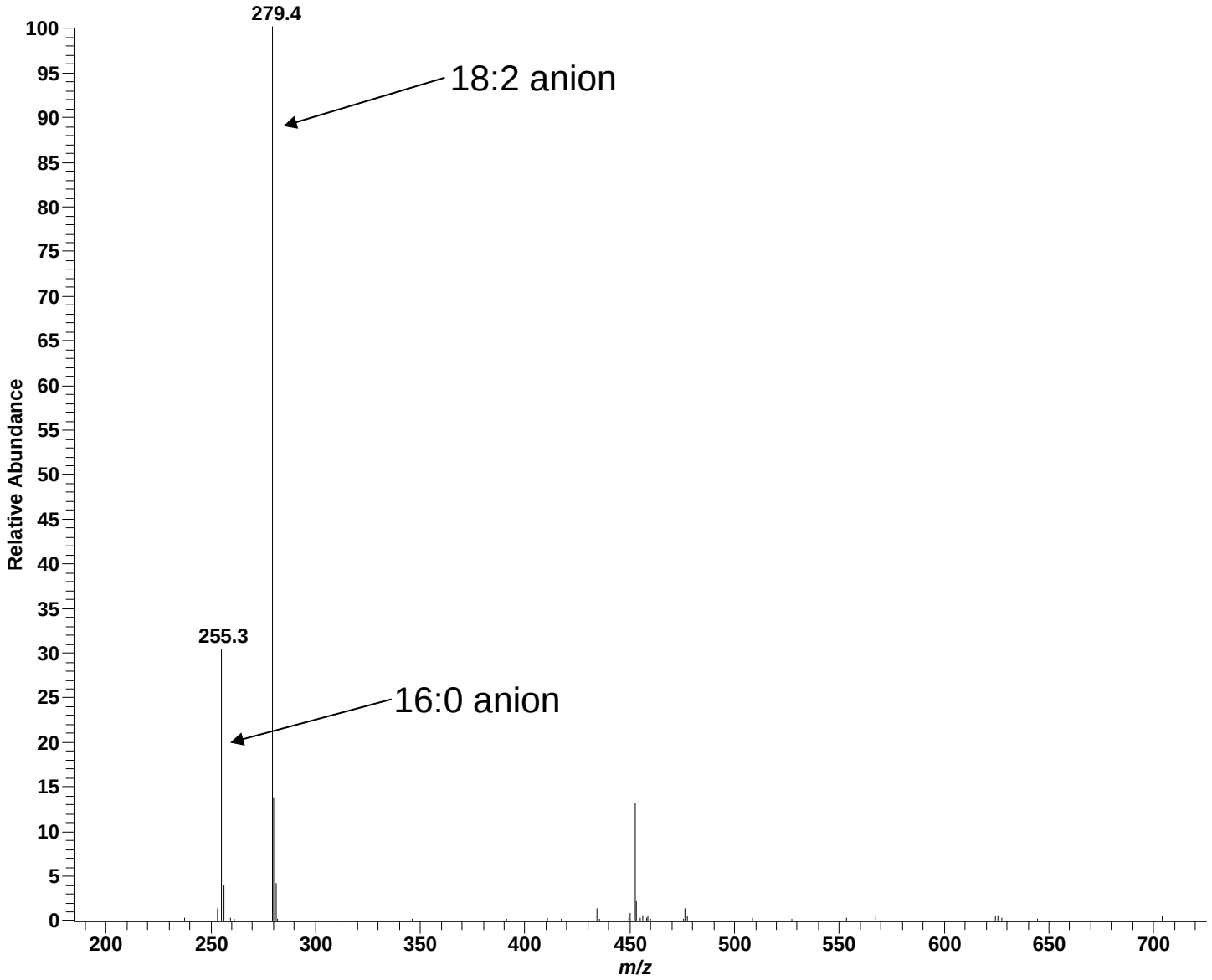

High mass measurement accuracy MS/MS utilizing LTQ-FT

Positive ESI: PE 16:0/18:1; $C_{39}H_{76}NO_8P$; theoretical *m/z* 718.5387, $(M+H)^+$

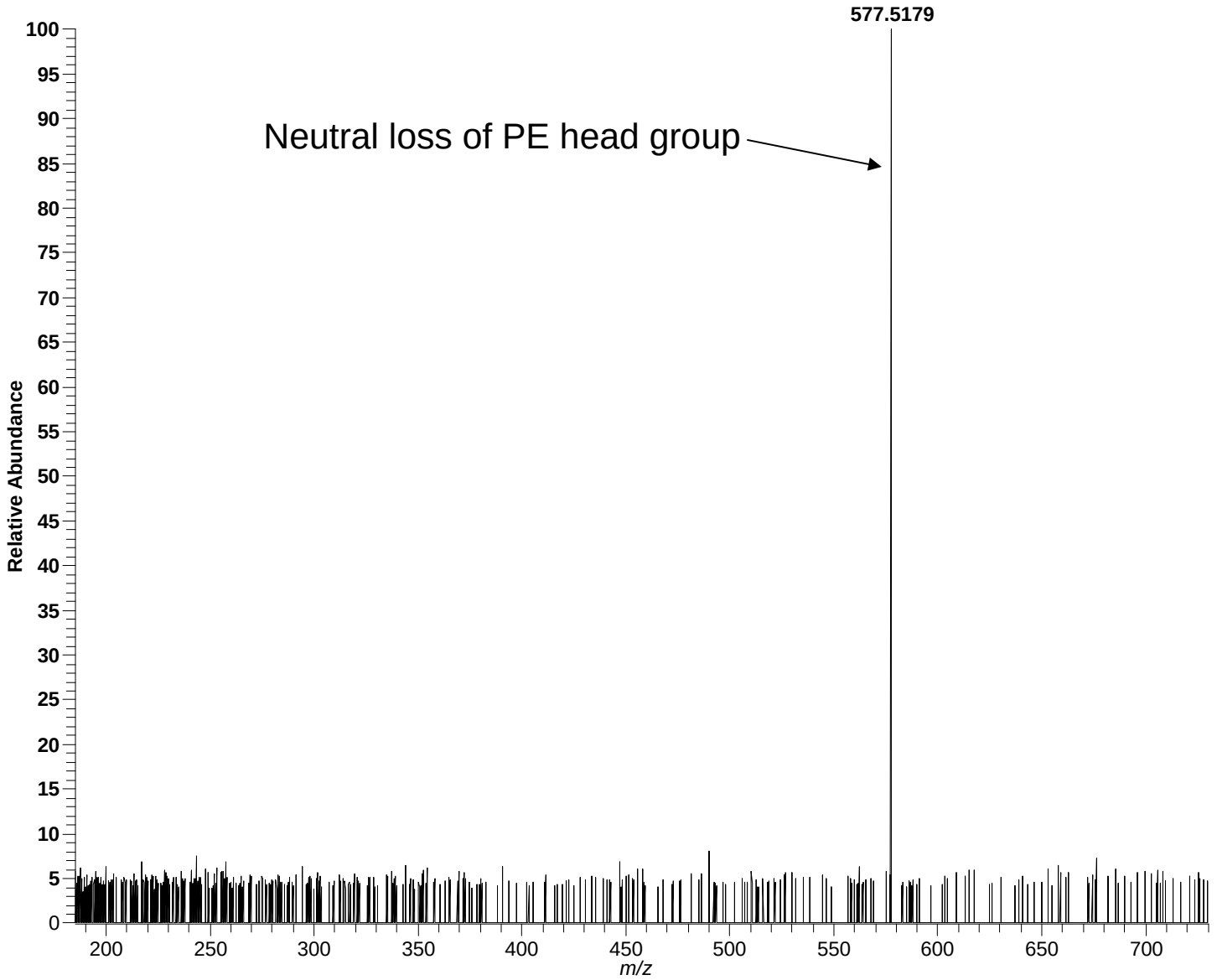

Low mass measurement accuracy MS/MS utilizing LTQ

Negative ESI: PE 16:0/18:1; $C_{39}H_{76}NO_8P$; theoretical *m/z* 716.5, $(M-H)^-$

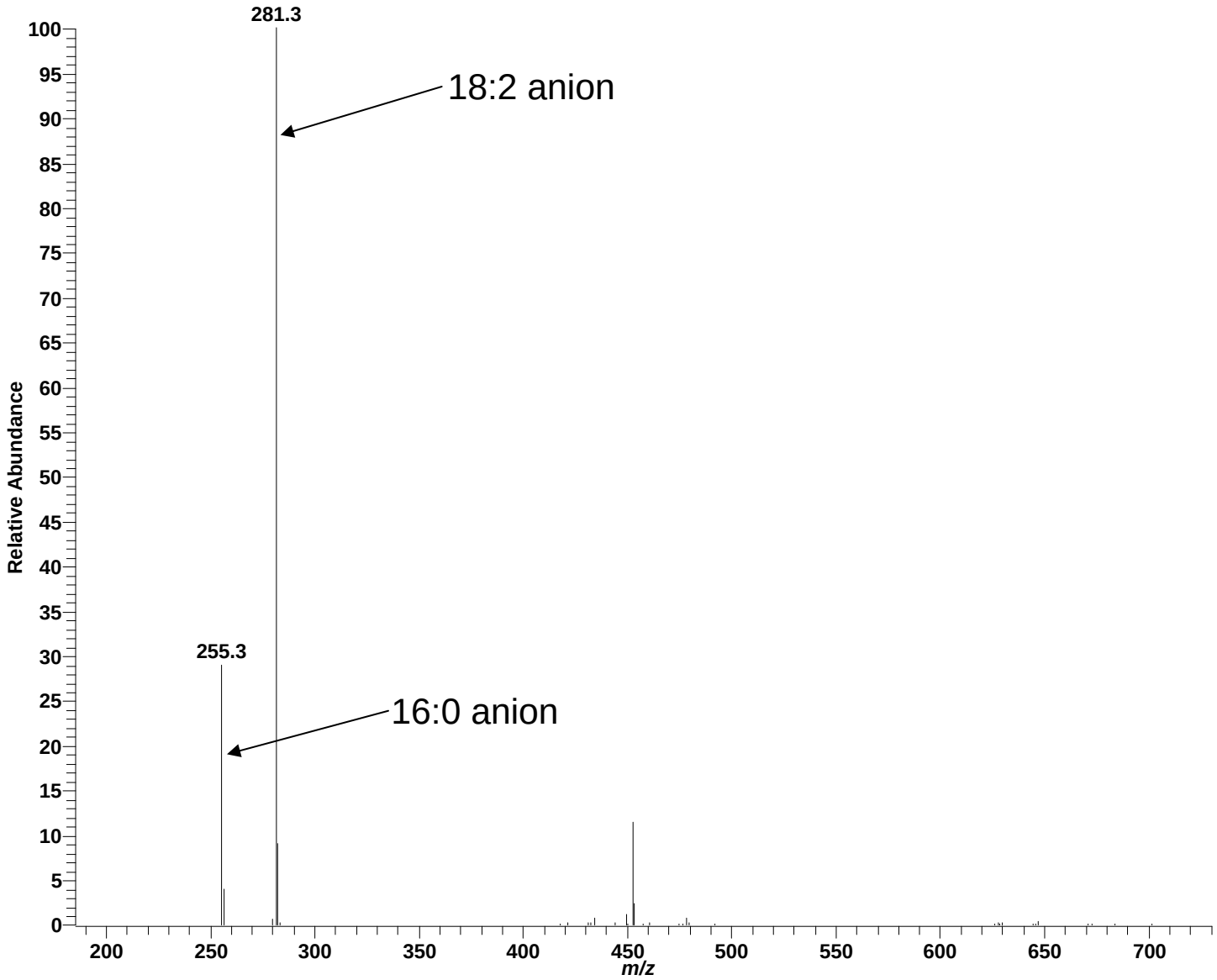

High mass measurement accuracy MS/MS utilizing LTQ-FT

Negative ESI: PE (18:0/6:0-dihydroxy); $C_{23}H_{44}NO_7P$; theoretical *m/z* 610.3720, $(M-H)^-$

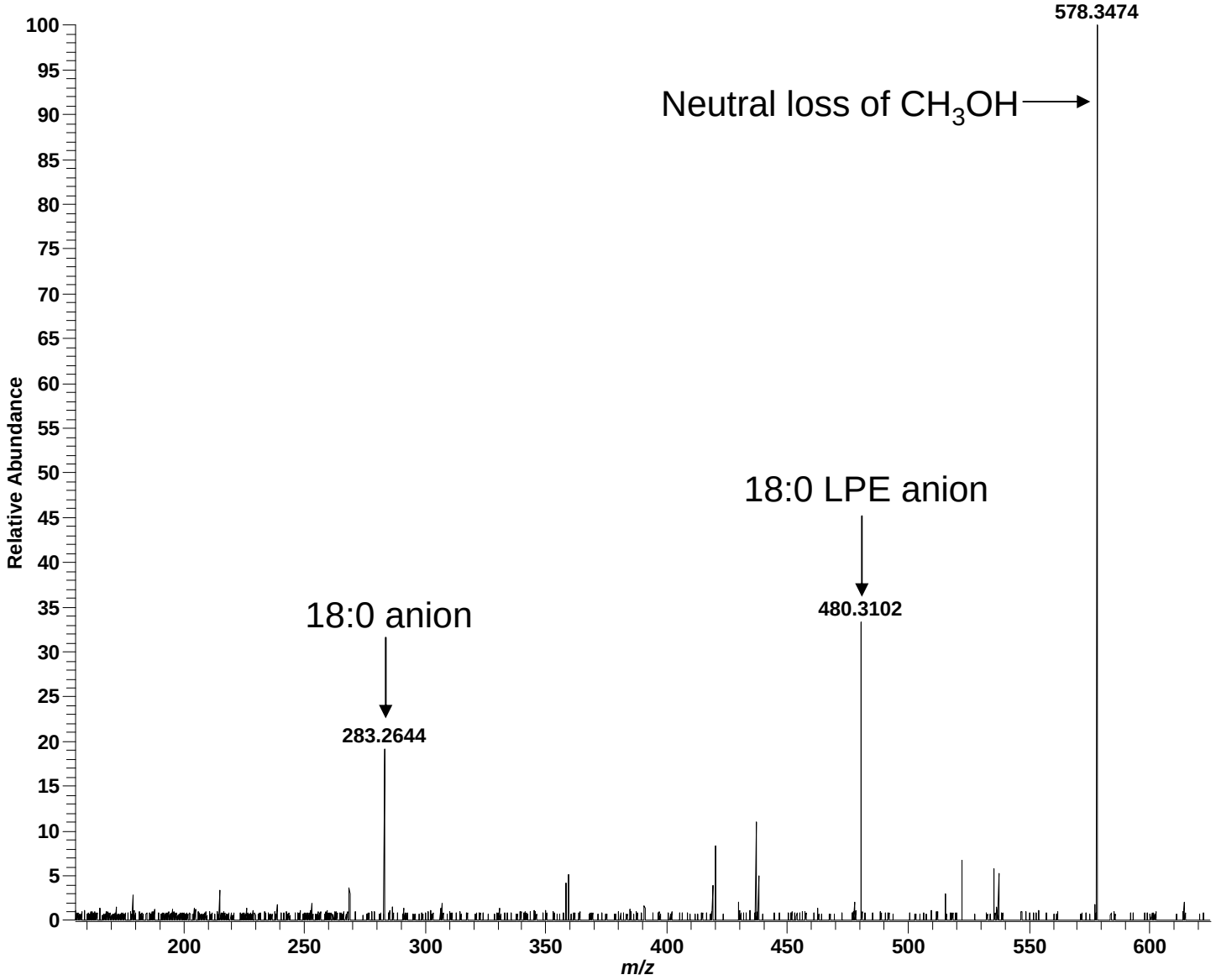

Low mass measurement accuracy MS/MS utilizing LTQ

Positive ESI: LPE (20:3); $C_{25}H_{46}NO_7P$; theoretical *m/z* 504.3, $(M+H)^+$

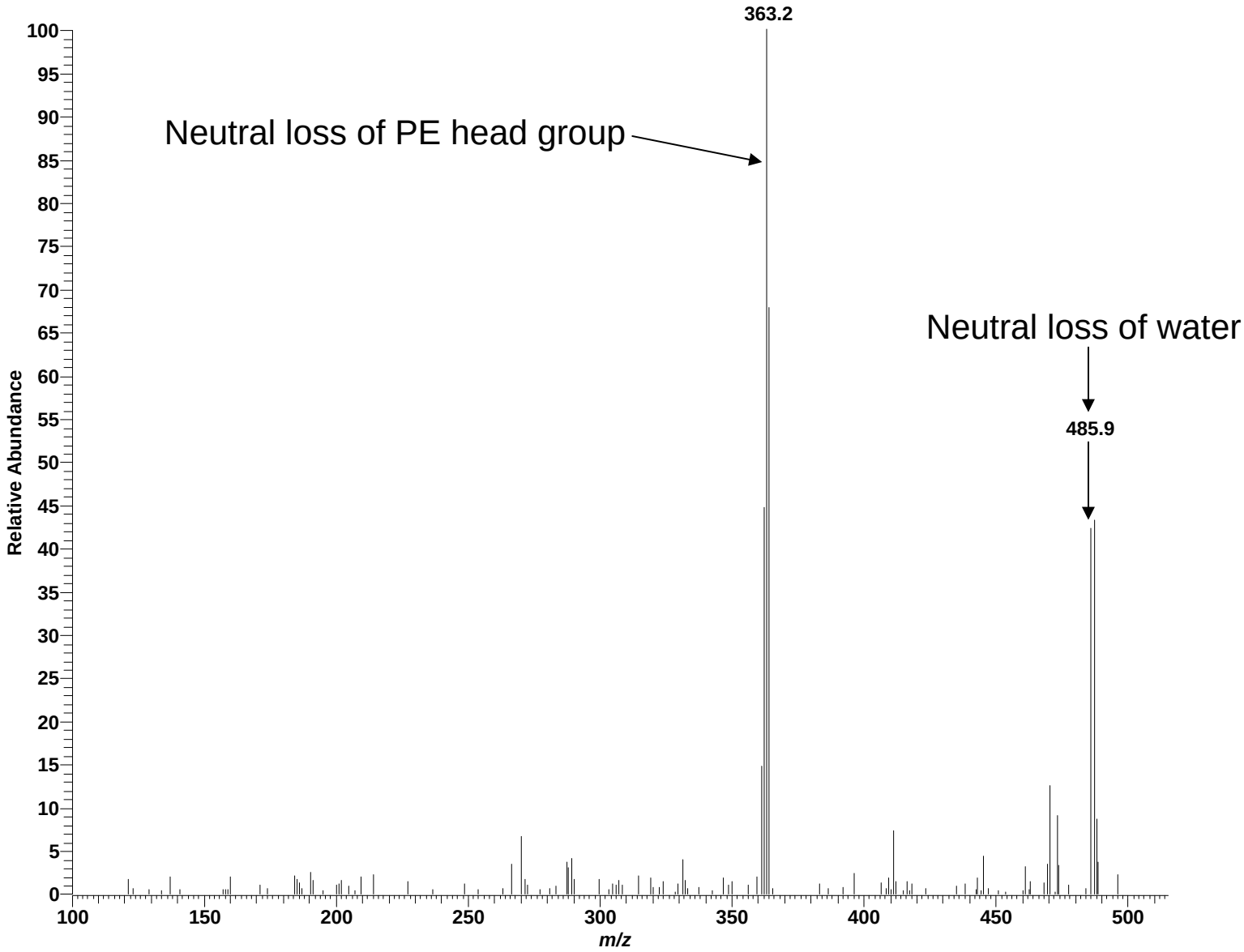

Glycerophosphocholines

Low mass measurement accuracy MS/MS utilizing LTQ

Positive ESI: LPC (15:0); $C_{23}H_{48}NO_7P$; theoretical *m/z* 482.3, $(M+H)^+$

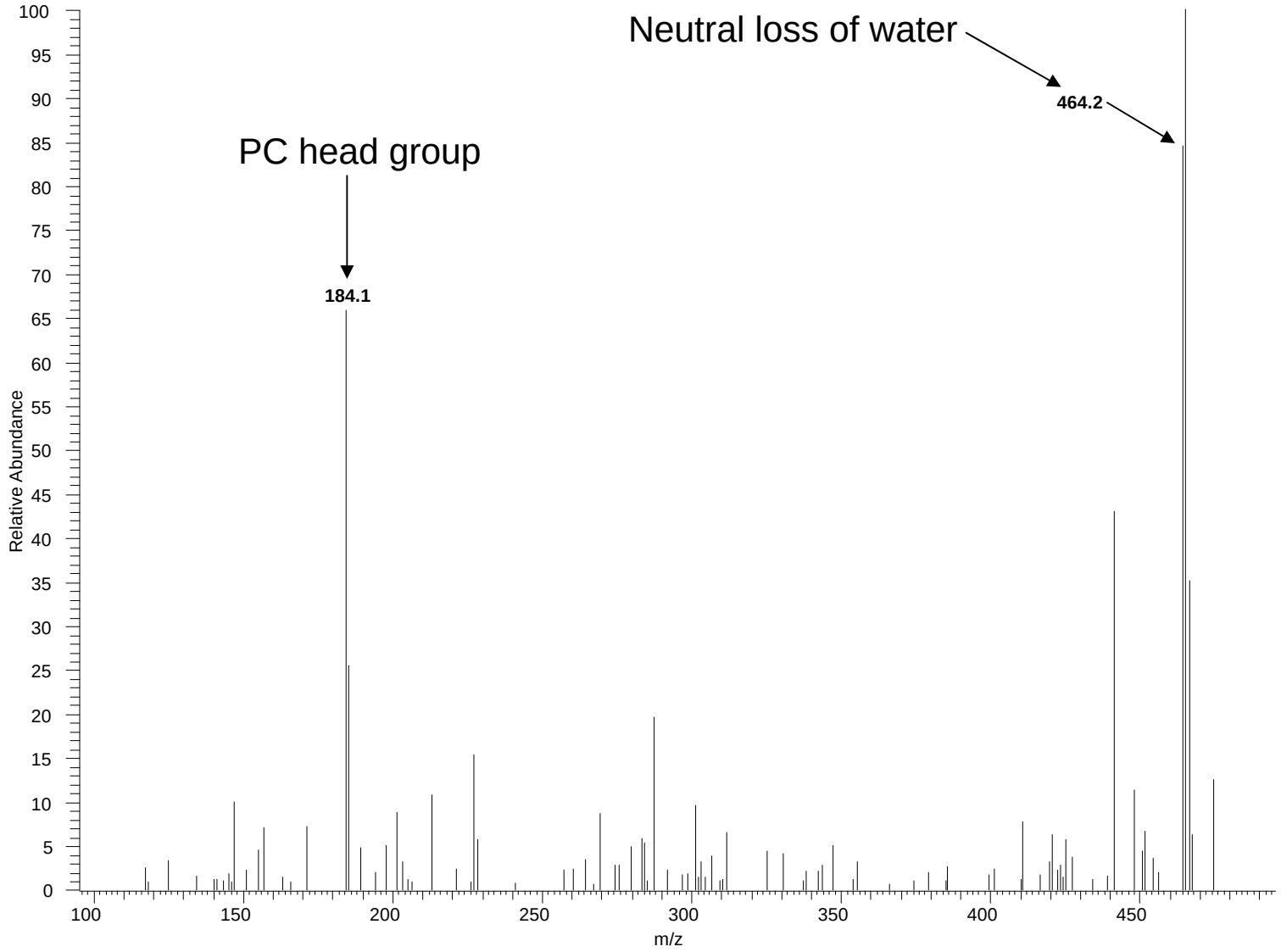

High mass measurement accuracy MS/MS utilizing LTQ-FT

Positive ESI: LPC 14:0; $C_{22}H_{46}NO_7P$; theoretical *m/z* 468.3090, $(M+H)^+$

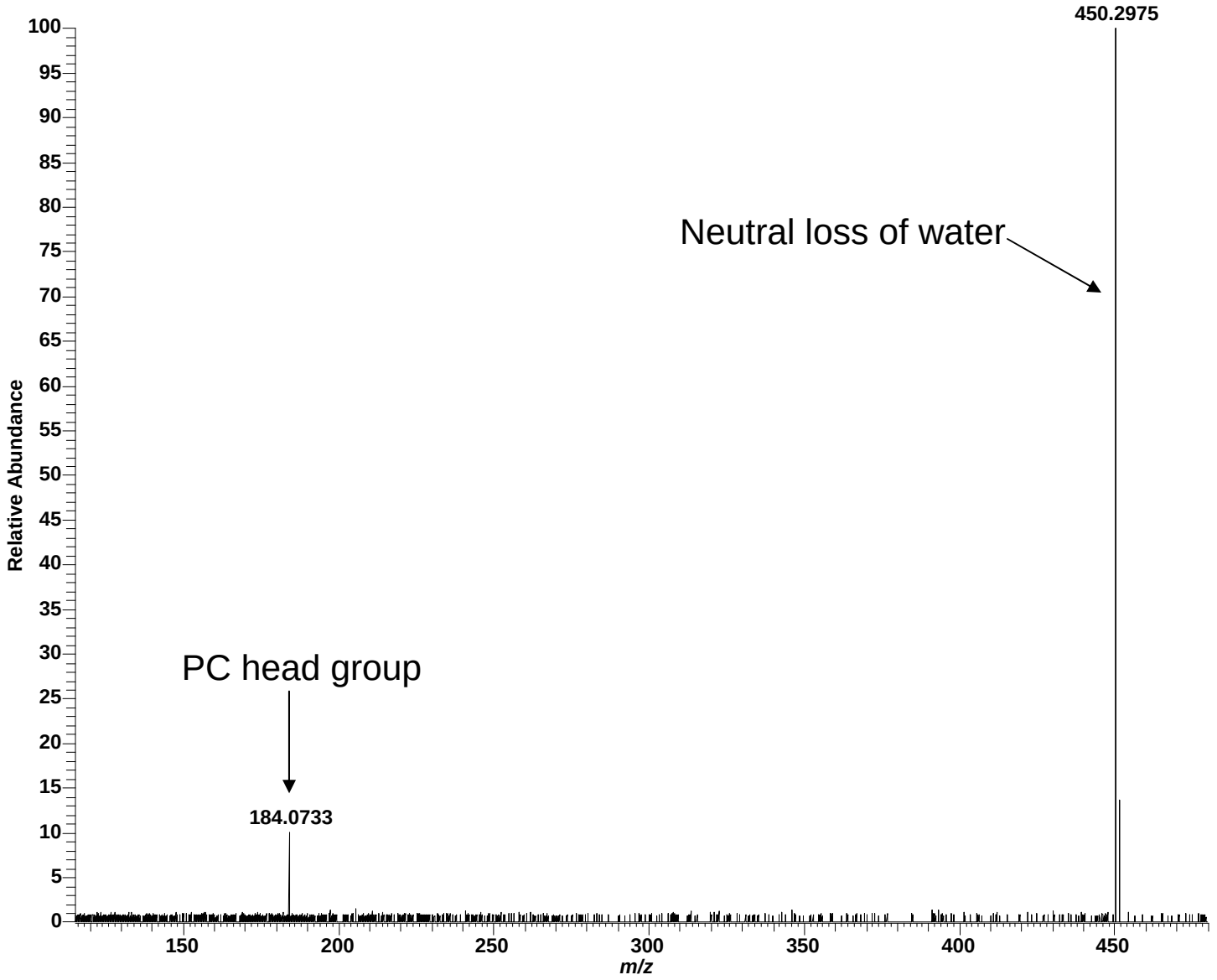

High mass measurement accuracy MS/MS utilizing LTQ-FT

Negative ESI: LPC 14:0; $C_{22}H_{46}NO_7P$; theoretical *m/z* 526.3145, $(M+CH_3COO)^-$

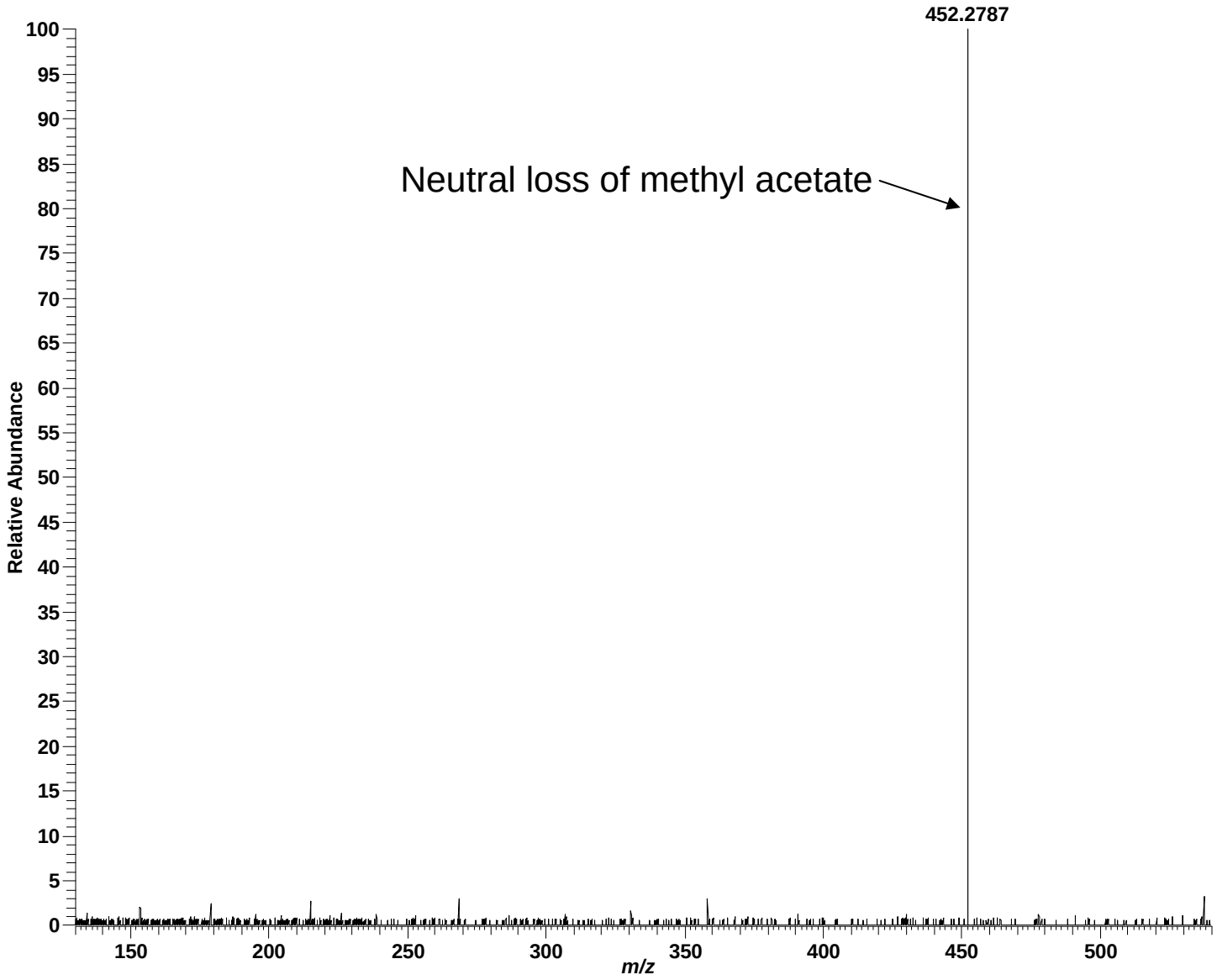

High mass measurement accuracy MS/MS utilizing LTQ-FT

Positive ESI: LPC 18:3; $C_{26}H_{48}NO_7P$; theoretical *m/z* 518.3246, $(M+H)^+$

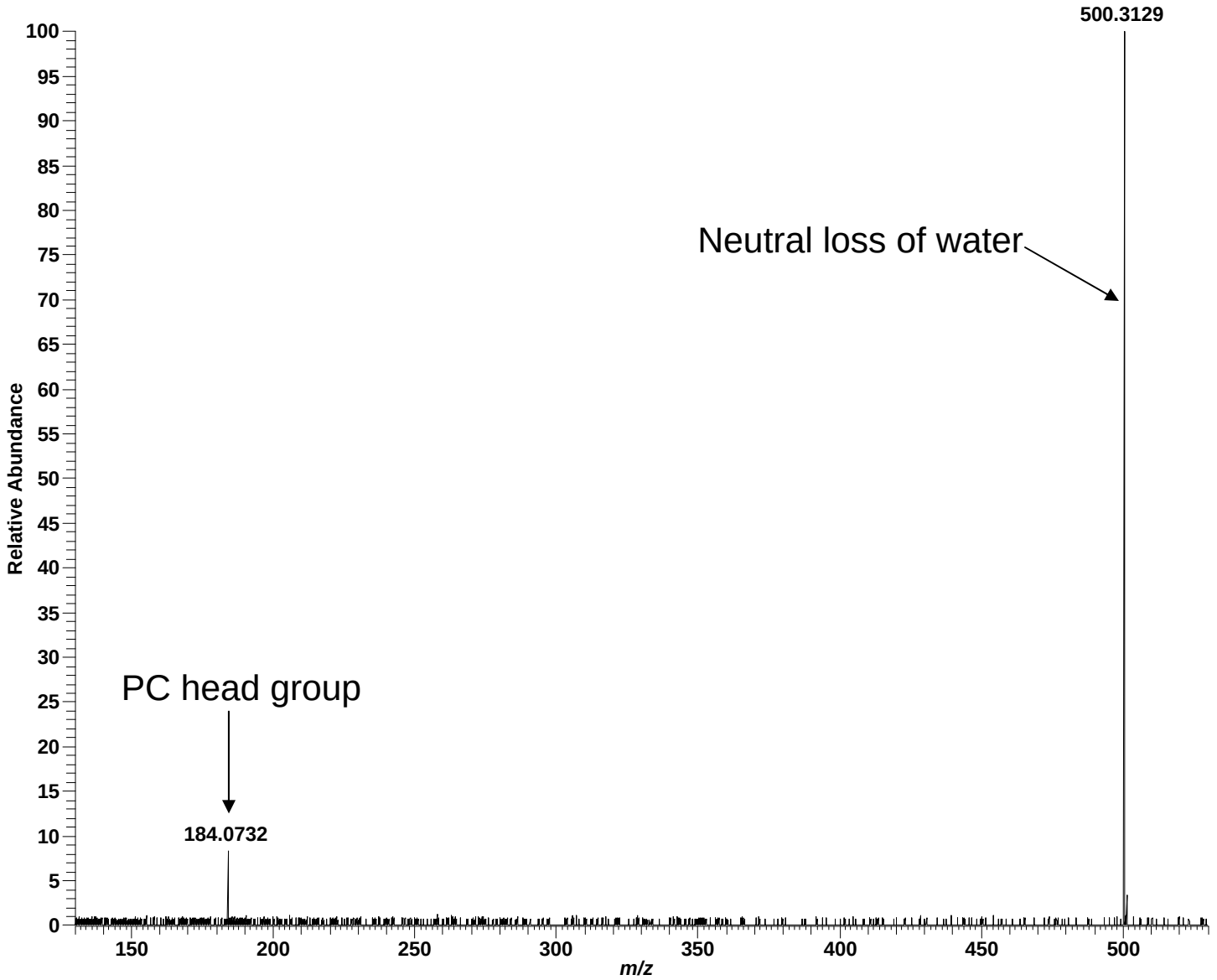

High mass measurement accuracy MS/MS utilizing LTQ-FT

Negative ESI: LPC 18:3; $C_{26}H_{48}NO_7P$; theoretical *m/z* 576.3301, $(M+CH_3COO)^-$

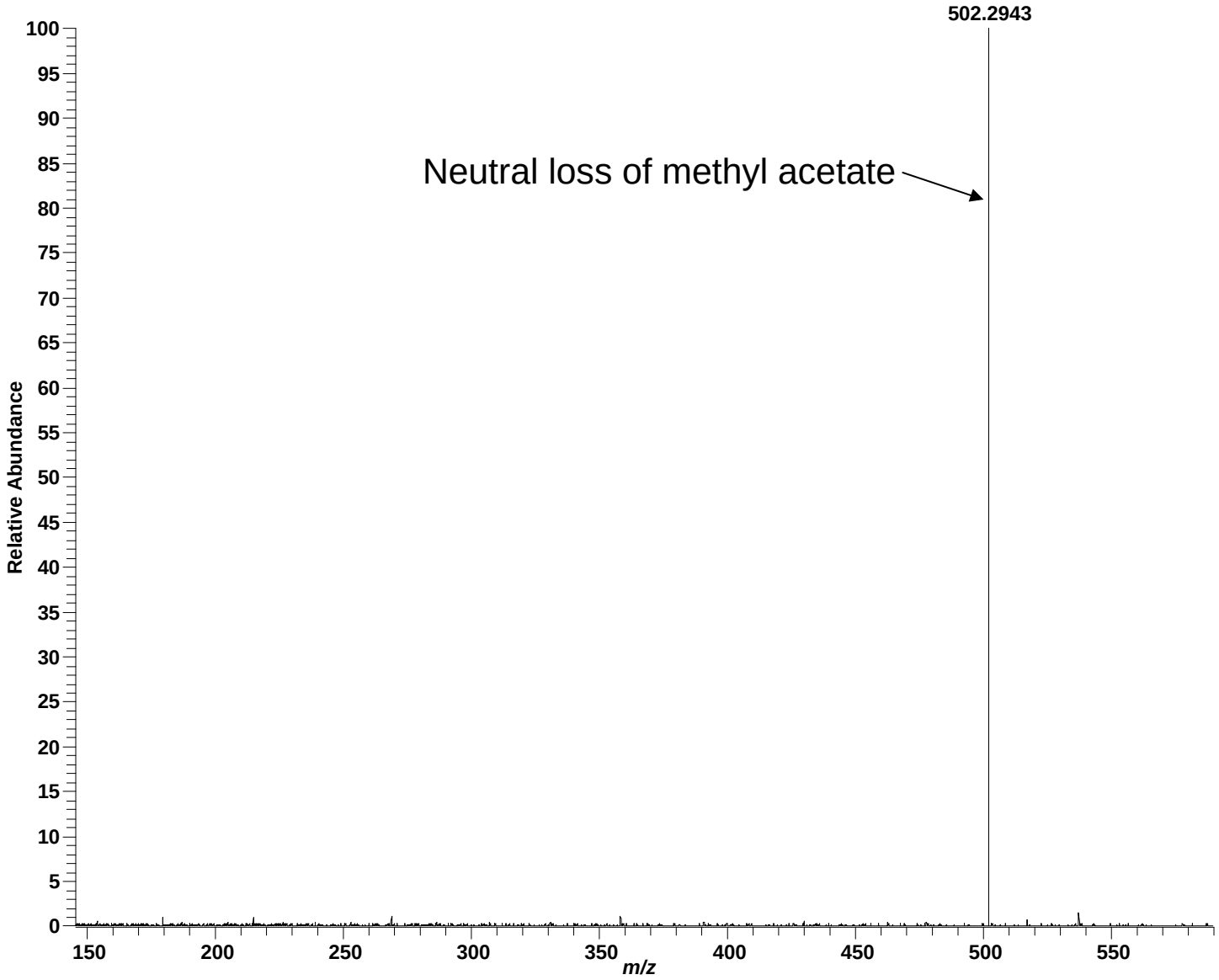

High mass measurement accuracy MS/MS utilizing LTQ-FT

Positive ESI: LPC 20:5; $C_{28}H_{48}NO_7P$; theoretical *m/z* 542.3246, $(M+H)^+$

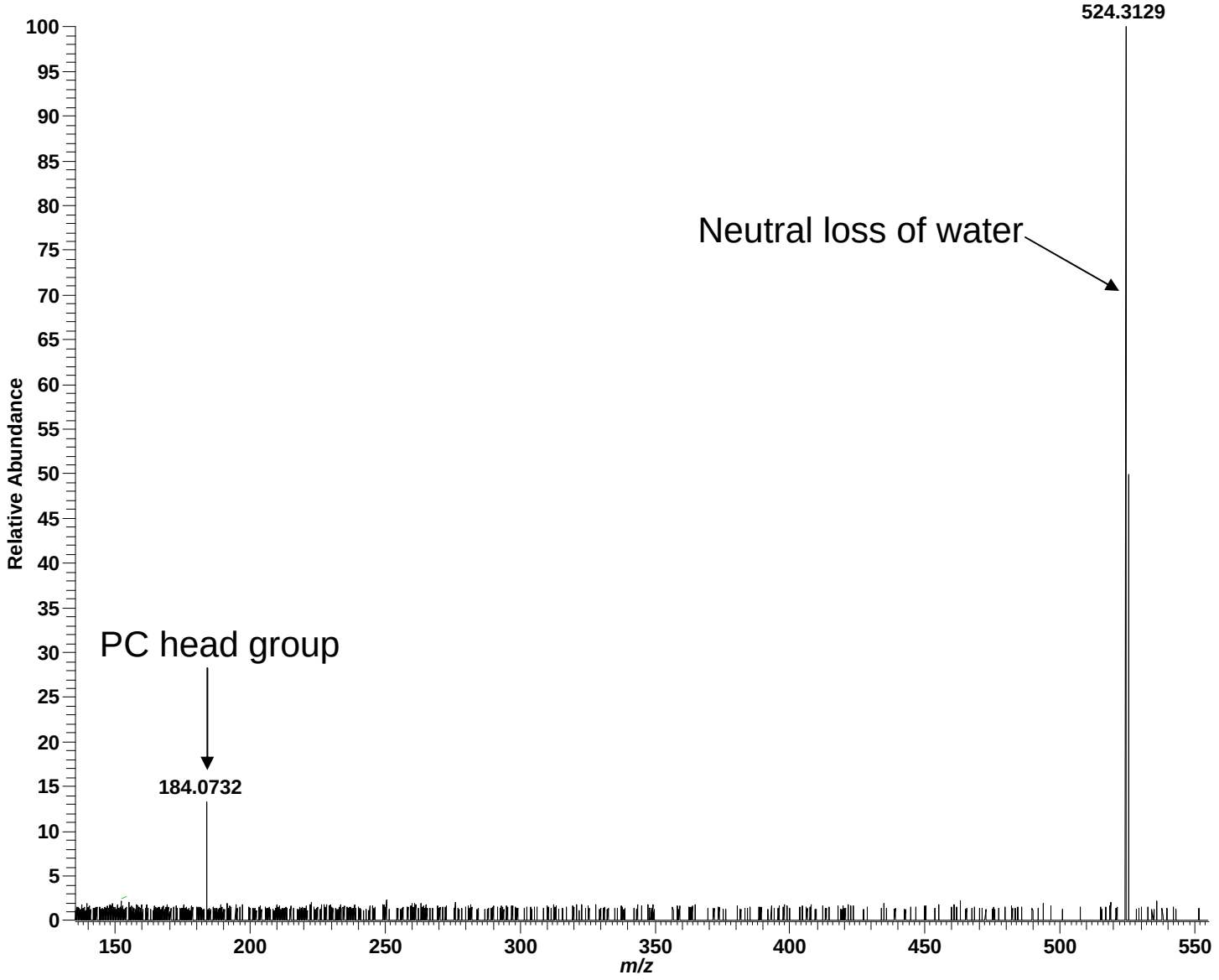

High mass measurement accuracy MS/MS utilizing LTQ-FT

Negative ESI: LPC 20:5; $C_{28}H_{48}NO_7P$; theoretical *m/z* 600.3301, $(M+CH_3COO)^-$

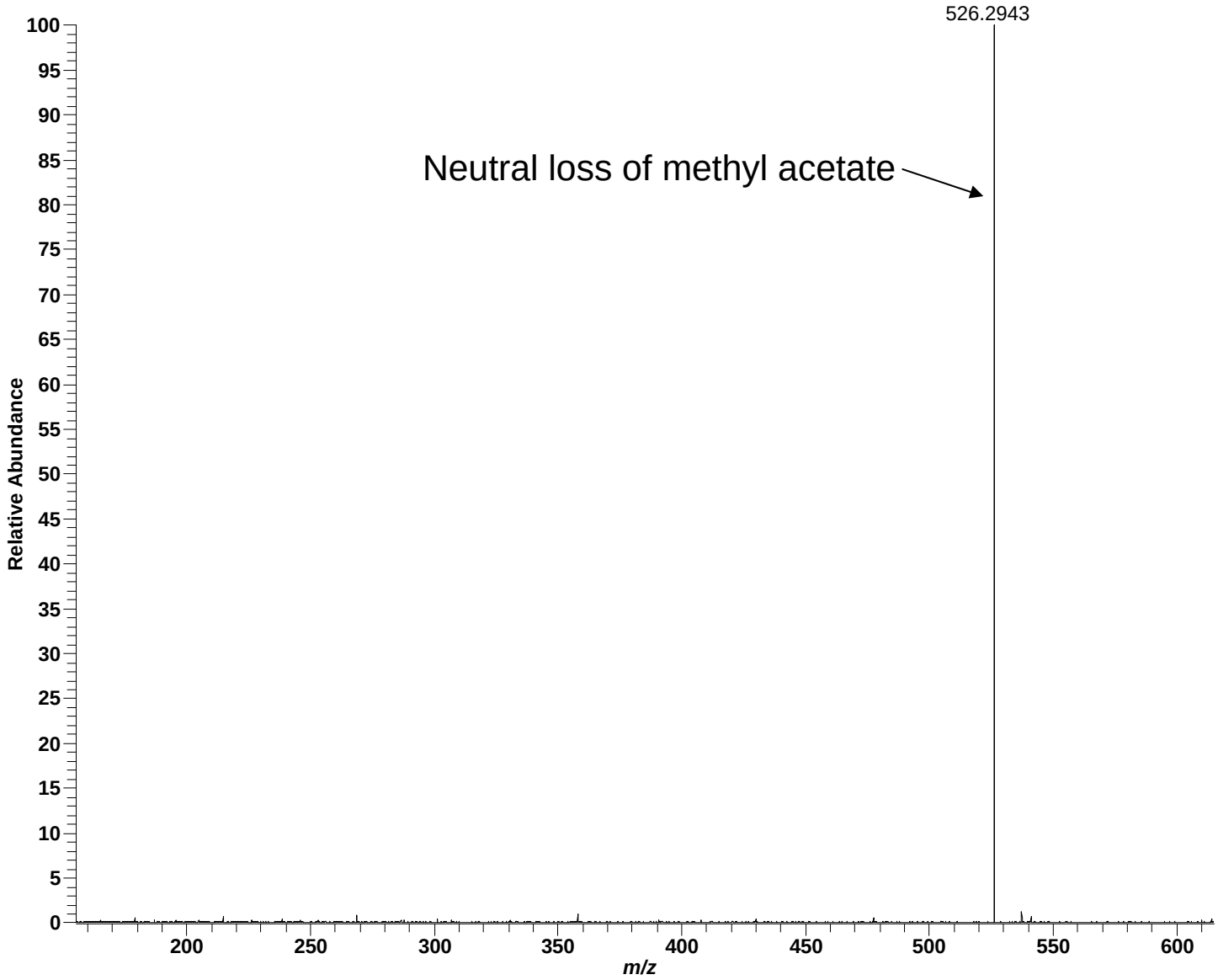

High mass measurement accuracy MS/MS utilizing LTQ-FT

Positive ESI: LPC 16:1; $C_{24}H_{48}NO_7P$; theoretical *m/z* 494.3247, $(M+H)^+$

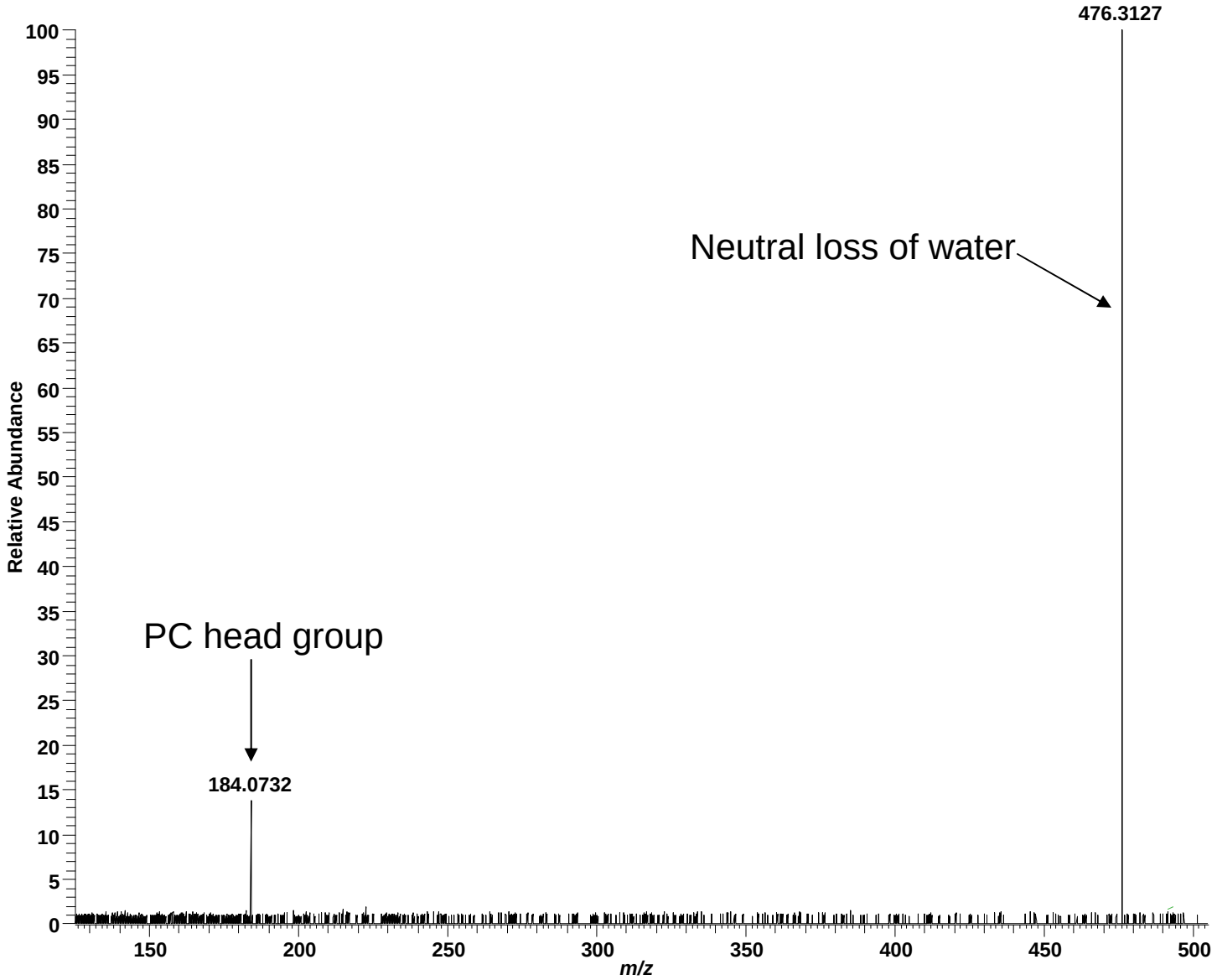

High mass measurement accuracy MS/MS utilizing LTQ-FT

Negative ESI: LPC 16:1; $C_{24}H_{48}NO_7P$; theoretical *m/z* 552.3301, $(M+CH_3COO)^-$

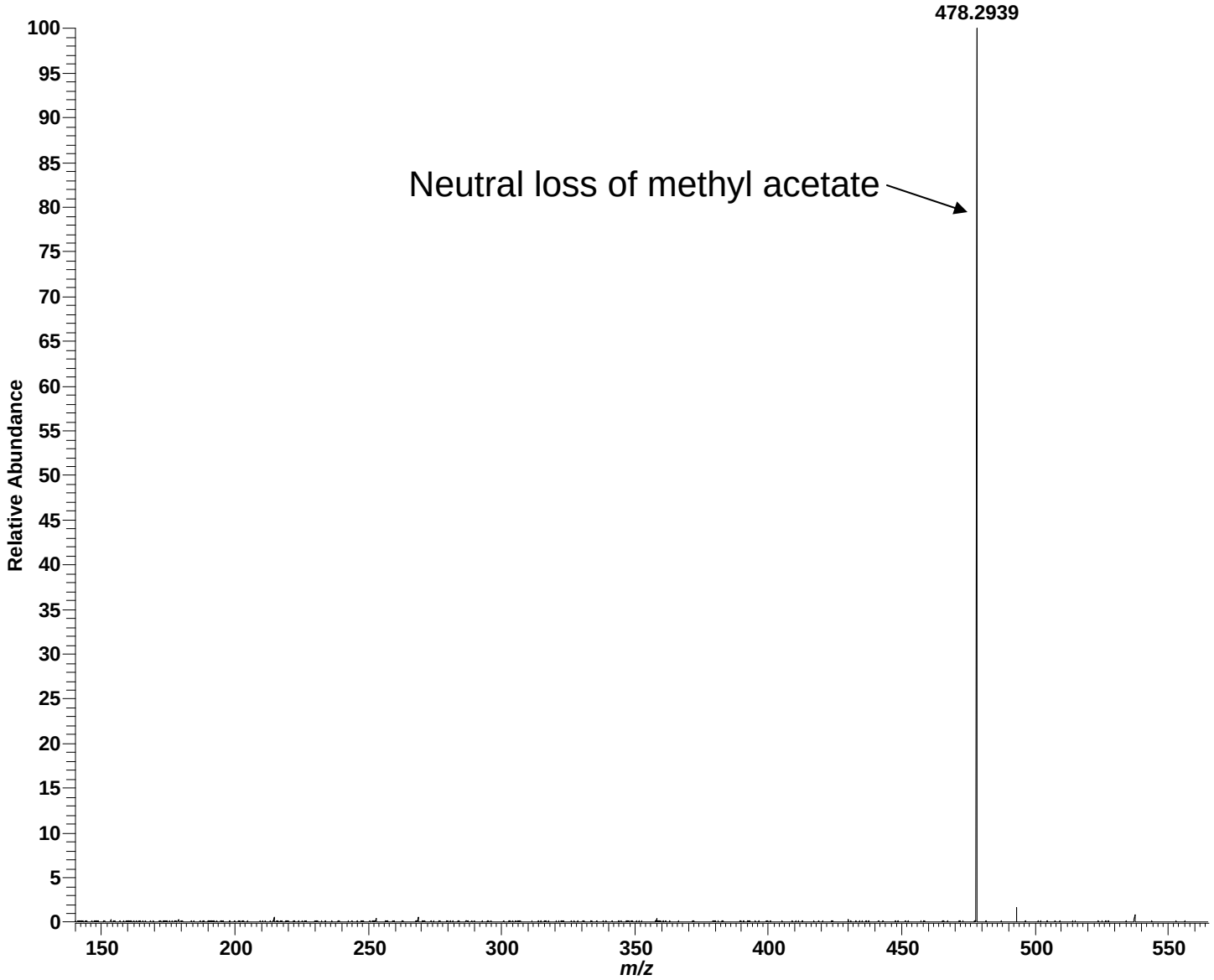

High mass measurement accuracy MS/MS utilizing LTQ-FT

Positive ESI: LPC 18:2; $C_{26}H_{50}NO_7P$; theoretical *m/z* 520.3403, $(M+H)^+$

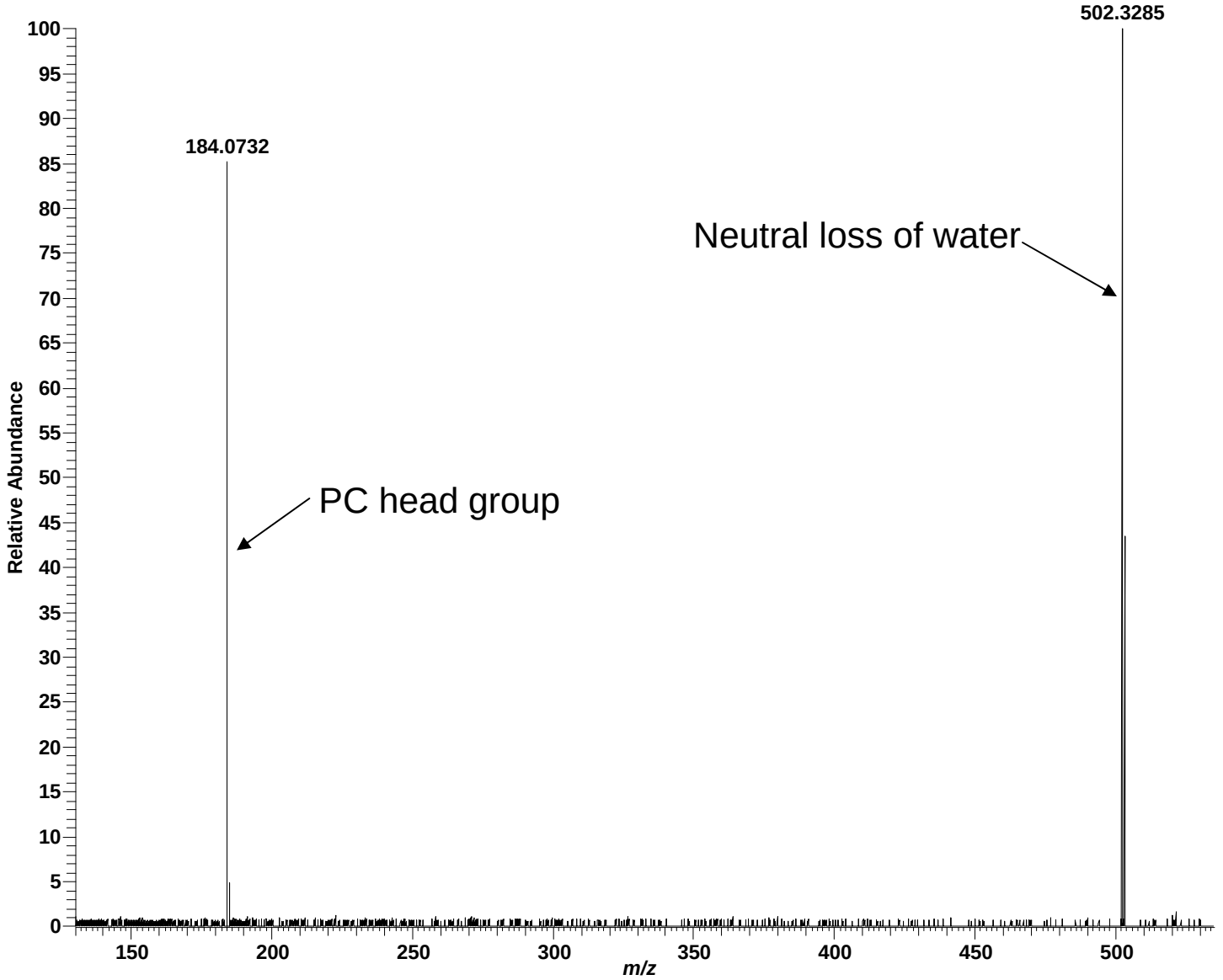

High mass measurement accuracy MS/MS utilizing LTQ-FT

Negative ESI: LPC 18:2; $C_{26}H_{50}NO_7P$; theoretical *m/z* 578.3458, $(M+CH_3COO)^-$

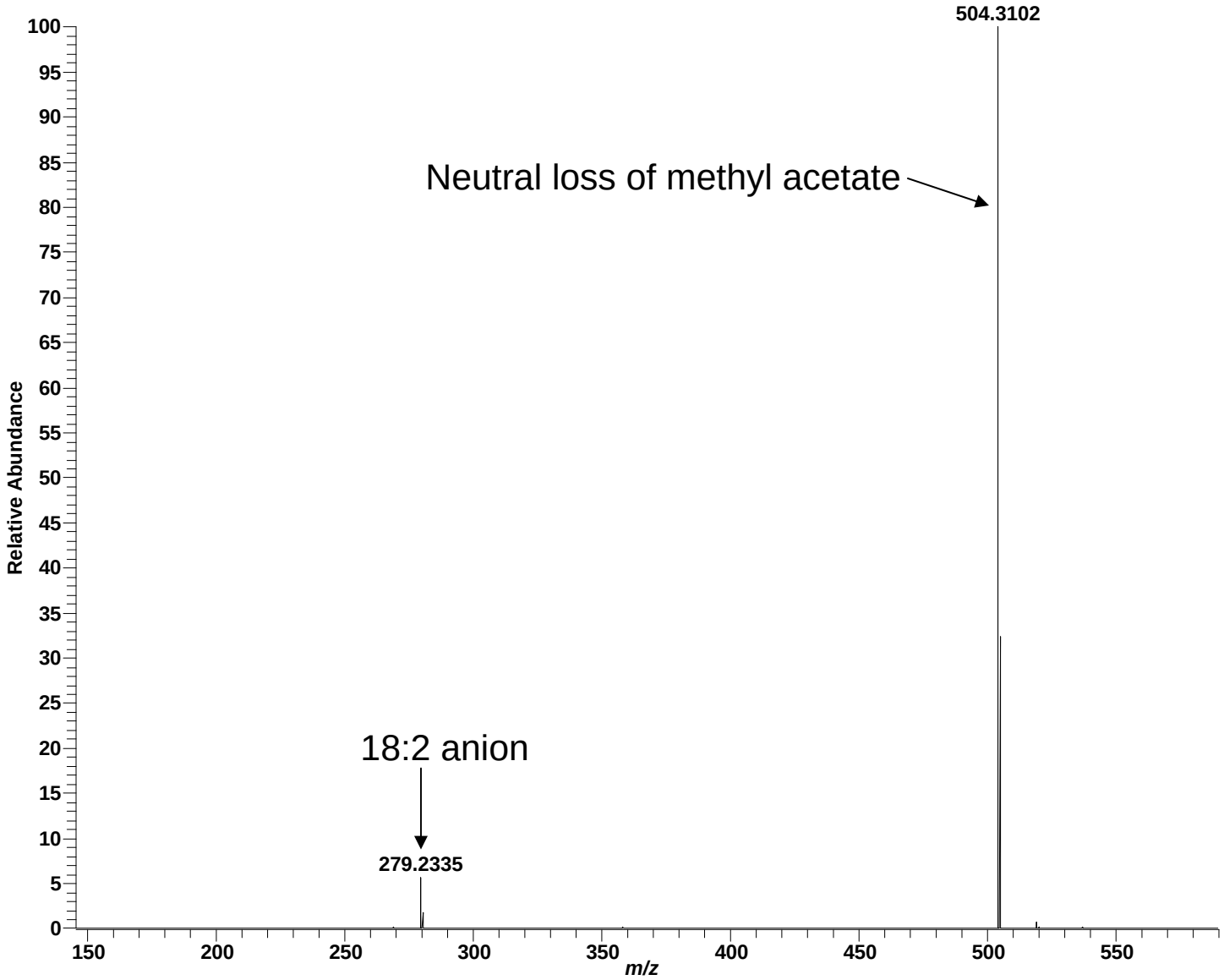

High mass measurement accuracy MS/MS utilizing LTQ-FT

Positive ESI: LPC 20:4; $C_{28}H_{50}NO_7P$; theoretical *m/z* 544.3403, $(M+H)^+$

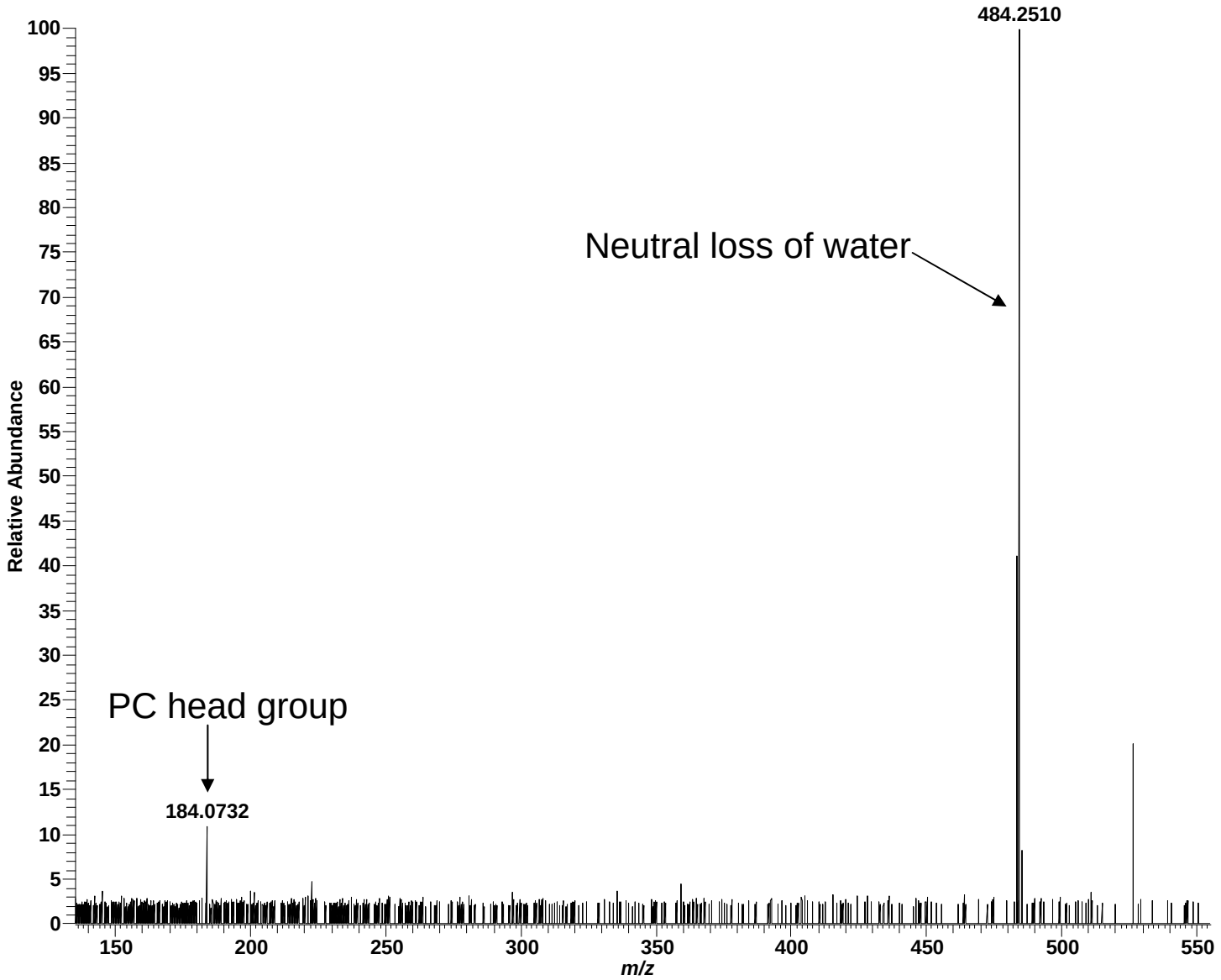

High mass measurement accuracy MS/MS utilizing LTQ-FT

Negative ESI: LPC 20:4; $C_{28}H_{50}NO_7P$; theoretical *m/z* 602.3458, $(M+CH_3COO)^-$

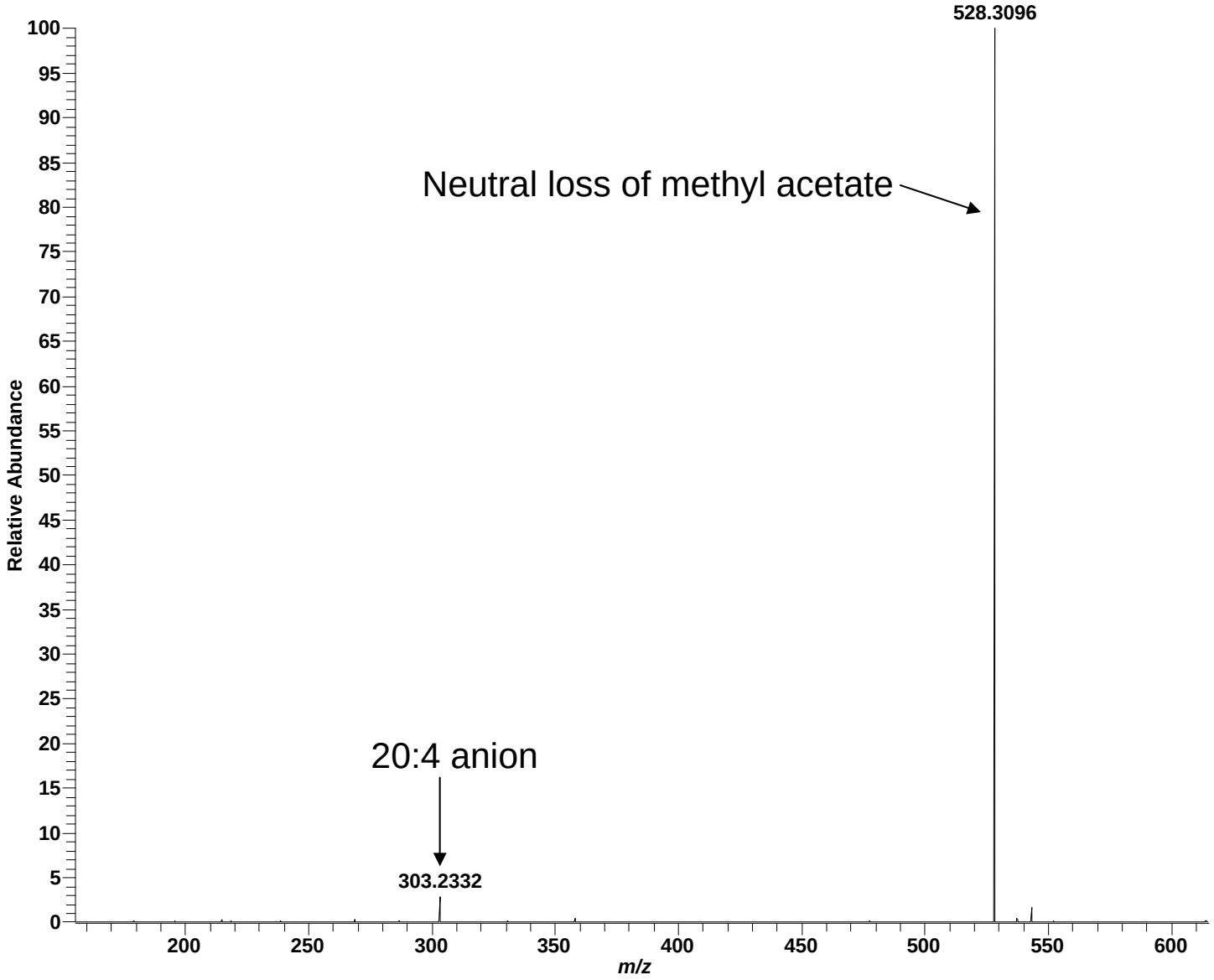

High mass measurement accuracy MS/MS utilizing LTQ-FT

Positive ESI: LPC 22:6; $C_{30}H_{50}NO_7P$; theoretical *m/z* 568.3403, $(M+H)^+$

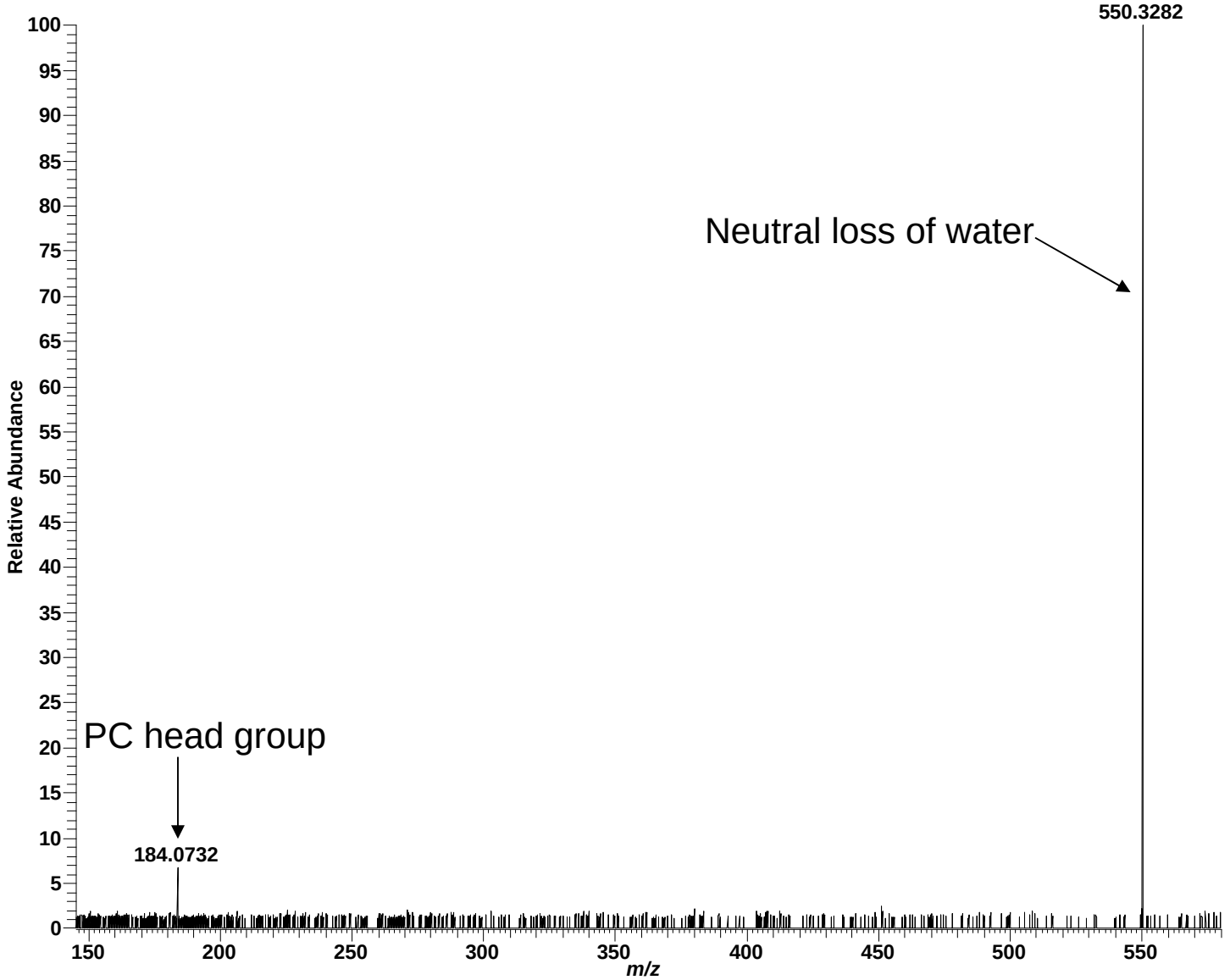

High mass measurement accuracy MS/MS utilizing LTQ-FT

Negative ESI: LPC 22:6; $C_{30}H_{50}NO_7P$; theoretical *m/z* 626.3458, $(M+CH_3COO)^-$

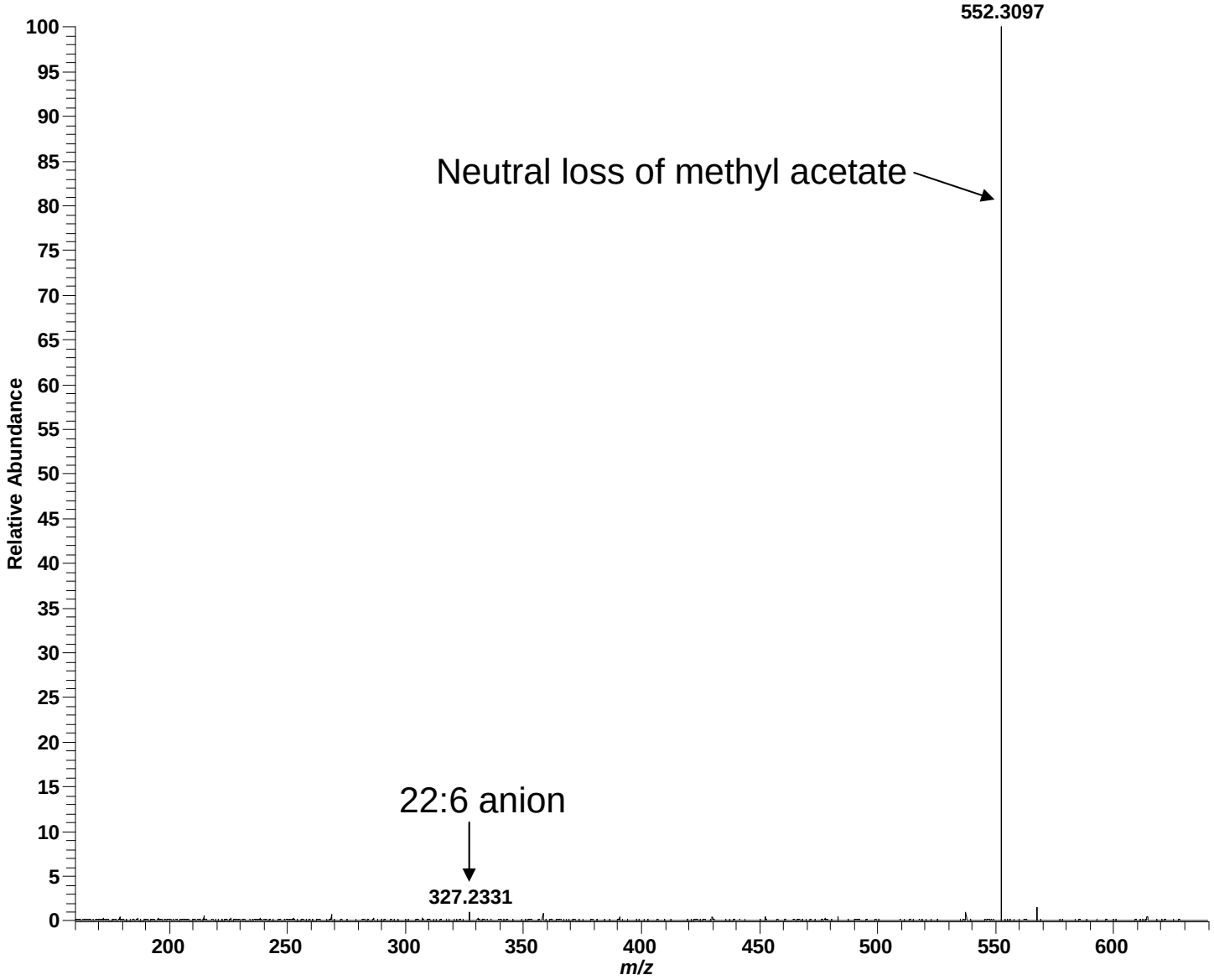

High mass measurement accuracy MS/MS utilizing LTQ-FT

Positive ESI: LPC 16:0; $C_{24}H_{50}NO_7P$; theoretical *m/z* 496.3403, $(M+H)^+$

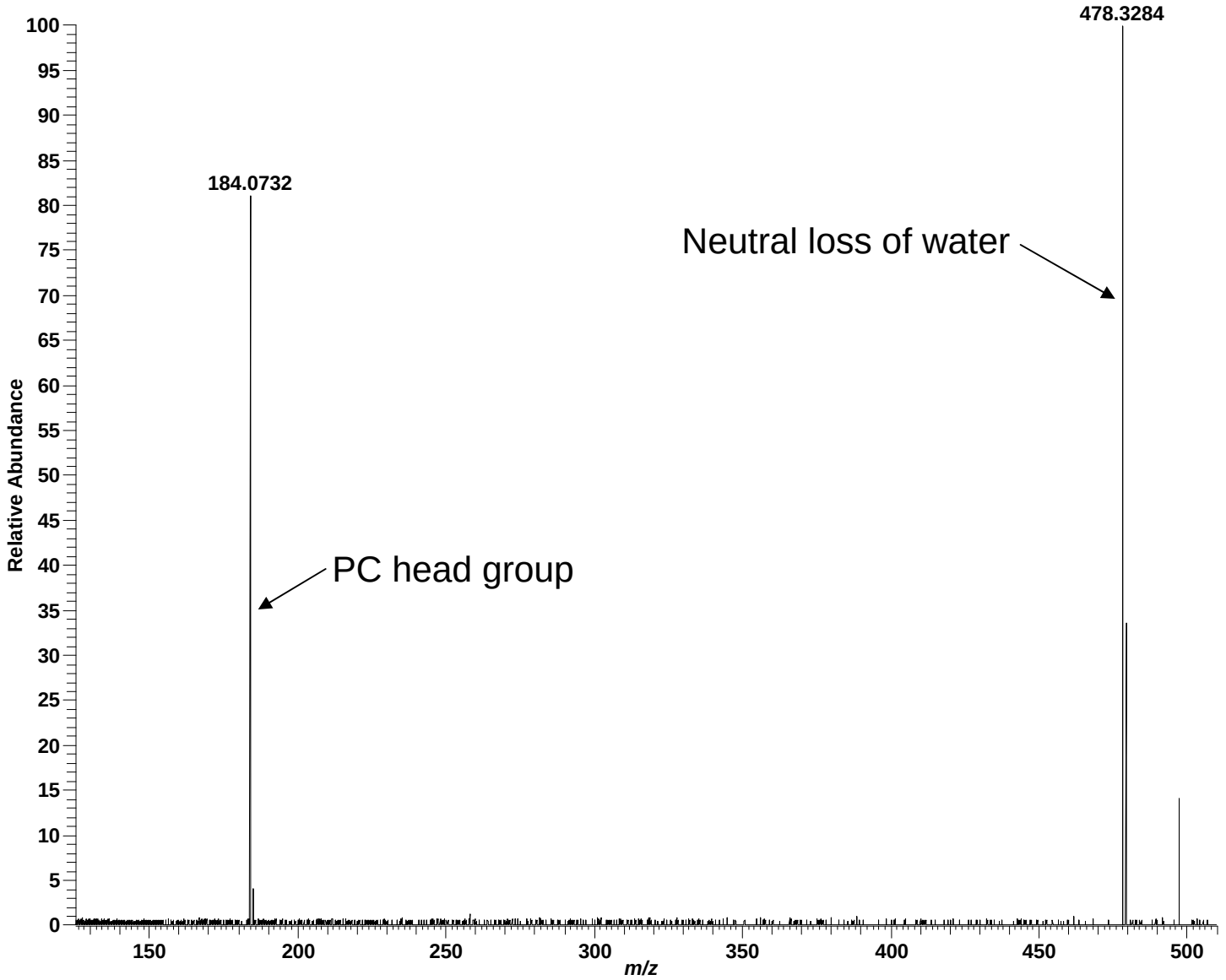

High mass measurement accuracy MS/MS utilizing LTQ-FT

Negative ESI: LPC 16:0; $C_{30}H_{50}NO_7P$; theoretical *m/z* 554.3458, $(M+CH_3COO)^-$

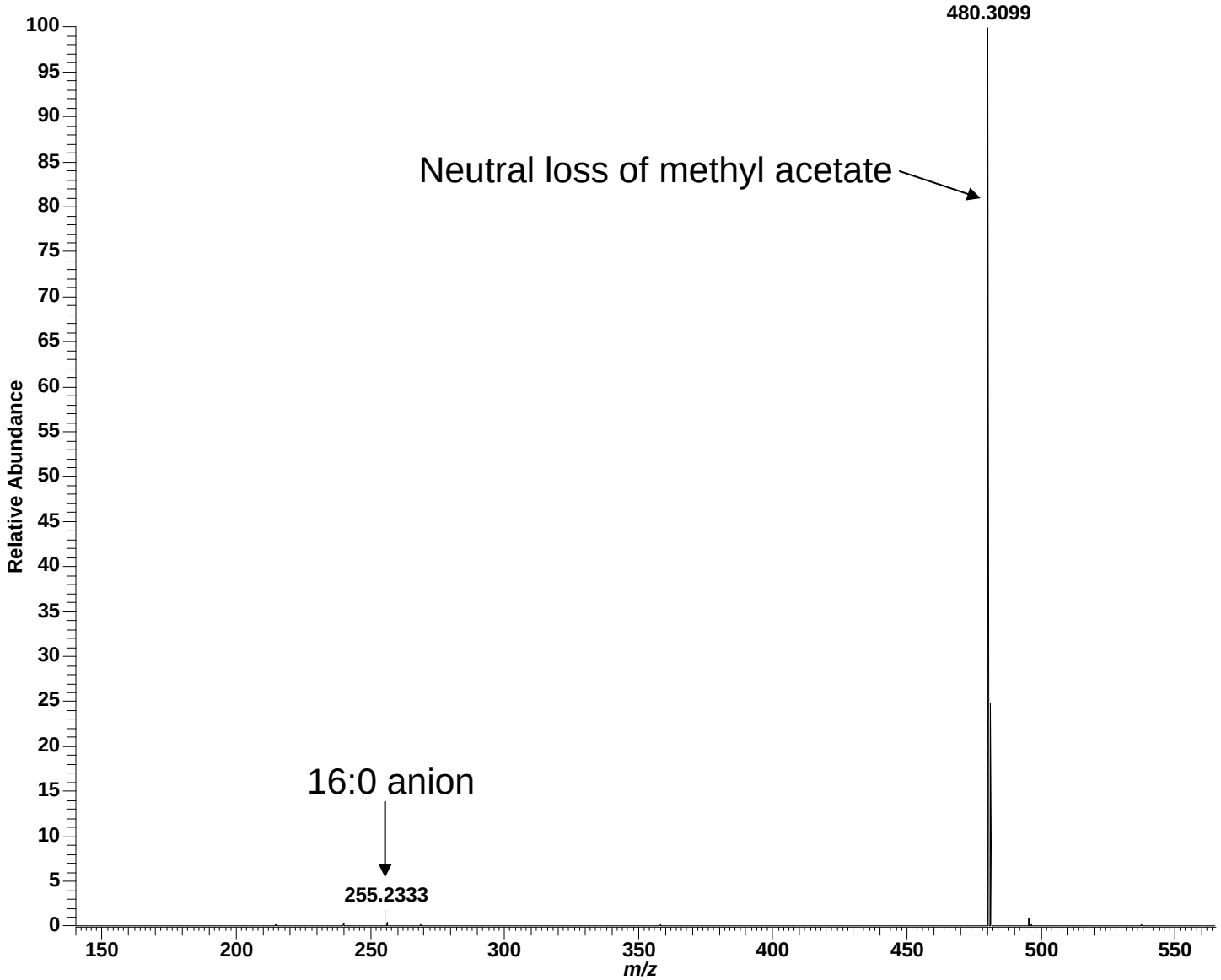

High mass measurement accuracy MS/MS utilizing LTQ-FT

Positive ESI: LPC 20:3; $C_{28}H_{52}NO_7P$; theoretical *m/z* 546.3559, $(M+H)^+$

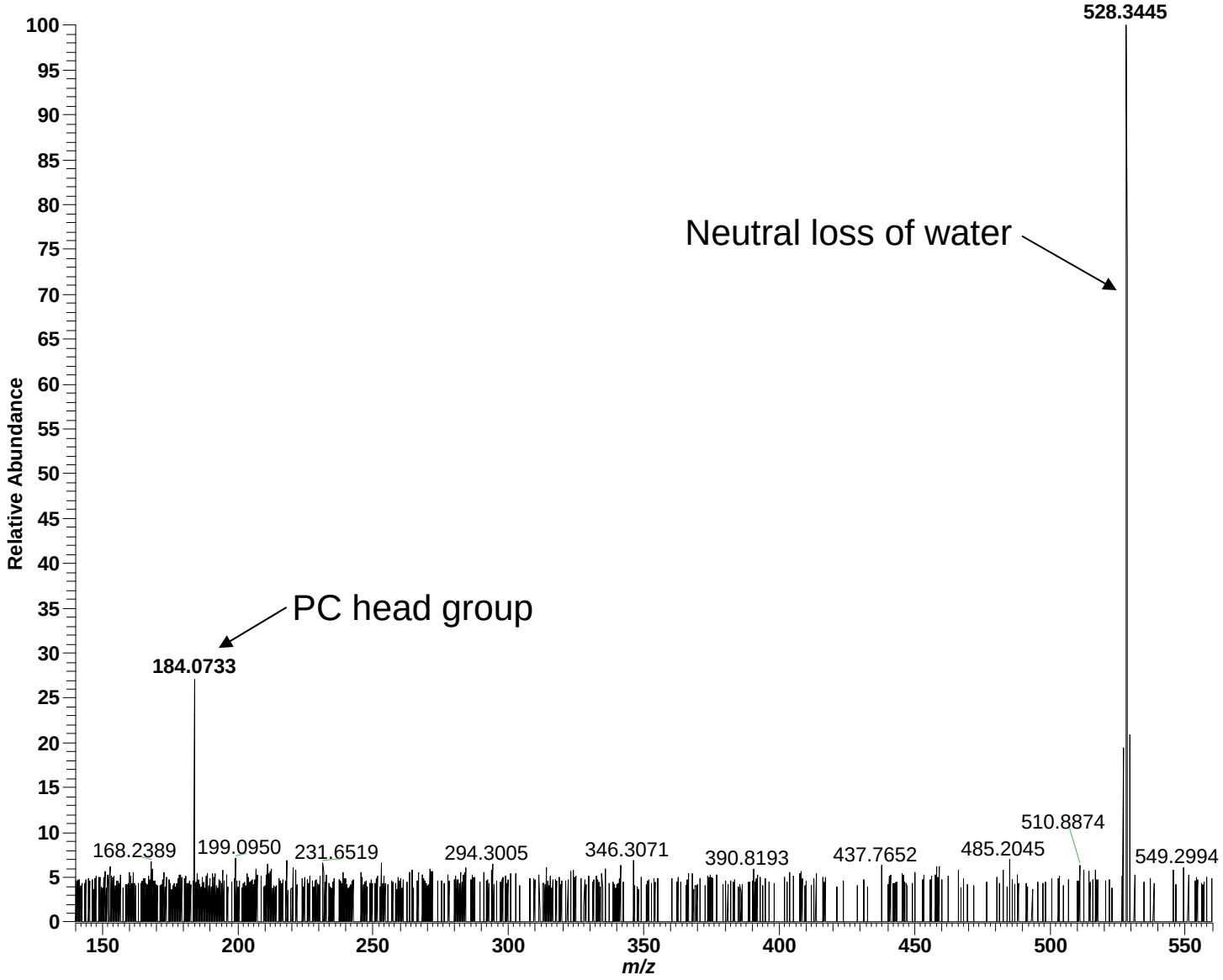

High mass measurement accuracy MS/MS utilizing LTQ-FT

Negative ESI: LPC 20:3; $C_{28}H_{52}NO_7P$; theoretical *m/z* 604.3614, $(M+CH_3COO)^-$

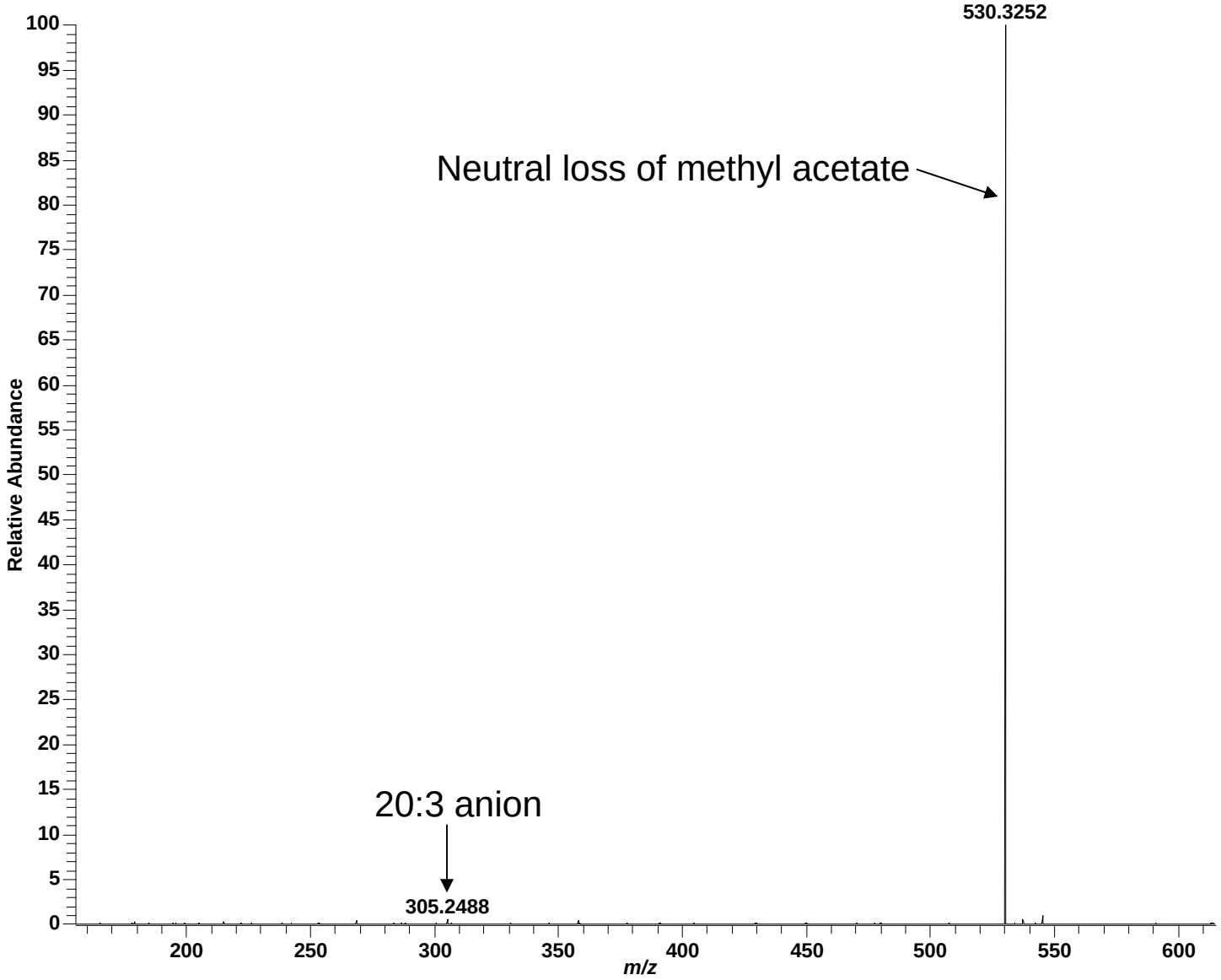

High mass measurement accuracy MS/MS utilizing LTQ-FT

Positive ESI: LPC 18:1; $C_{26}H_{52}NO_7P$; theoretical *m/z* 522.3559, $(M+H)^+$

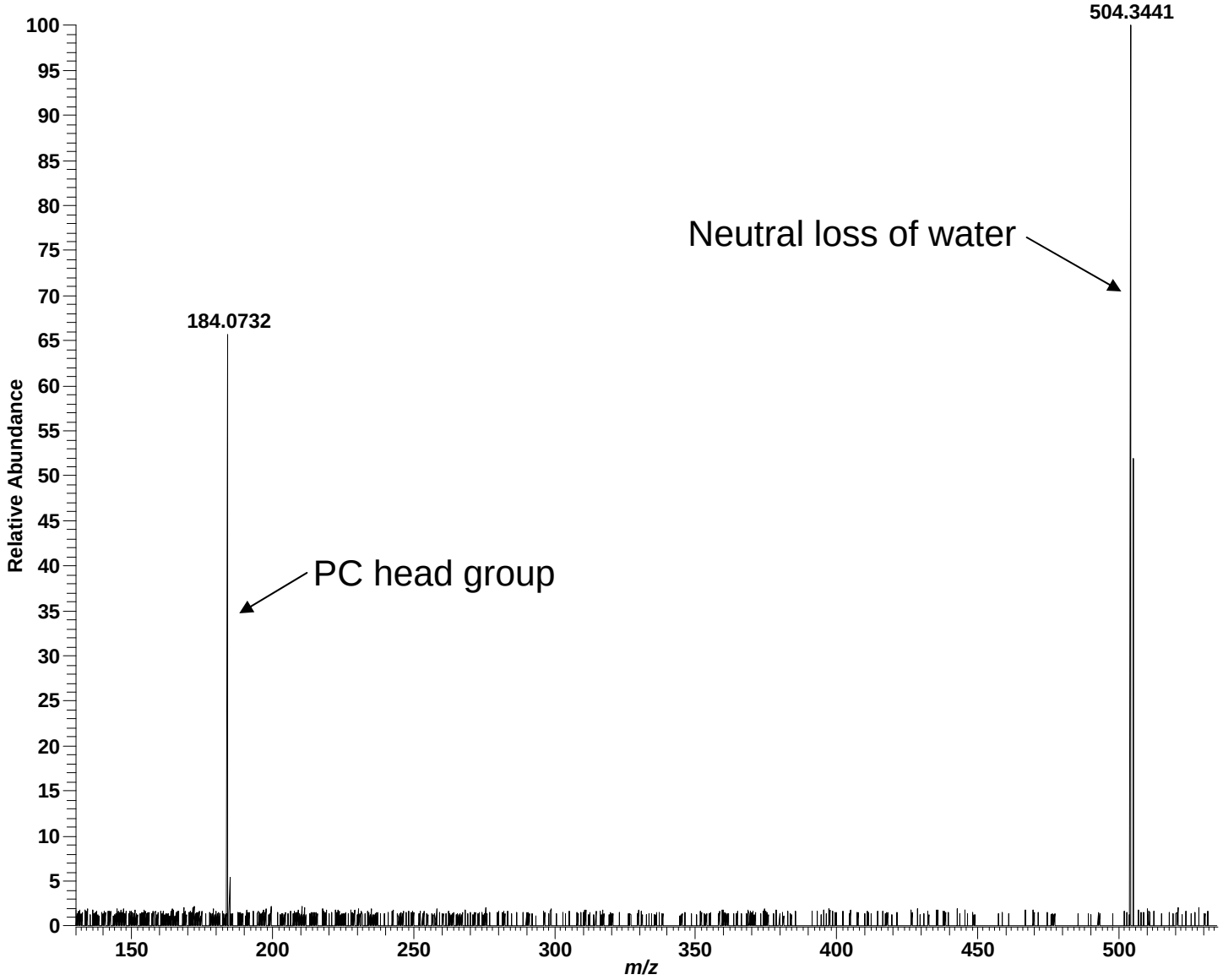

High mass measurement accuracy MS/MS utilizing LTQ-FT

Negative ESI: LPC 18:1; $C_{26}H_{52}NO_7P$; theoretical *m/z* 580.3614, $(M+CH_3COO)^-$

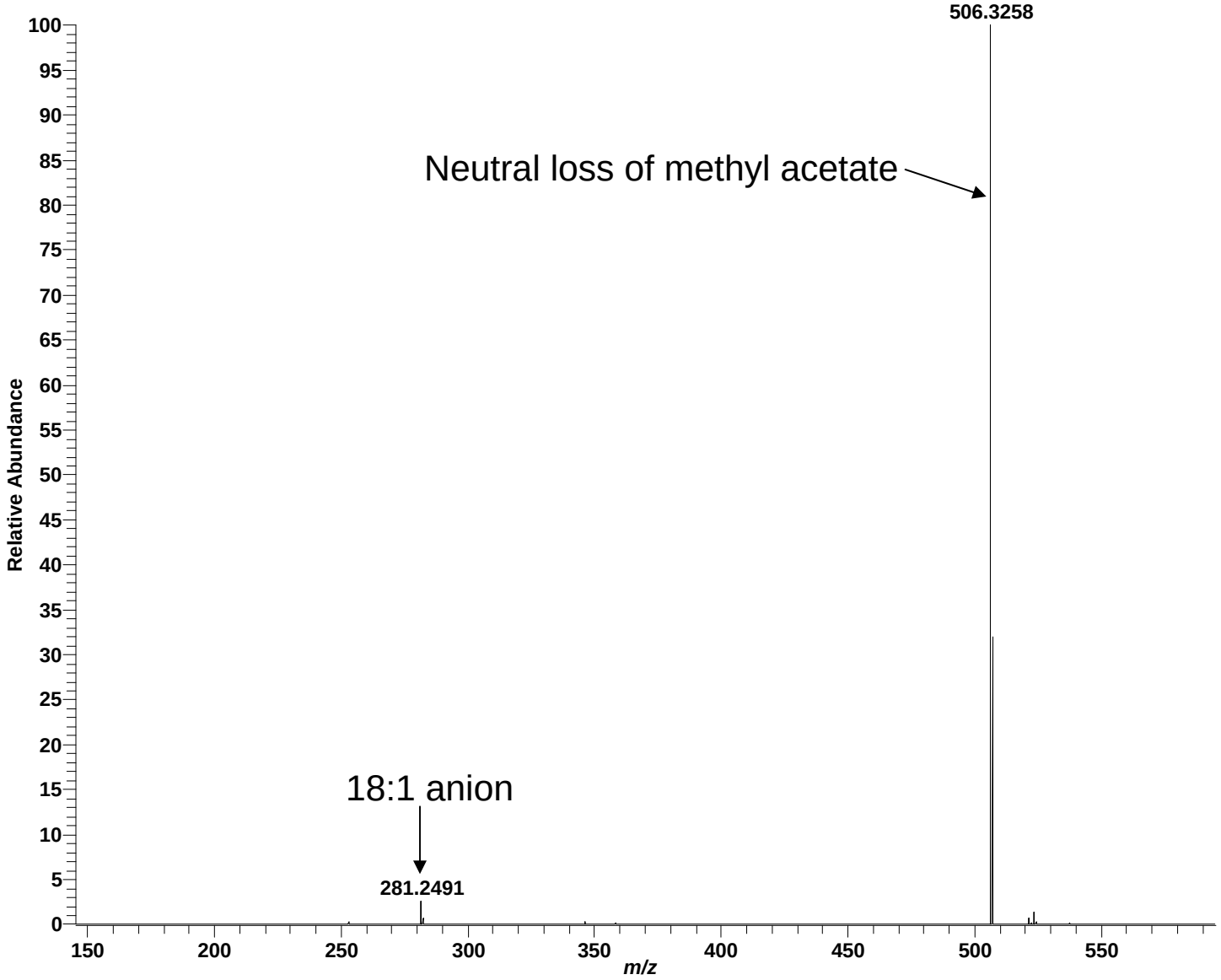

High mass measurement accuracy MS/MS utilizing LTQ-FT

Positive ESI: LPC 17:0; $C_{25}H_{52}NO_7P$; theoretical *m/z* 510.3559, $(M+H)^+$

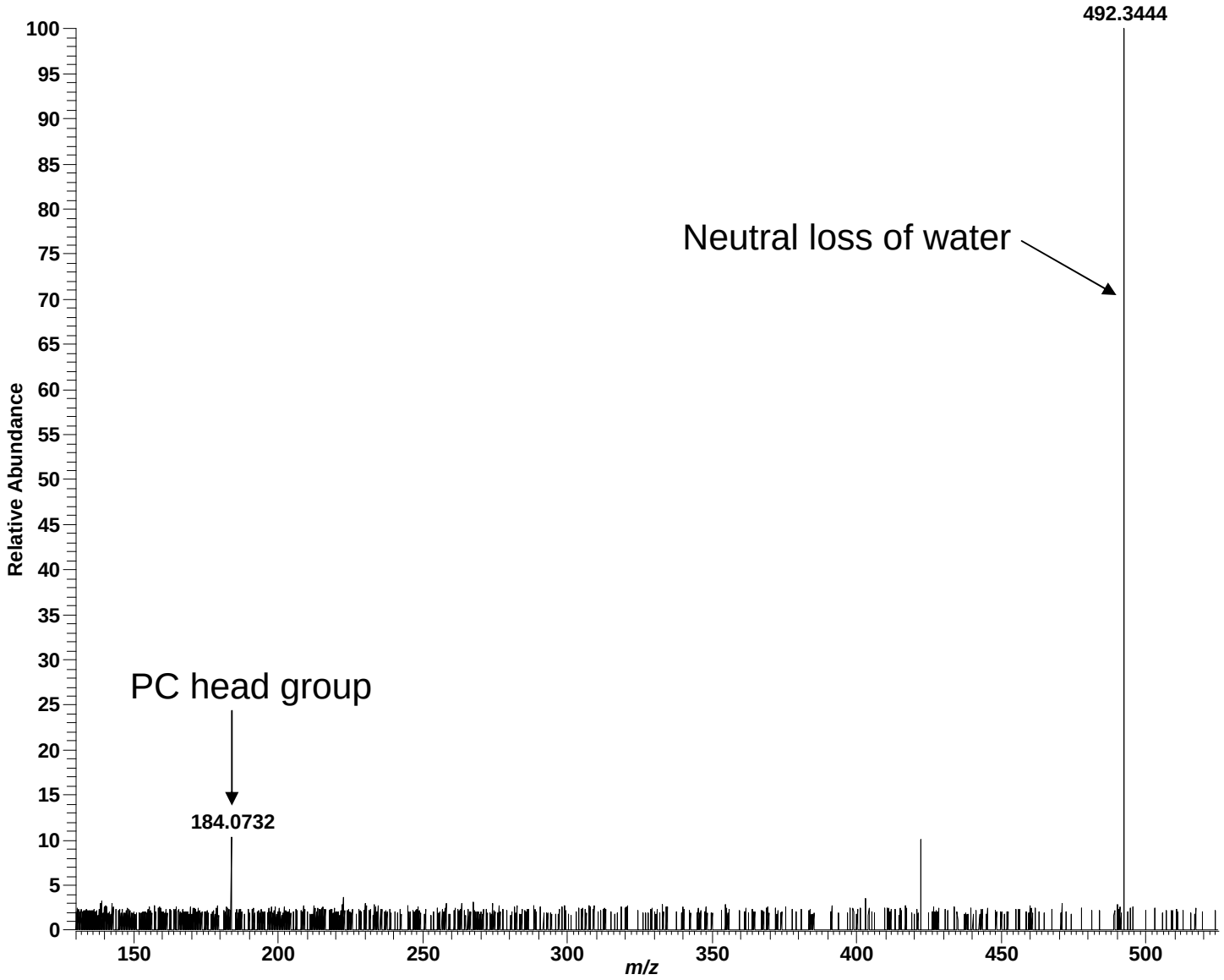

High mass measurement accuracy MS/MS utilizing LTQ-FT

Negative ESI: LPC 17:0; $C_{25}H_{52}NO_7P$; theoretical *m/z* 568.3614, $(M+CH_3COO)^-$

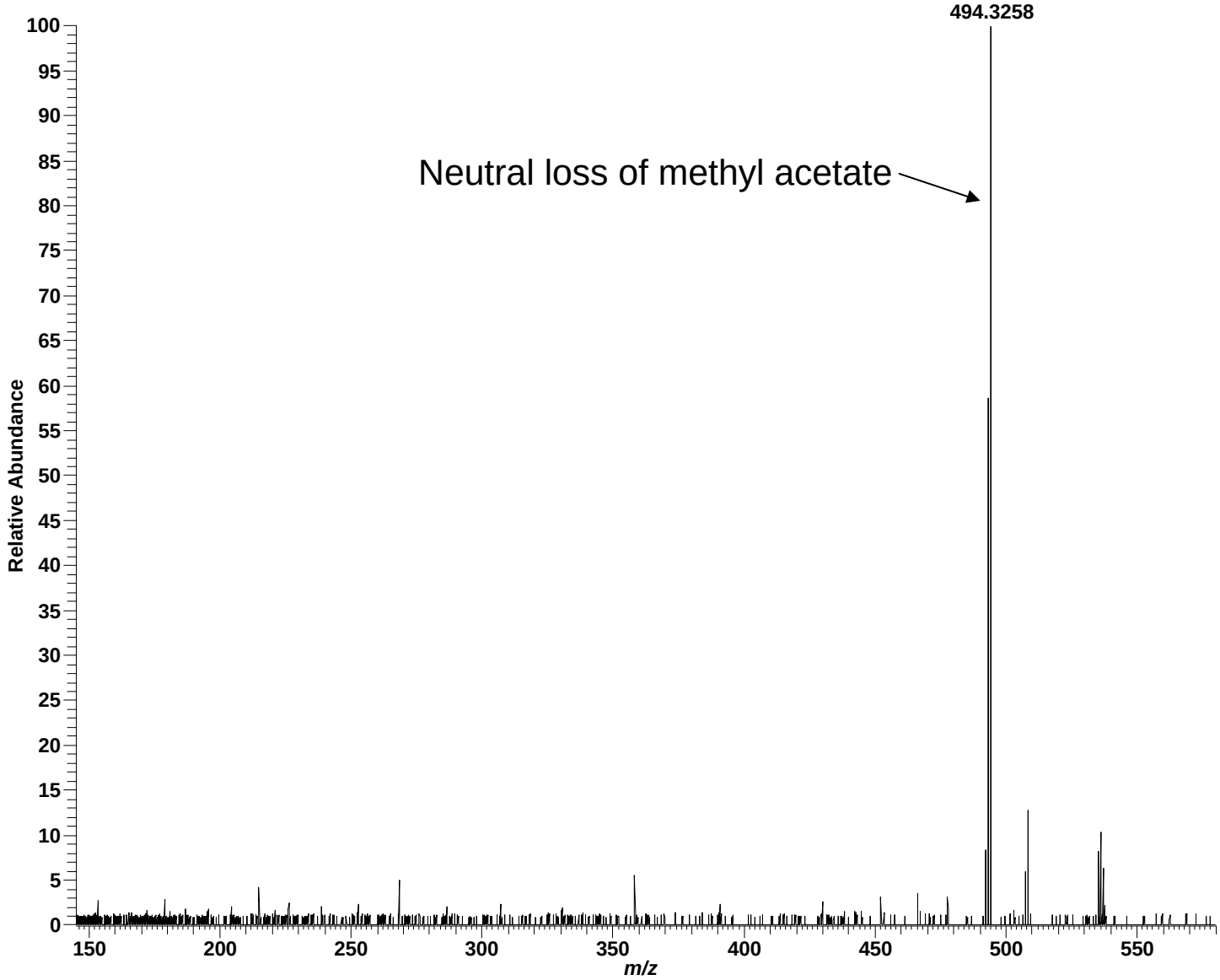

High mass measurement accuracy MS/MS utilizing LTQ-FT

Positive ESI: LPC 18:0; $C_{26}H_{54}NO_7P$; theoretical *m/z* 524.3716, $(M+H)^+$

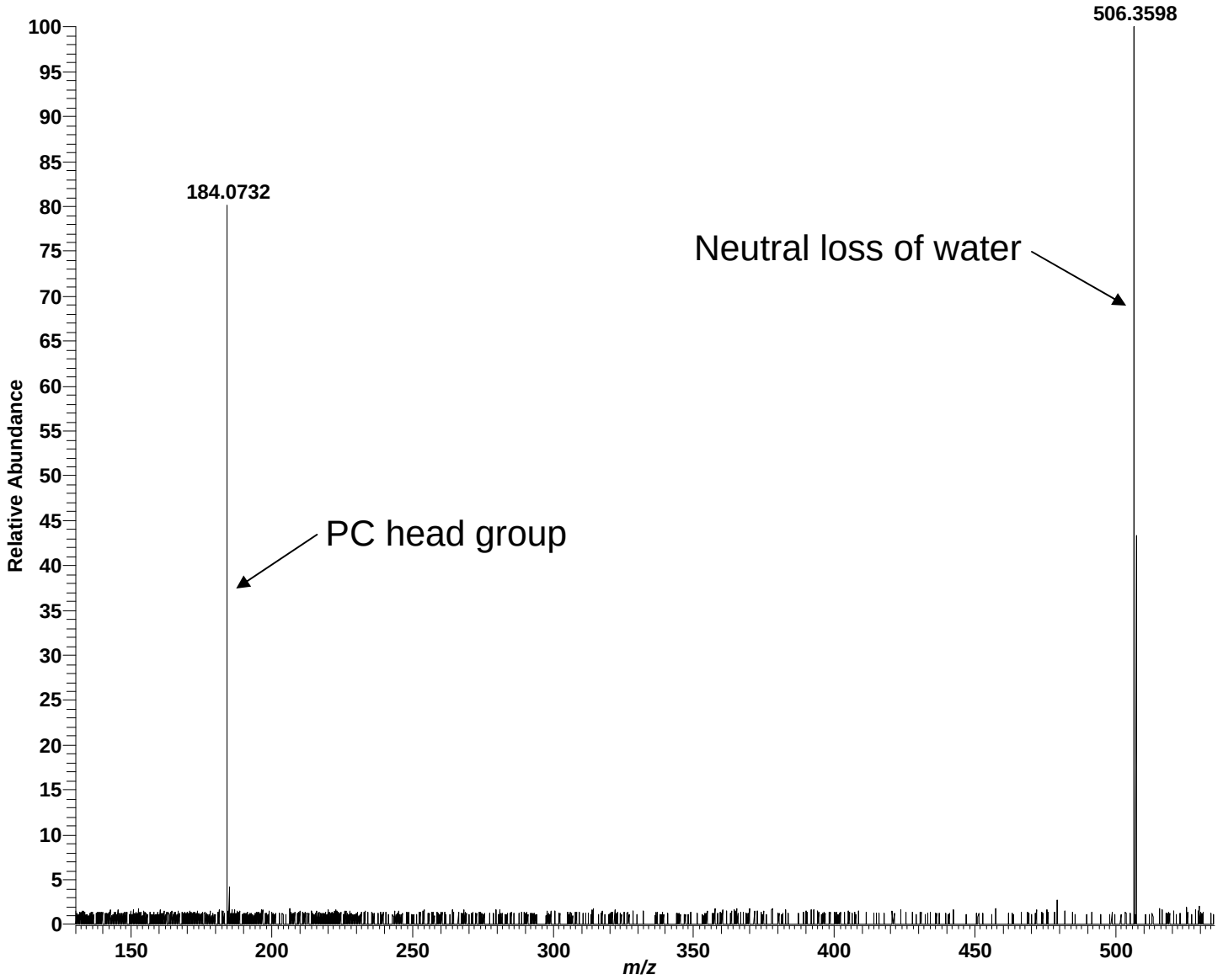

High mass measurement accuracy MS/MS utilizing LTQ-FT

Negative ESI: LPC 18:0; $C_{26}H_{54}NO_7P$; theoretical *m/z* 582.3771, $(M+CH_3COO)^-$

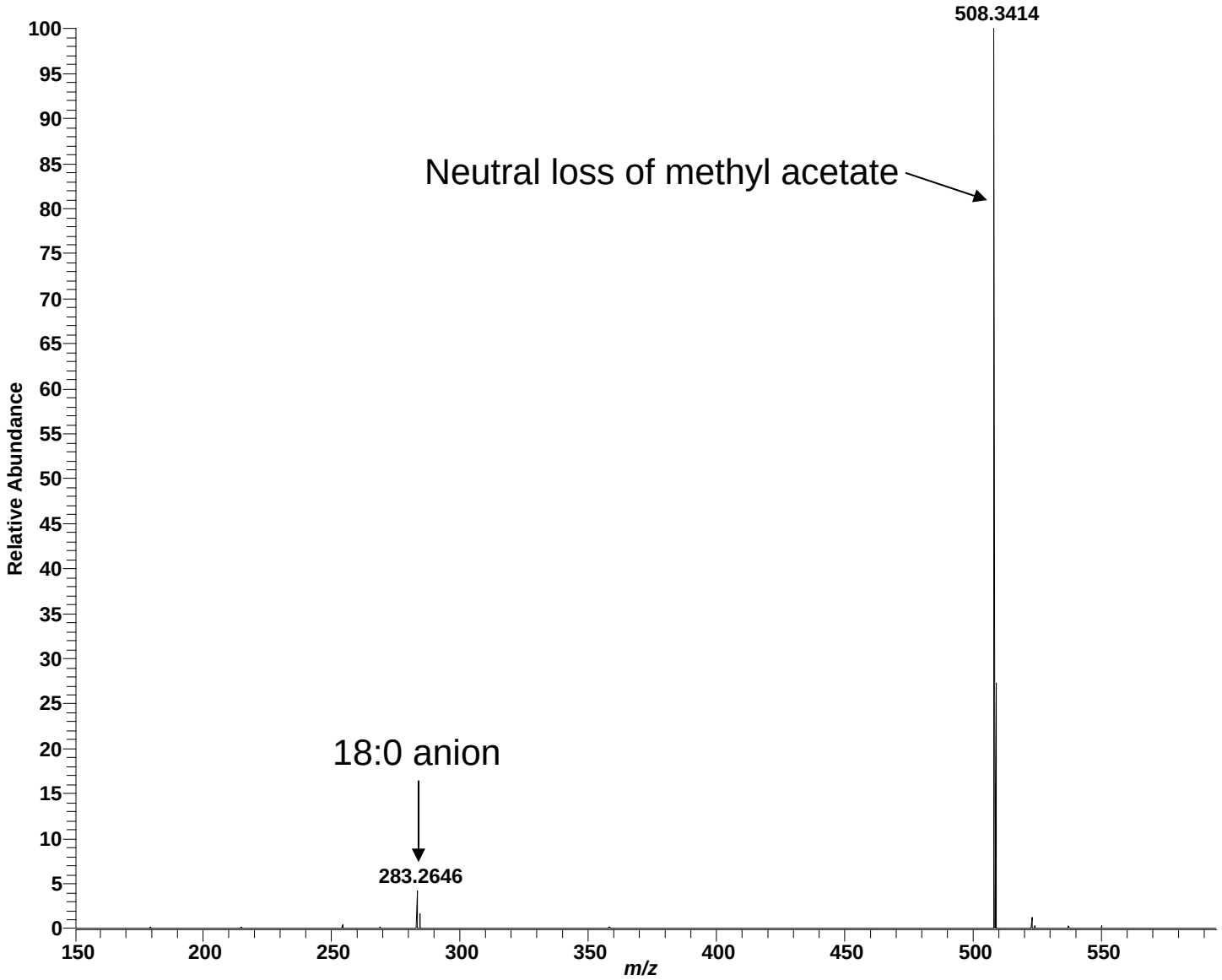

High mass measurement accuracy MS/MS utilizing LTQ-FT

Positive ESI: Oxidized PC 16:0/9:0-hydroxy; $C_{33}H_{64}NO_9P$; theoretical *m/z* 650.4397, $(M+H)^+$

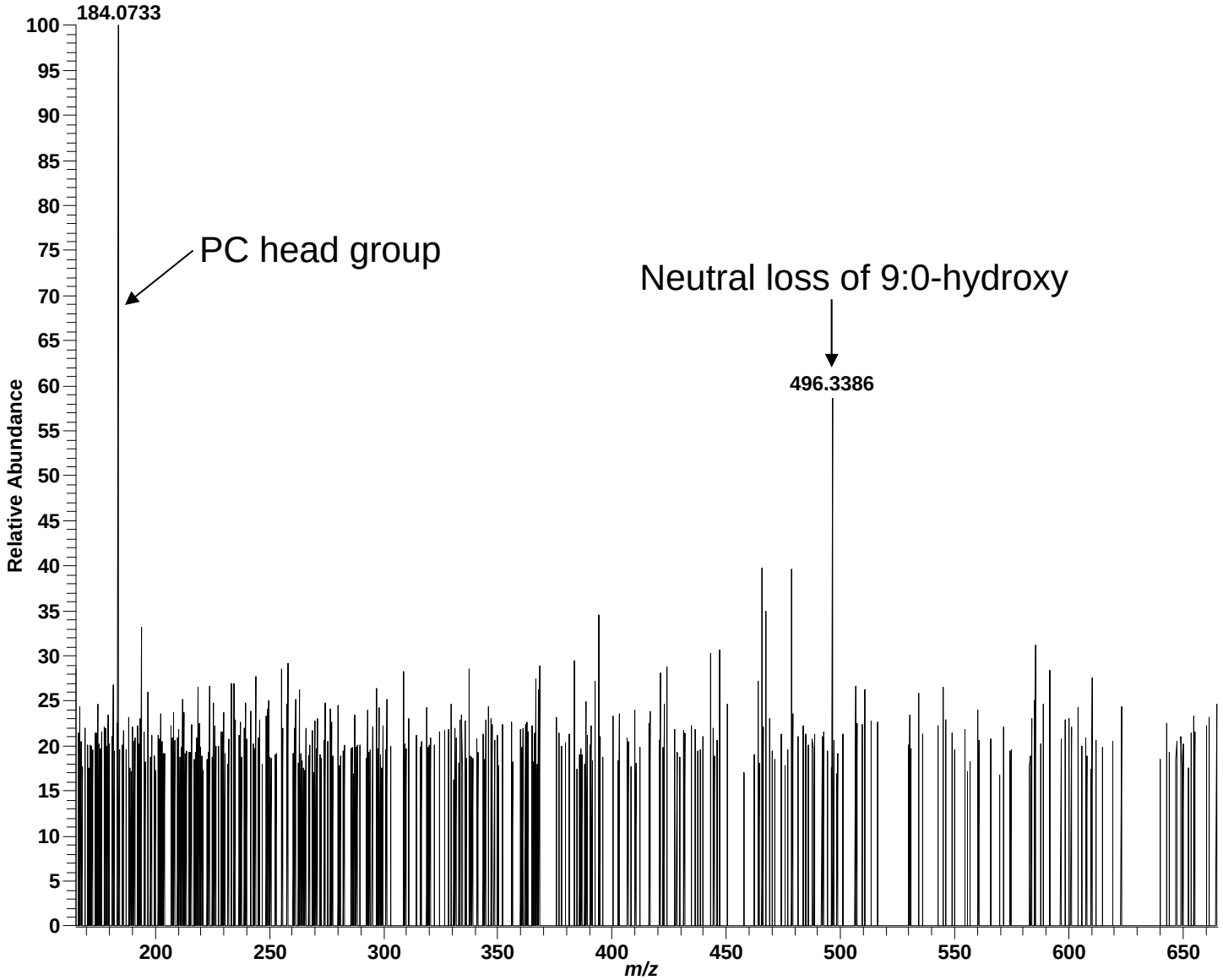

High mass measurement accuracy MS/MS utilizing LTQ-FT

Positive ESI: PC 18:2/18:2; $C_{44}H_{80}NO_8P$; theoretical *m/z* 782.5699, $(M+H)^+$

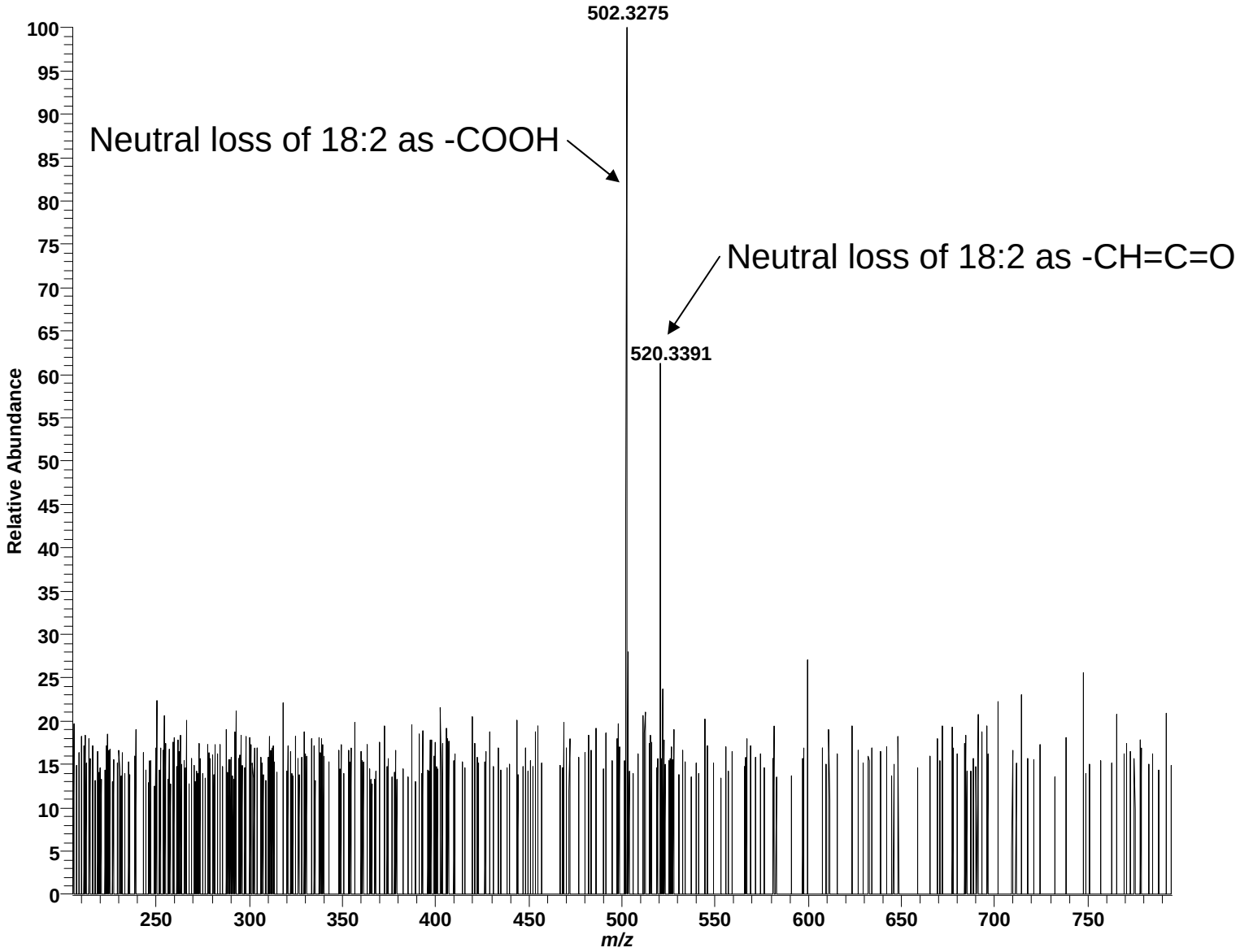

High mass measurement accuracy MS/MS utilizing LTQ-FT

Positive ESI: PC 16:0/22:6; $C_{46}H_{80}NO_8P$; theoretical *m/z* 806.5699, $(M+H)^+$

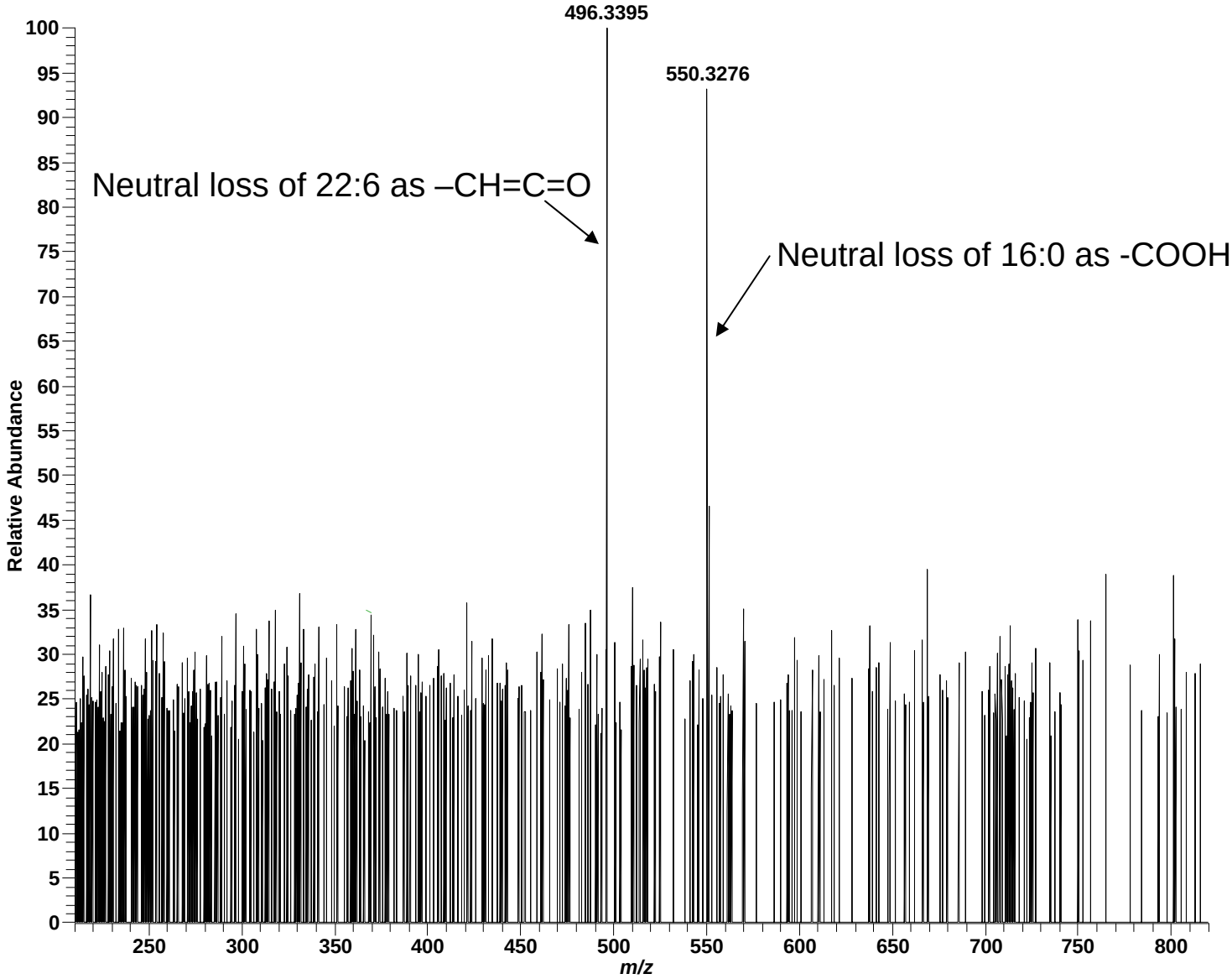

High mass measurement accuracy MS/MS utilizing LTQ-FT

Negative ESI: PC 16:0/22:6; $C_{46}H_{80}NO_8P$; theoretical *m/z* 864.5754, $(M+CH_3COO)^-$

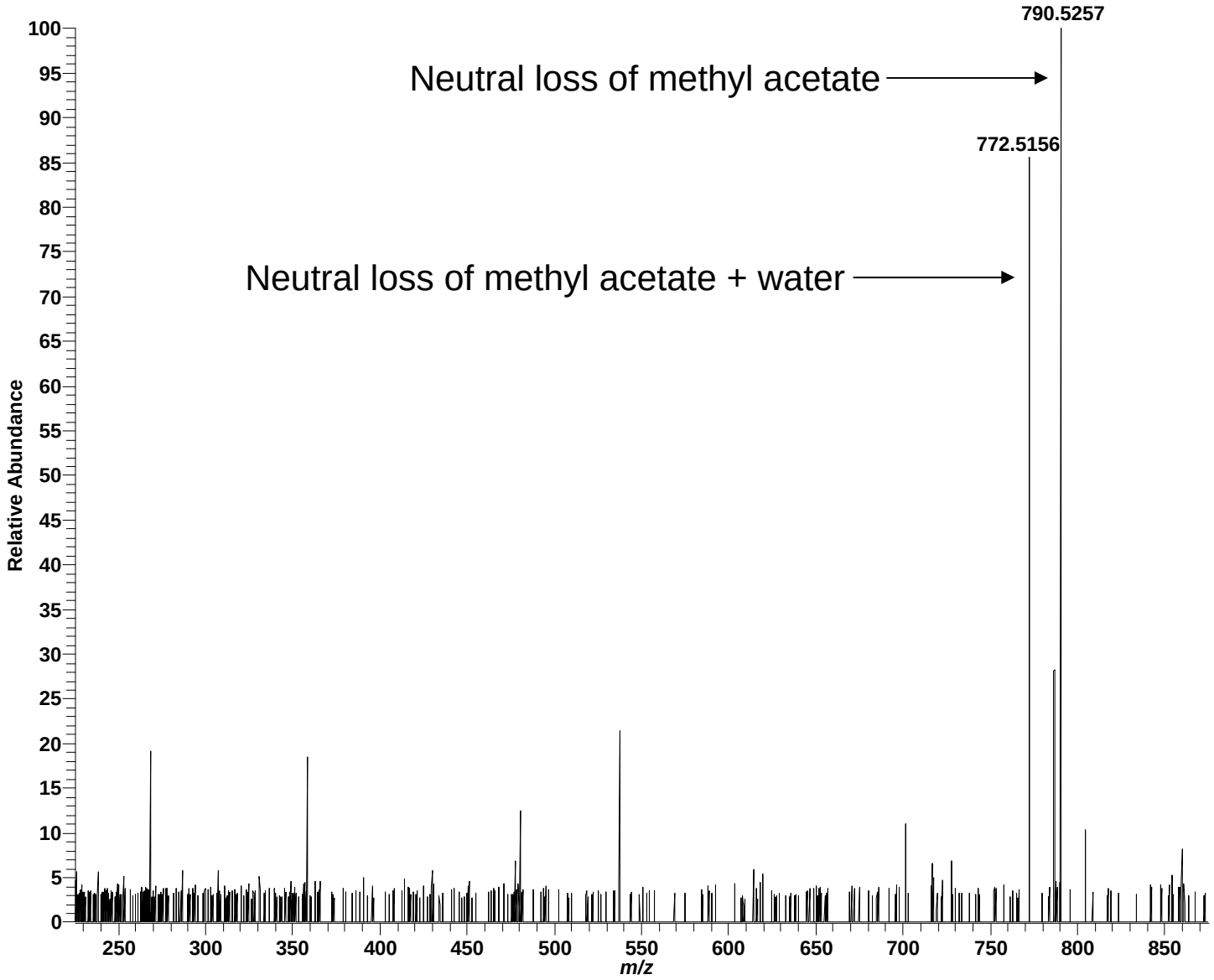

High mass measurement accuracy MS/MS utilizing LTQ-FT

Positive ESI: PC 18:1/18:2; $C_{44}H_{82}NO_8P$; theoretical *m/z* 784.5856, $(M+H)^+$

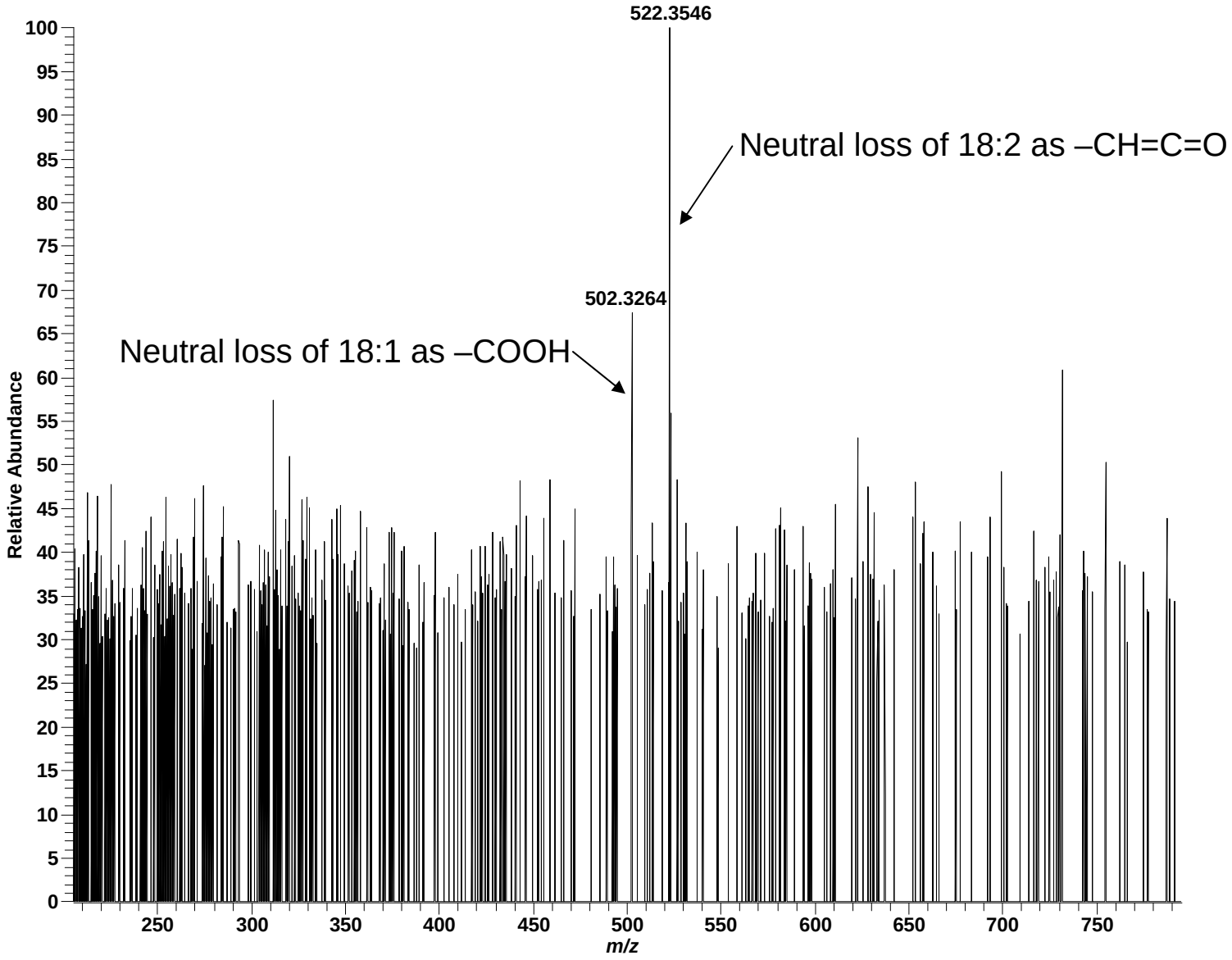

High mass measurement accuracy MS/MS utilizing LTQ-FT

Positive ESI: PC 18:0/22:6; $C_{48}H_{84}NO_8P$; theoretical *m/z* 834.6013, $(M+H)^+$

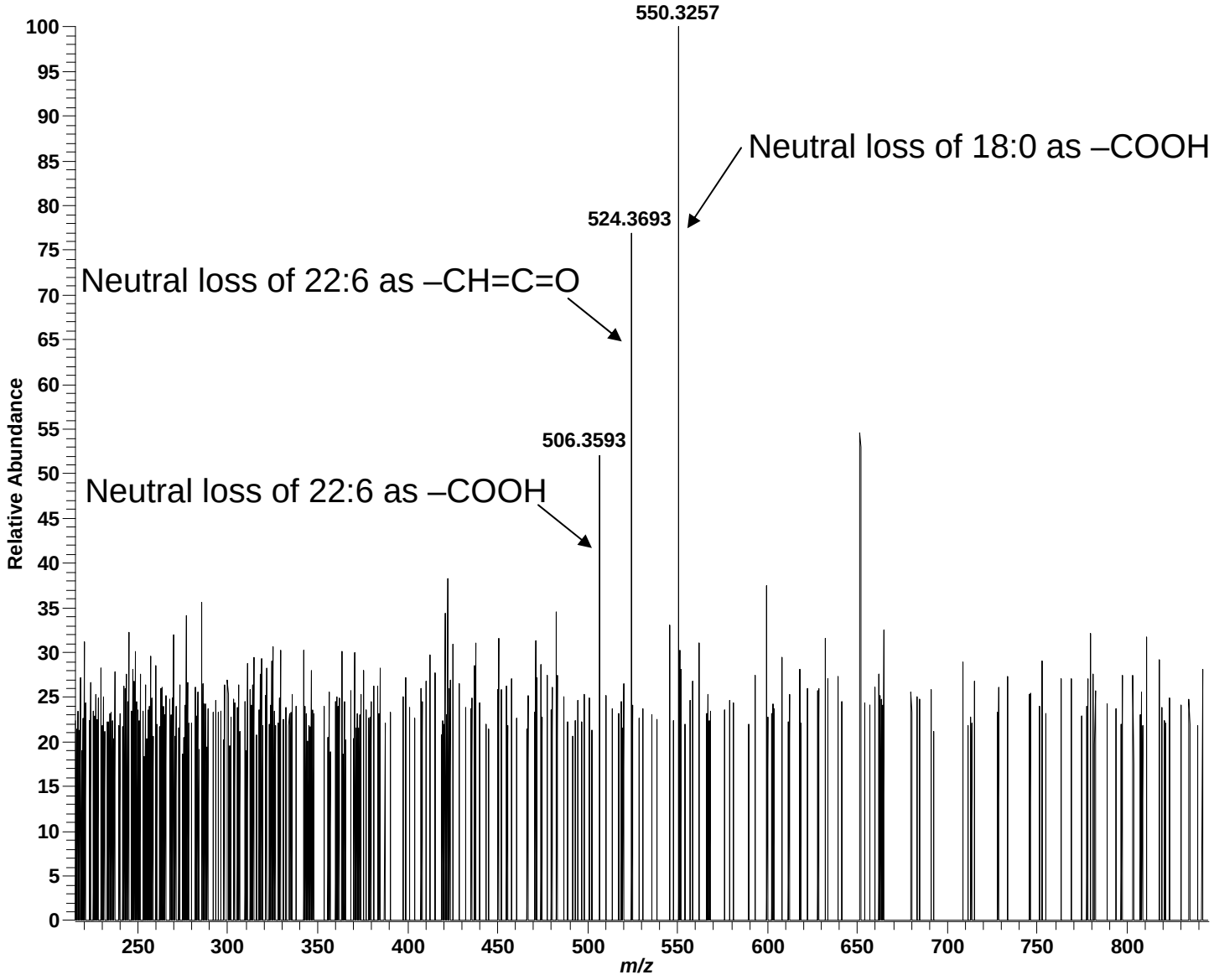

Cholesterol and its esters

Characteristic daughter ion: 369.3521
(Neutral loss of NH_4 + OH)

High mass measurement accuracy MS/MS utilizing LTQ-FT

Positive ESI: Cholesterol; $C_{27}H_{46}O$; theoretical *m/z* 404.3892, $(M+NH_4)^+$

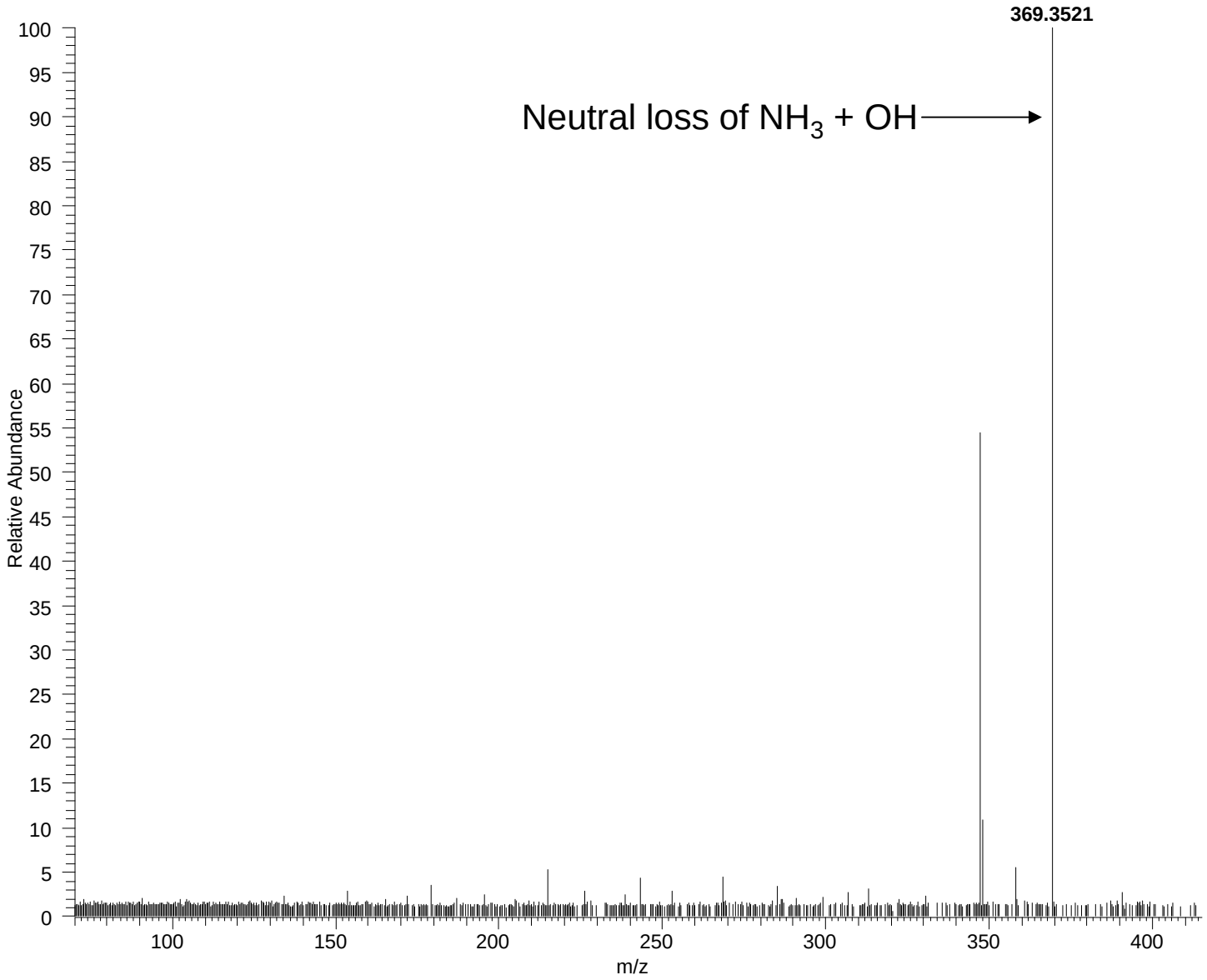

High mass measurement accuracy MS/MS utilizing LTQ-FT

Positive ESI: CE 20:5; $C_{47}H_{74}O2$; theoretical *m/z* 688.6032, $(M+NH_4)^+$

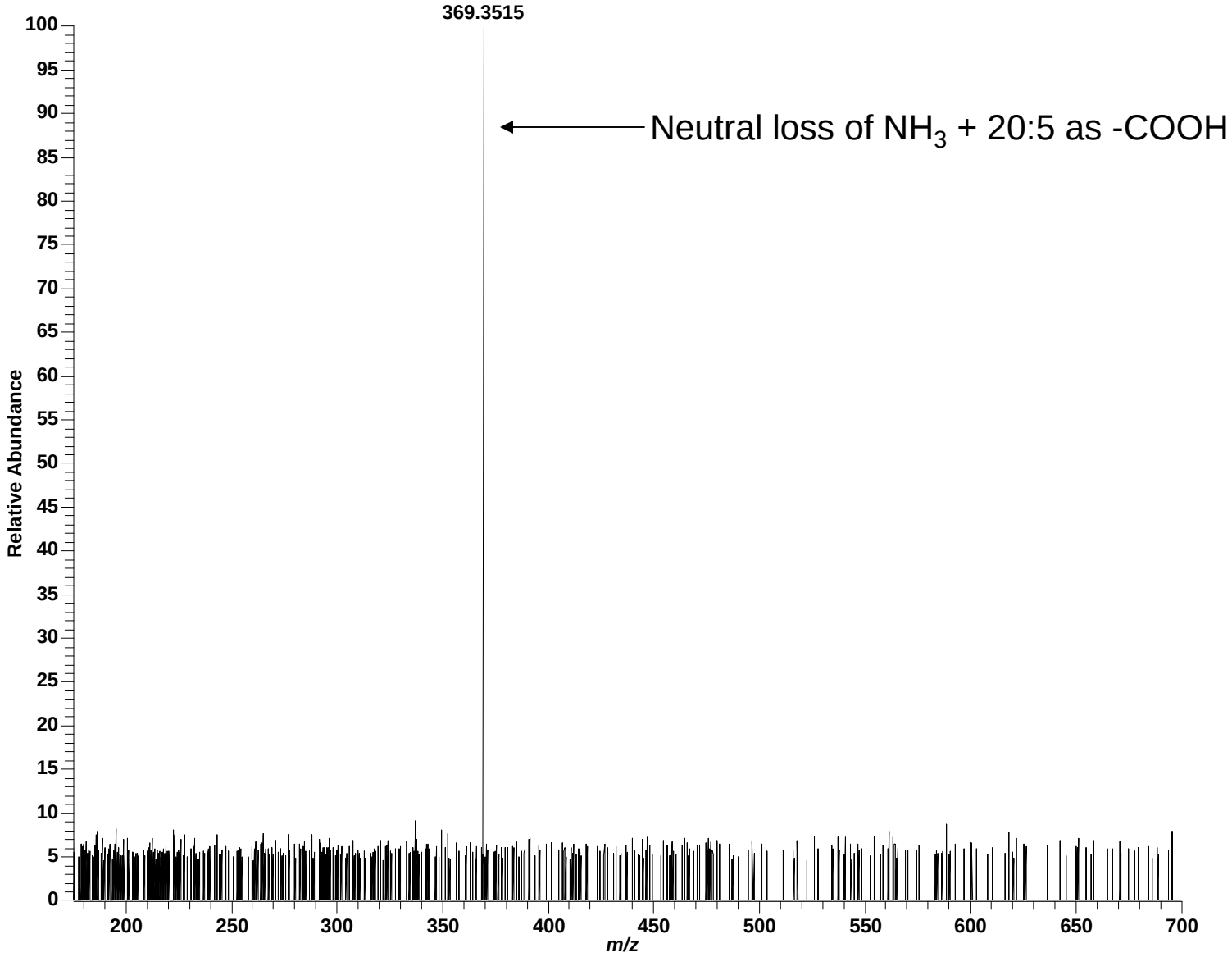

High mass measurement accuracy MS/MS utilizing LTQ-FT

Positive ESI: CE 20:4; $C_{47}H_{76}O_2$; theoretical *m/z* 690.6189, $(M+NH_4)^+$

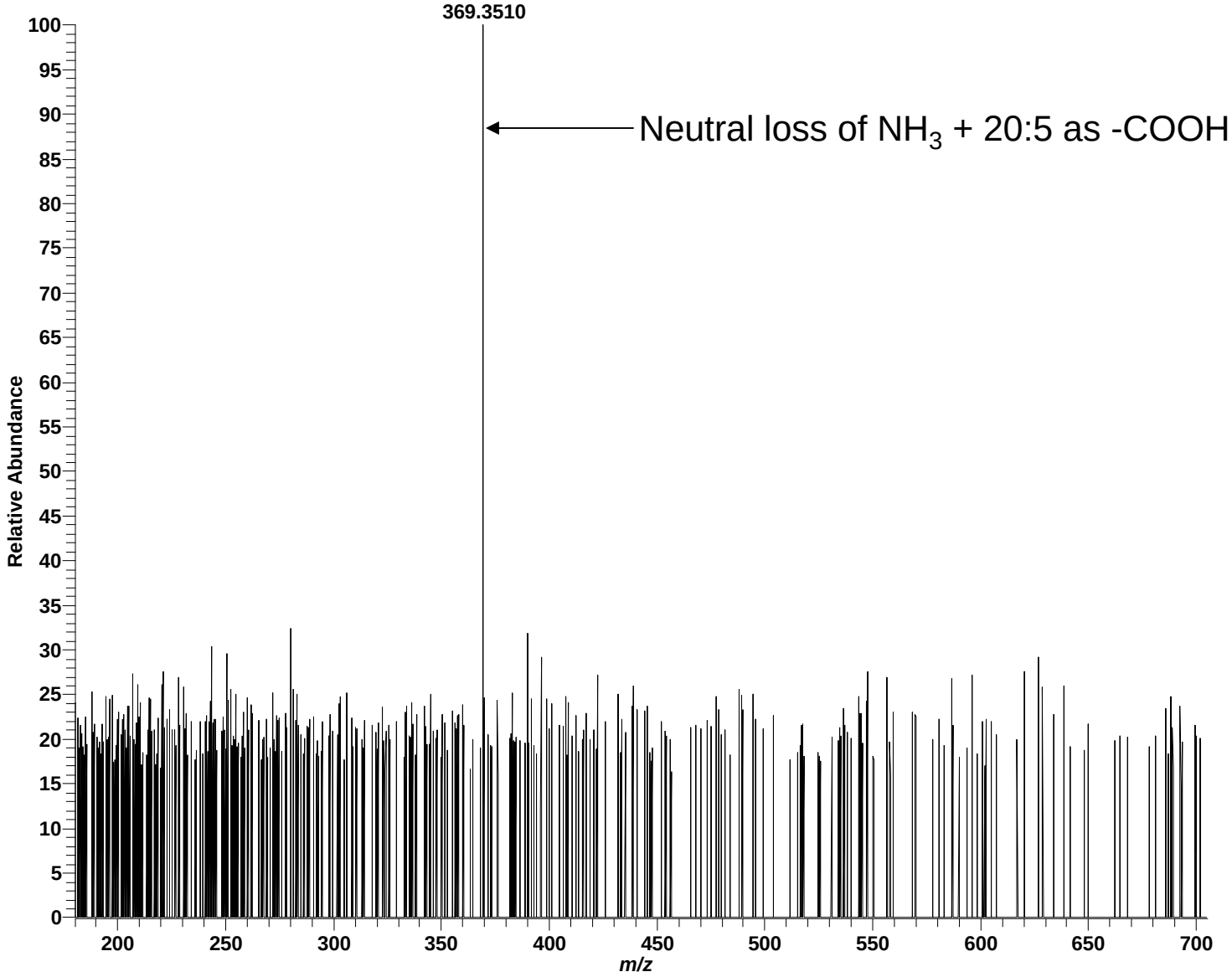

High mass measurement accuracy MS/MS utilizing LTQ-FT

Positive ESI: CE 18:3; $C_{45}H_{74}O_2$; theoretical *m/z* 664.6032, $(M+NH_4)^+$

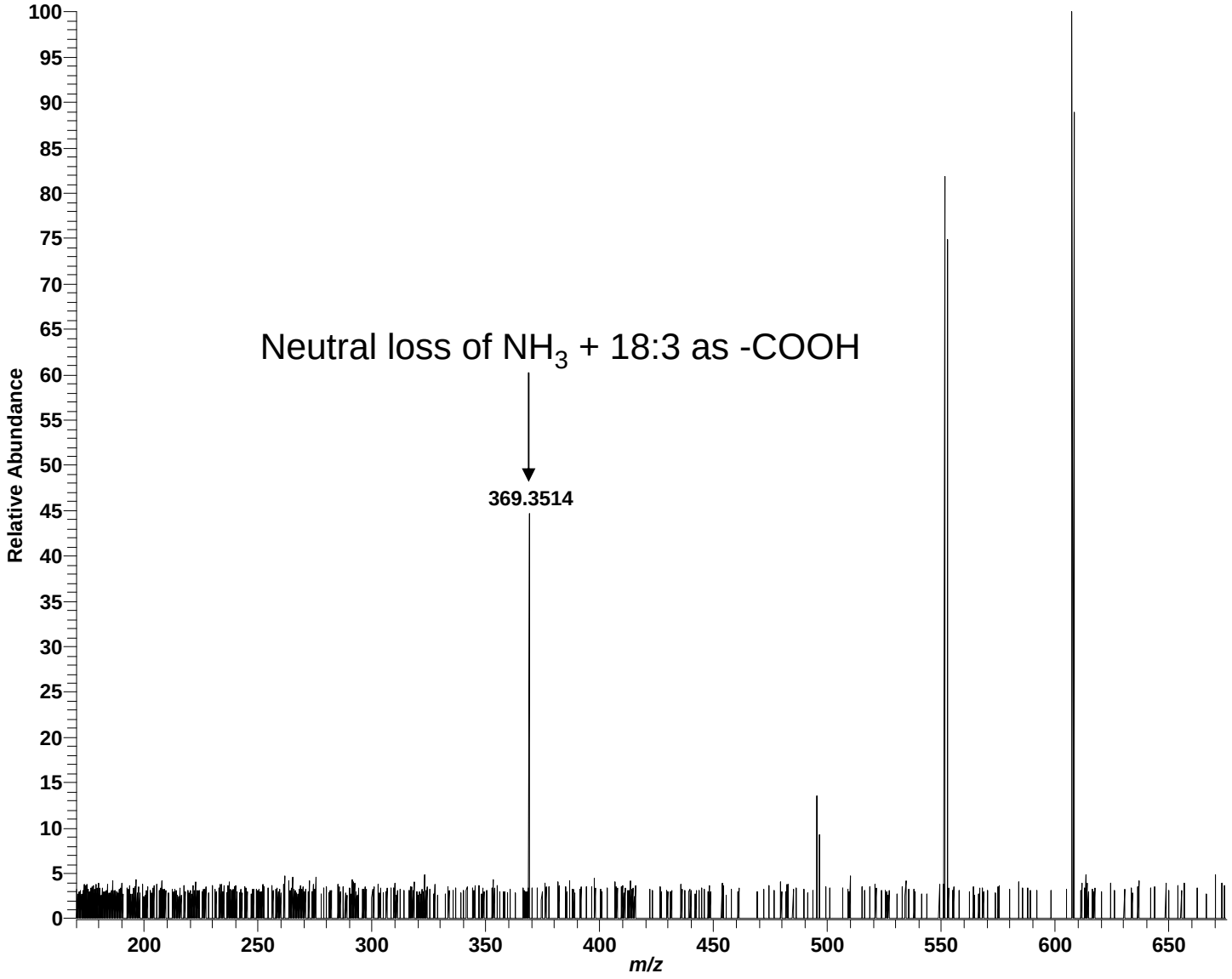

High mass measurement accuracy MS/MS utilizing LTQ-FT

Positive ESI: CE 18:2; $C_{45}H_{76}O_2$; theoretical *m/z* 666.6189, $(M+NH_4)^+$

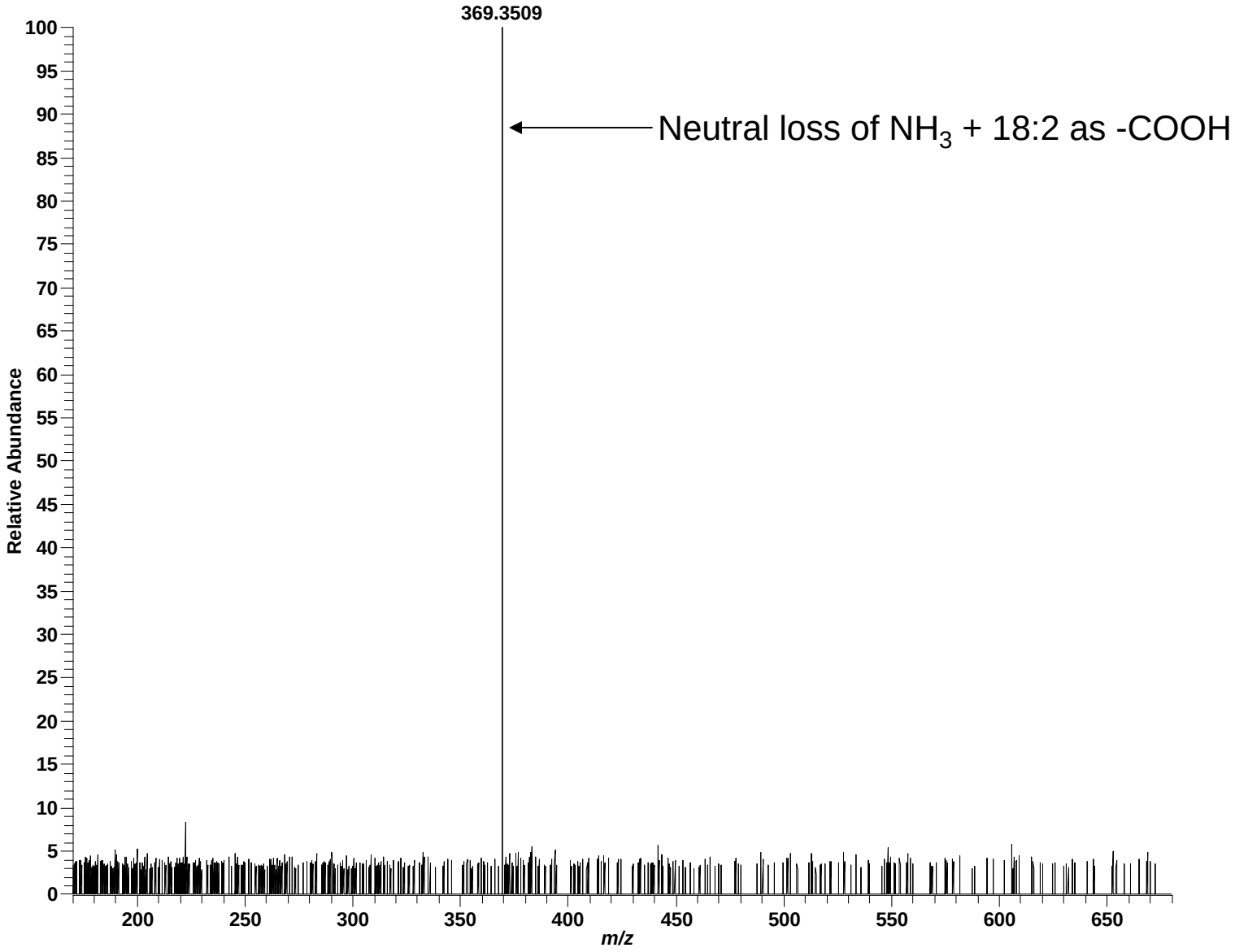

Triacylglycerols

High mass measurement accuracy MS/MS utilizing LTQ-FT

Positive ESI: TAG (18:2,18:2,18:3); $C_{57}H_{96}O_6$; theoretical *m/z* 894.7551, $(M+NH_4)^+$

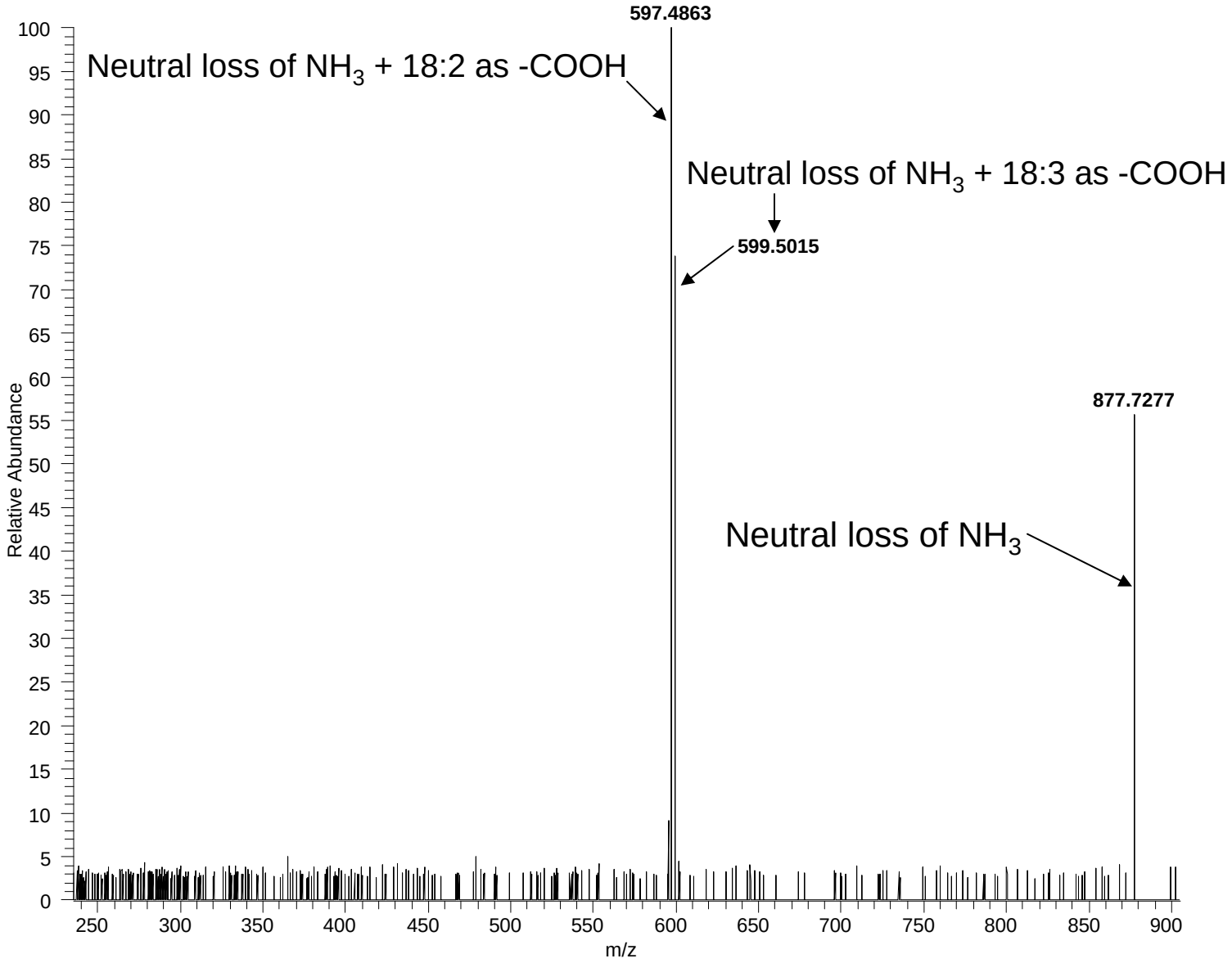

High mass measurement accuracy MS/MS utilizing LTQ-FT

Positive ESI: TAG (14:0,18:2,18:2); $C_{53}H_{94}O_6$; theoretical *m/z* 844.7394, $(M+NH_4)^+$

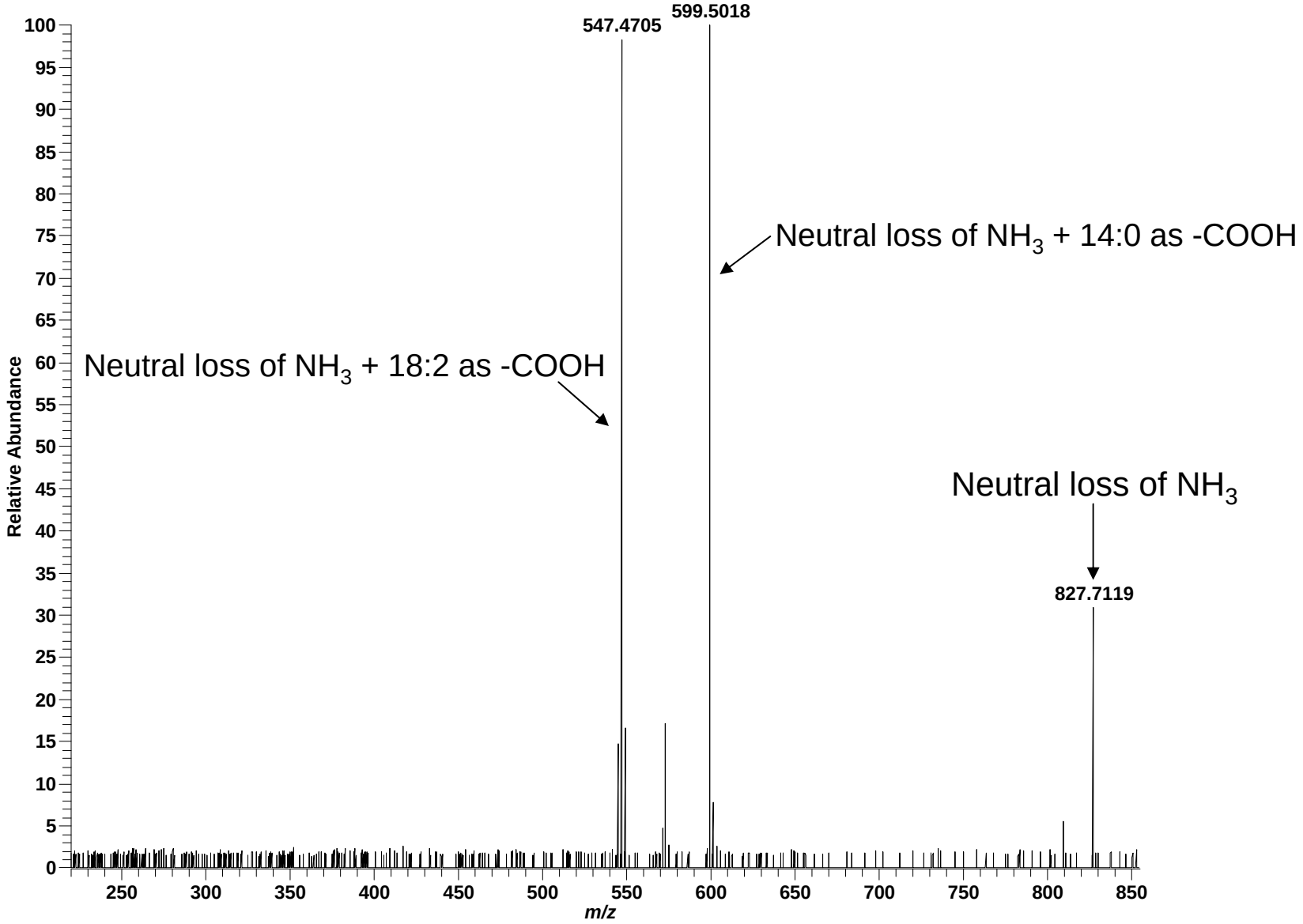

High mass measurement accuracy MS/MS utilizing LTQ-FT

Positive ESI: TAG (16:1,18:2,18:2); $C_{55}H_{96}O_6$; theoretical *m/z* 870.7550, $(M+NH_4)^+$

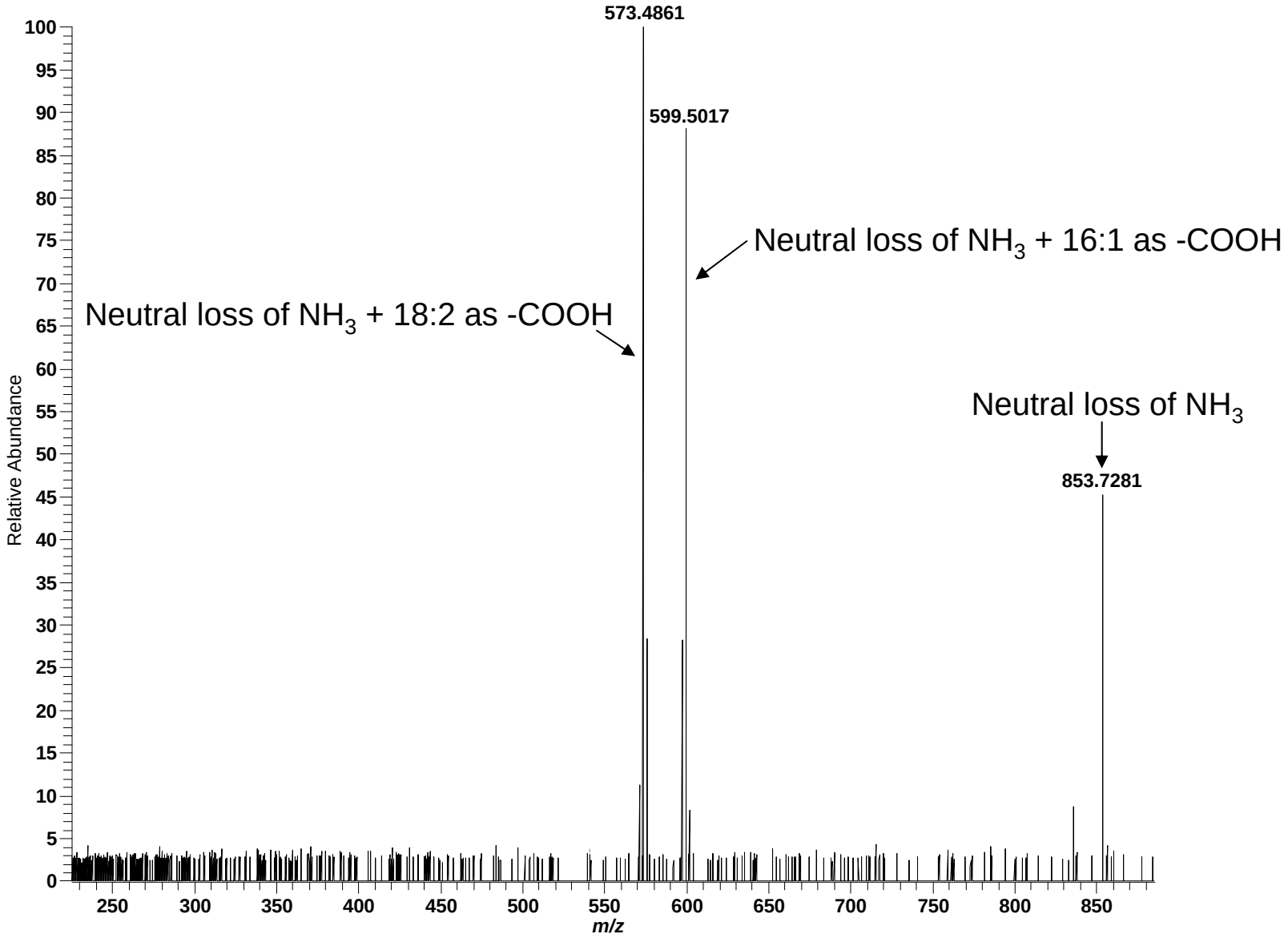

High mass measurement accuracy MS/MS utilizing LTQ-FT

Positive ESI: TAG (16:0,18:2,18:3); $C_{55}H_{96}O_6$; theoretical *m/z* 870.7550, $(M+NH_4)^+$

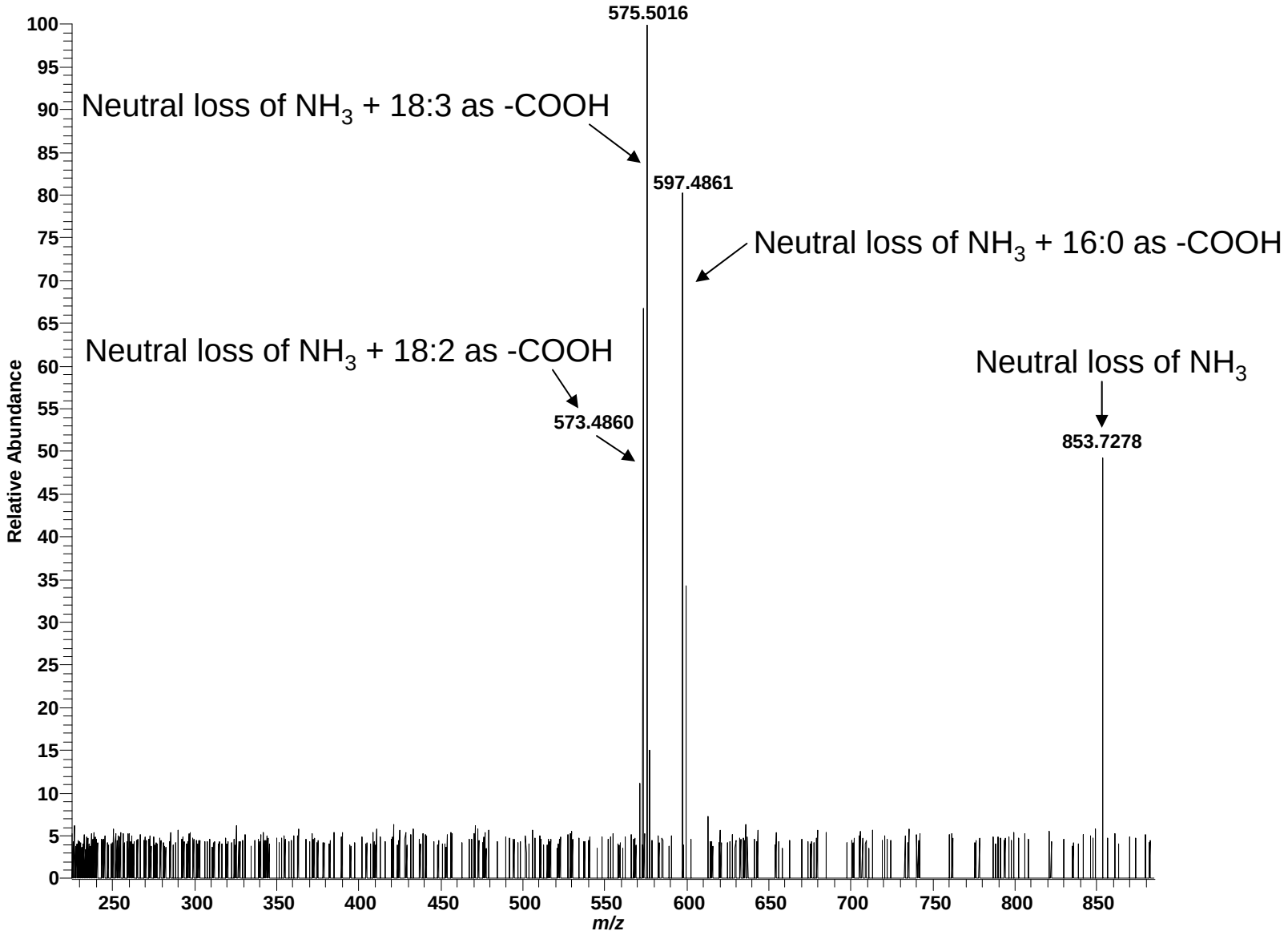

High mass measurement accuracy MS/MS utilizing LTQ-FT

Positive ESI: TAG (16:0,18:2,22:6); $C_{59}H_{98}O_6$; theoretical *m/z* 920.7707, $(M+NH_4)^+$

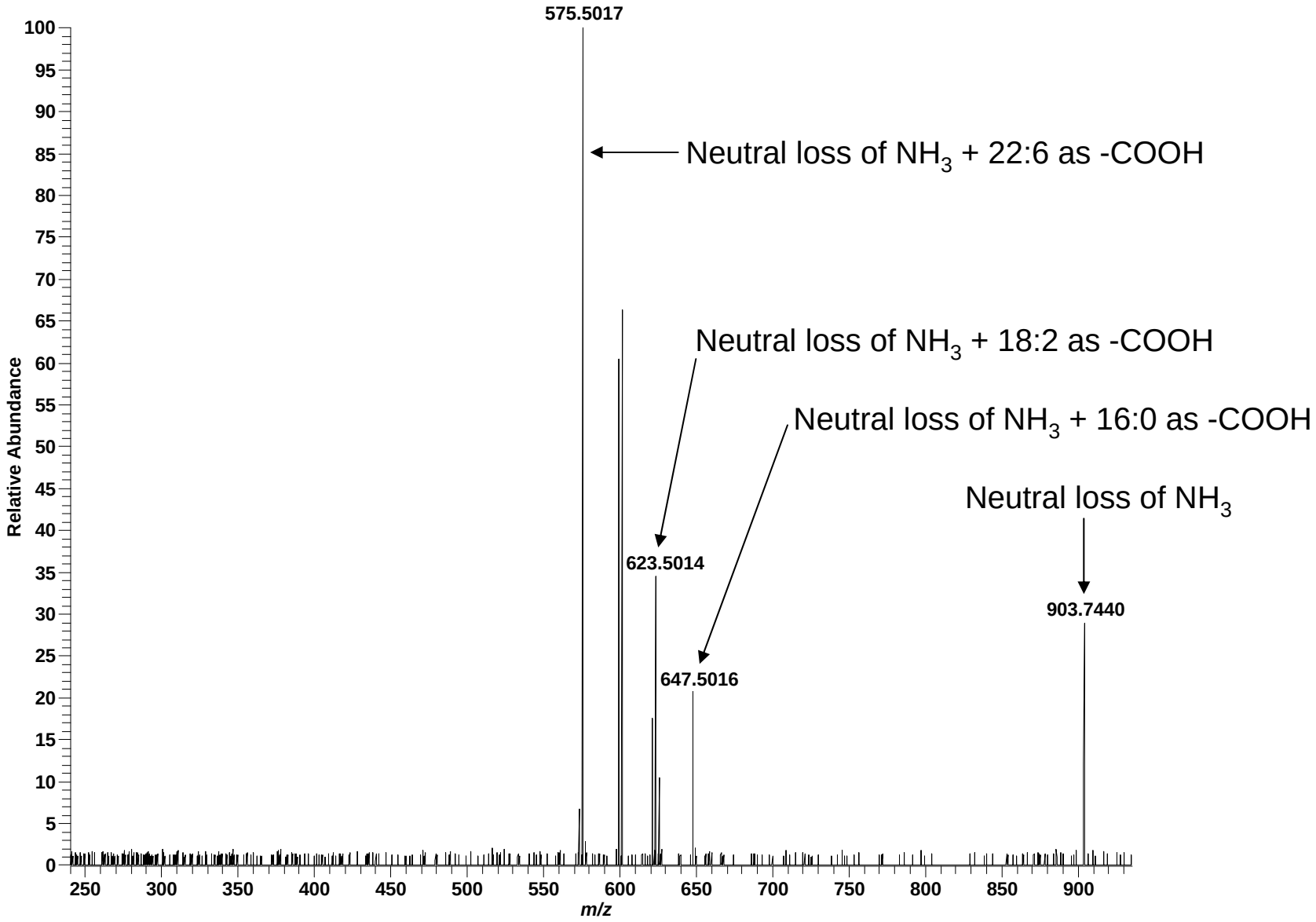

High mass measurement accuracy MS/MS utilizing LTQ-FT

Positive ESI: TAG (18:1,18:2,20:4); $C_{59}H_{100}O_6$; theoretical *m/z* 922.7864, $(M+NH_4)^+$

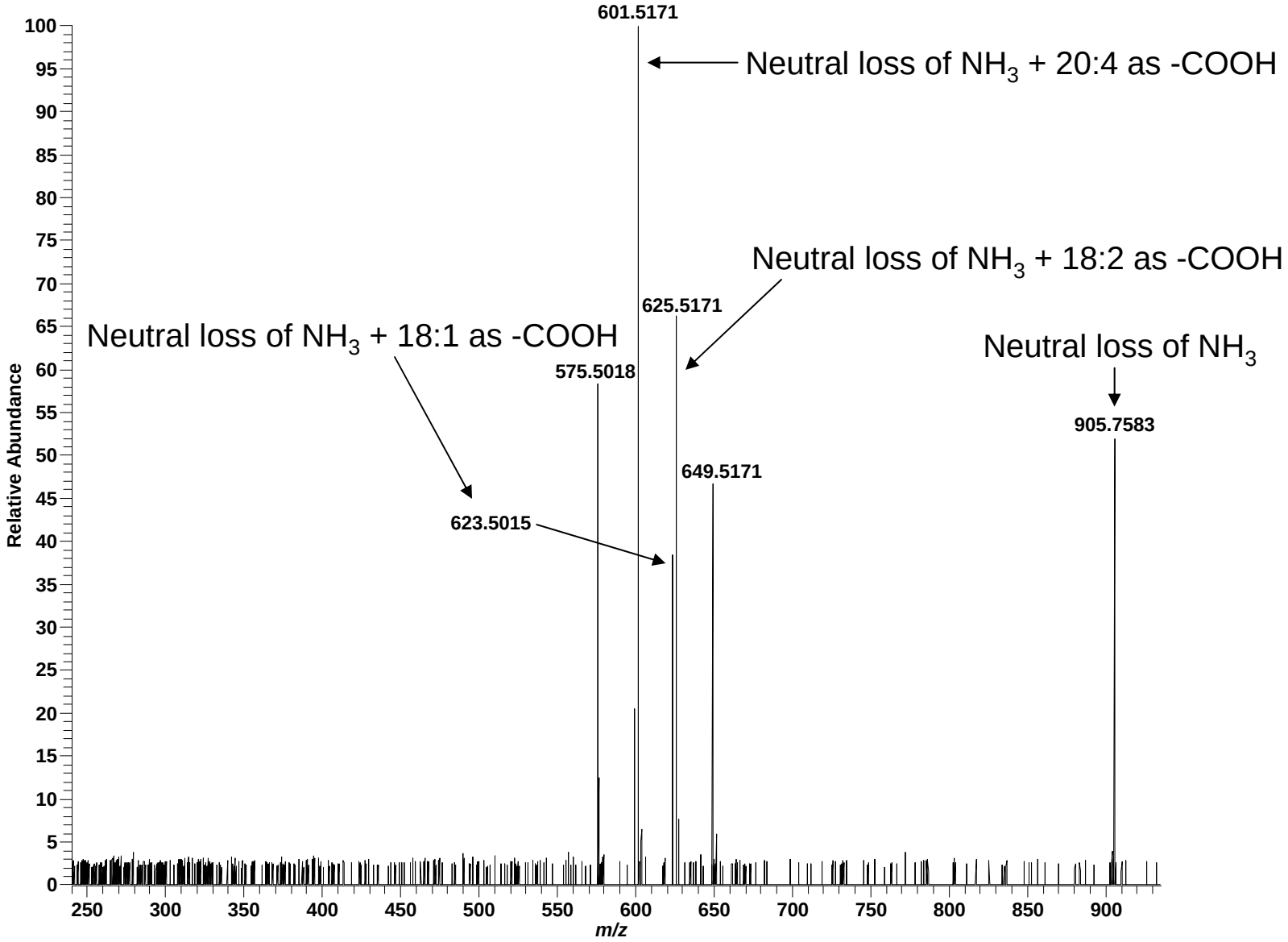

High mass measurement accuracy MS/MS utilizing LTQ-FT

Positive ESI: TAG (16:0,20:3,20:4); $C_{59}H_{100}O_6$; theoretical *m/z* 922.7864, $(M+NH_4)^+$

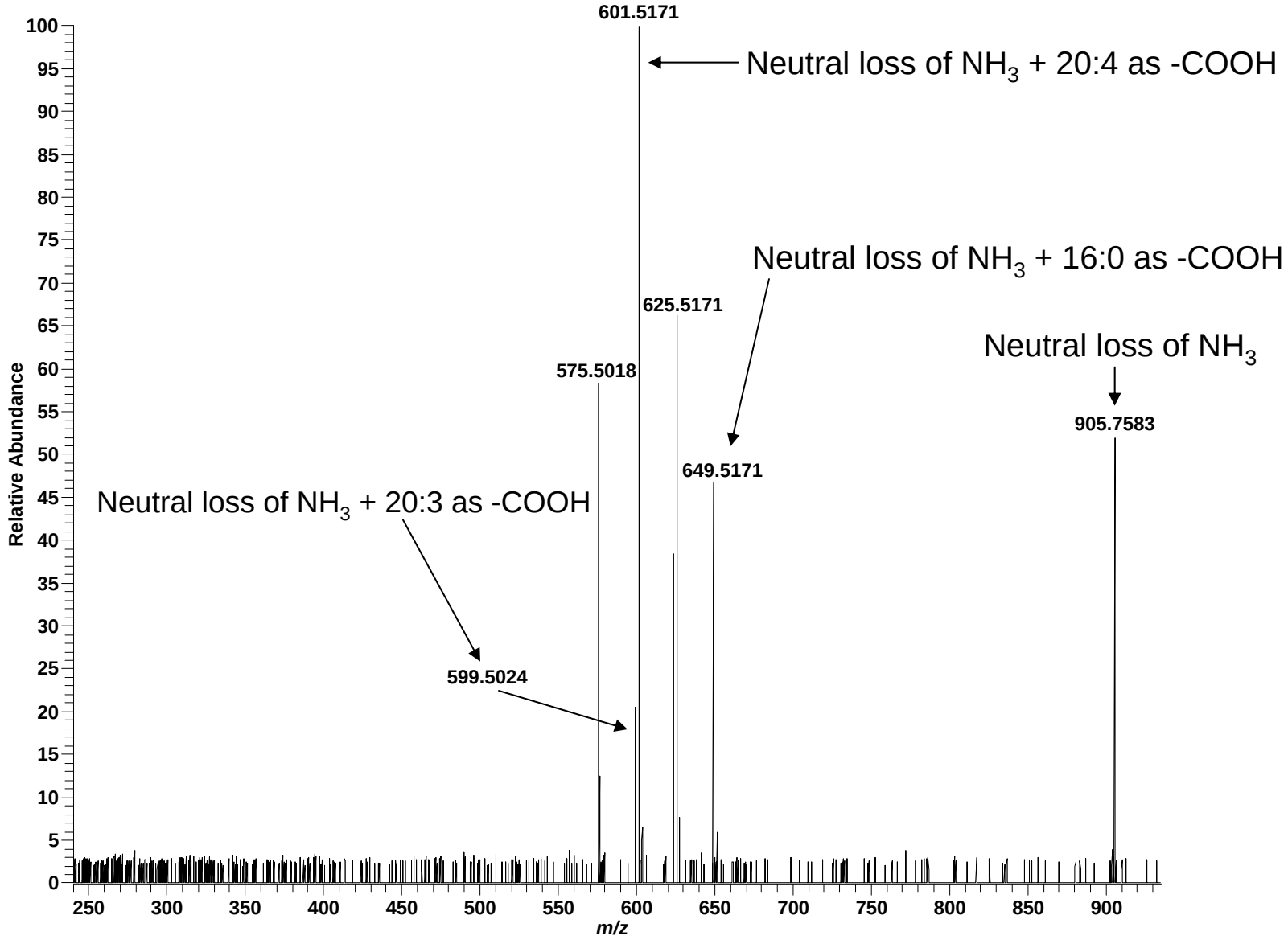

High mass measurement accuracy MS/MS utilizing LTQ-FT

Positive ESI: TAG (16:0,18:2,20:4); $C_{57}H_{98}O_6$; theoretical *m/z* 896.7707, $(M+NH_4)^+$

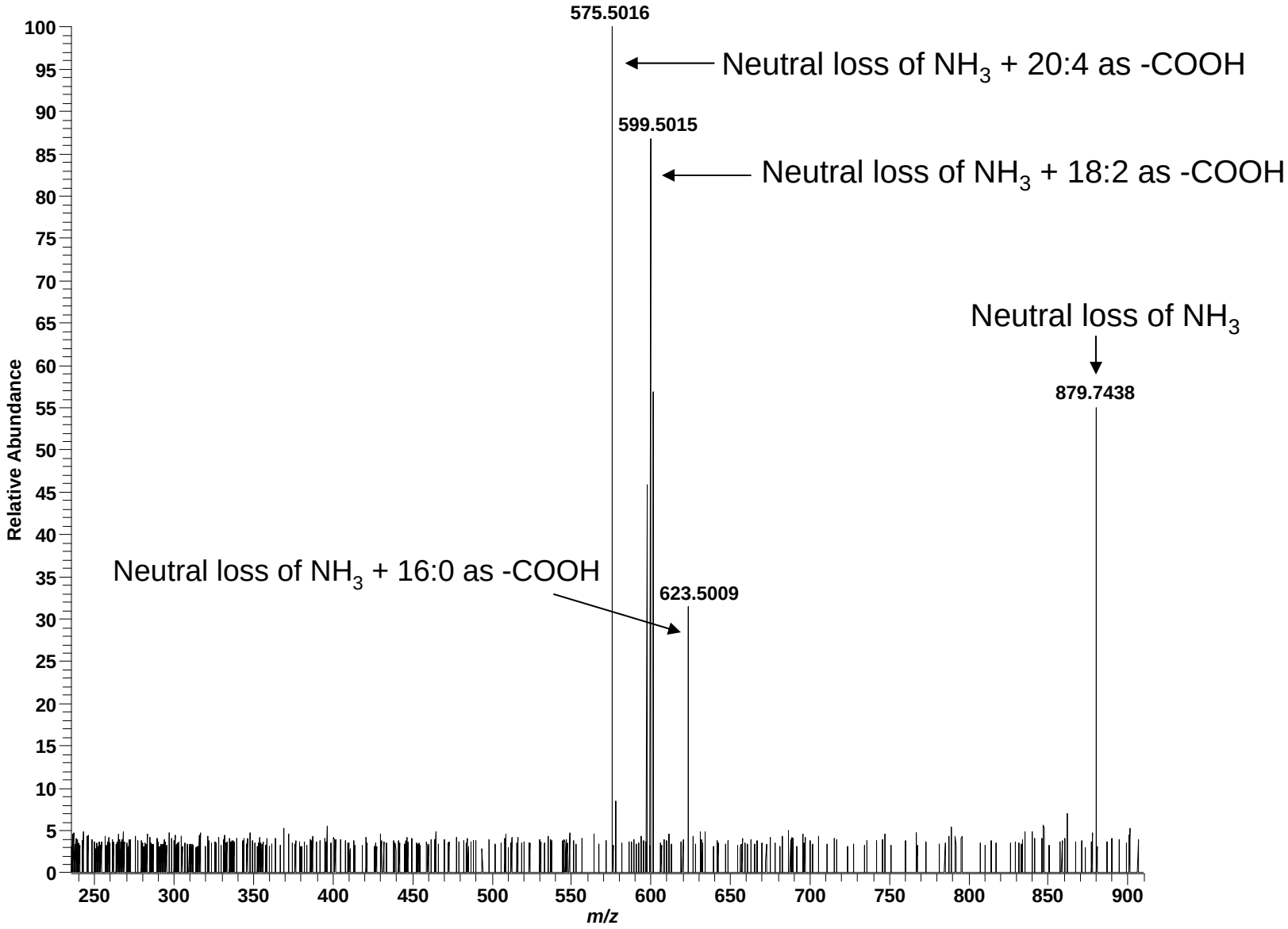

High mass measurement accuracy MS/MS utilizing LTQ-FT

Positive ESI: TAG (18:1,18:2,18:3); $C_{57}H_{98}O_6$; theoretical *m/z* 896.7707, $(M+NH_4)^+$

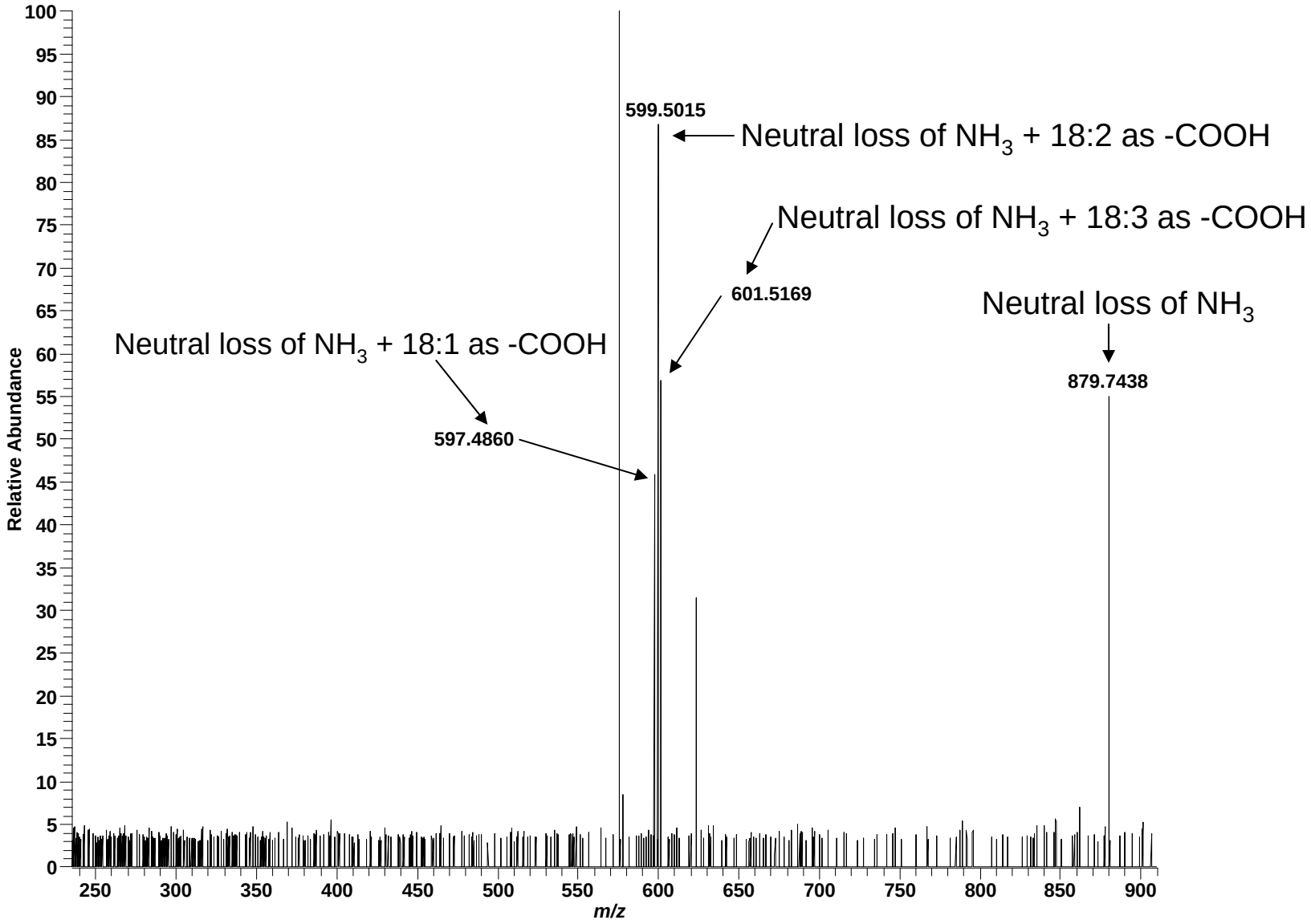

High mass measurement accuracy MS/MS utilizing LTQ-FT

Positive ESI: TAG (14:0,18:1,18:2); $C_{53}H_{96}O_6$; theoretical *m/z* 846.7551, $(M+NH_4)^+$

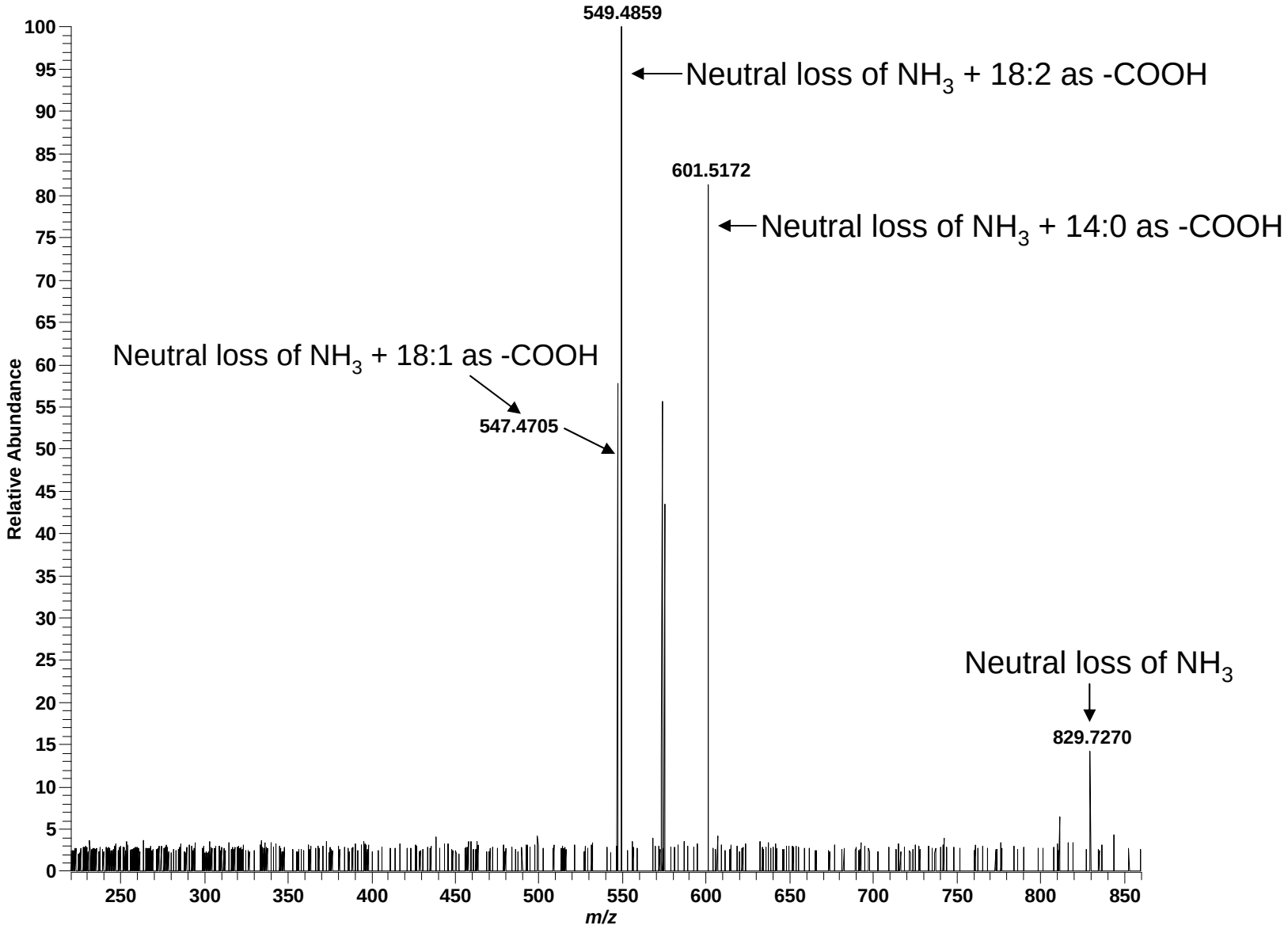

High mass measurement accuracy MS/MS utilizing LTQ-FT

Positive ESI: TAG (16:0,16:1,18:2); $C_{53}H_{96}O_6$; theoretical *m/z* 846.7551, $(M+NH_4)^+$

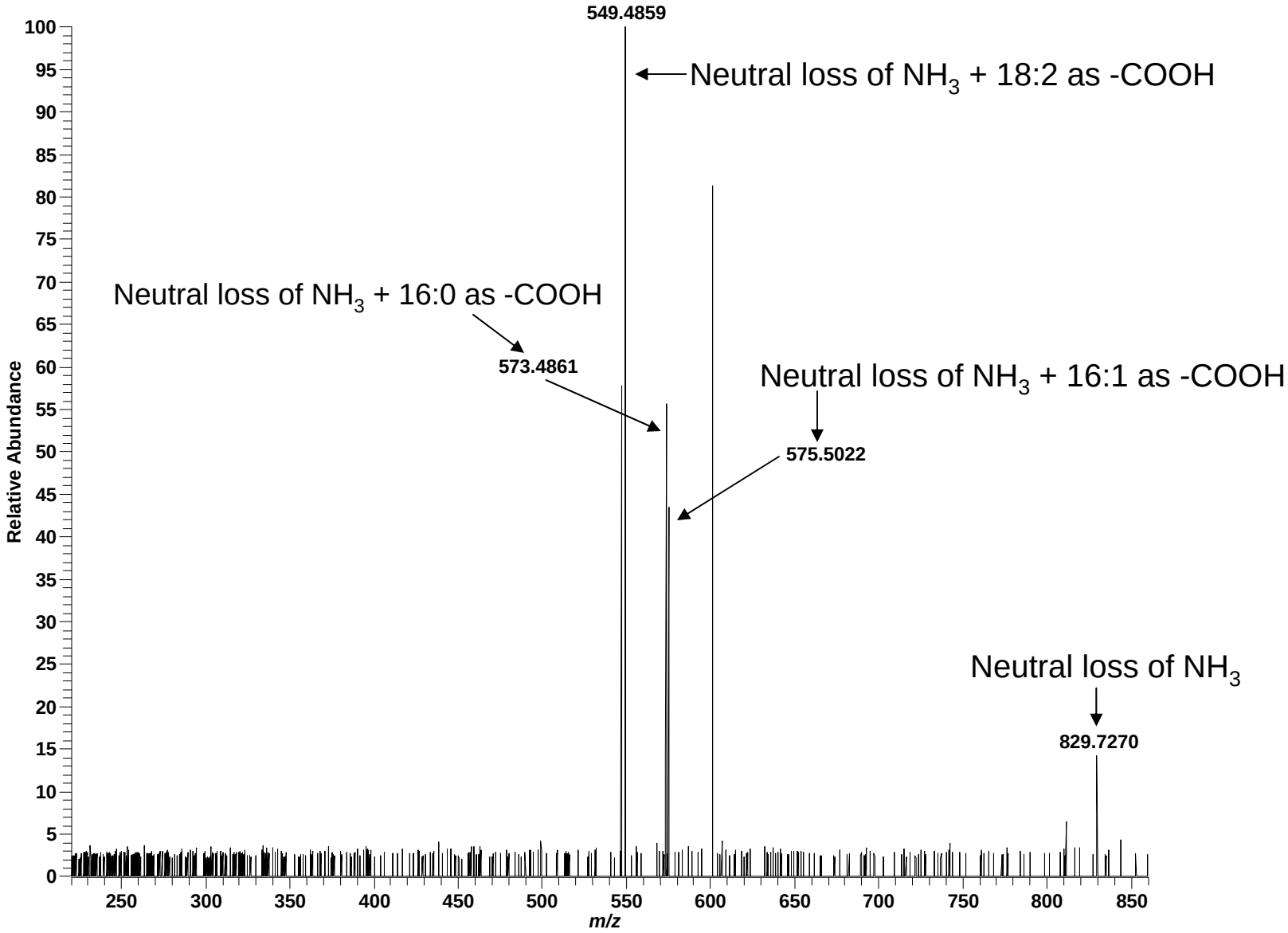

High mass measurement accuracy MS/MS utilizing LTQ-FT

Positive ESI: TAG (16:0,18:2,18:2); $C_{55}H_{98}O_6$; theoretical *m/z* 872.7707, $(M+NH_4)^+$

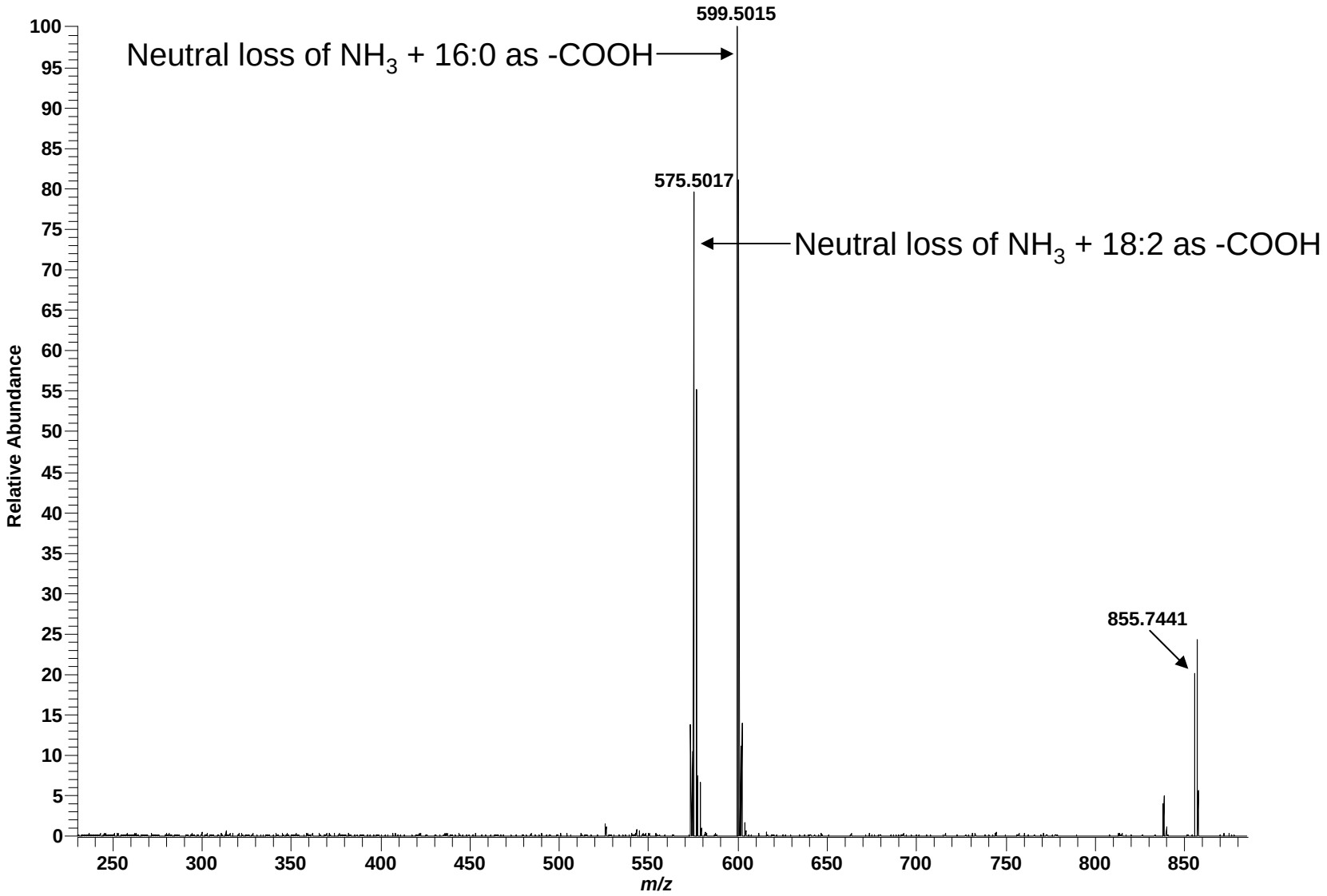

High mass measurement accuracy MS/MS utilizing LTQ-FT

Positive ESI: TAG (16:0,18:2,18:3); $C_{55}H_{98}O_6$; theoretical *m/z* 872.7707, $(M+NH_4)^+$

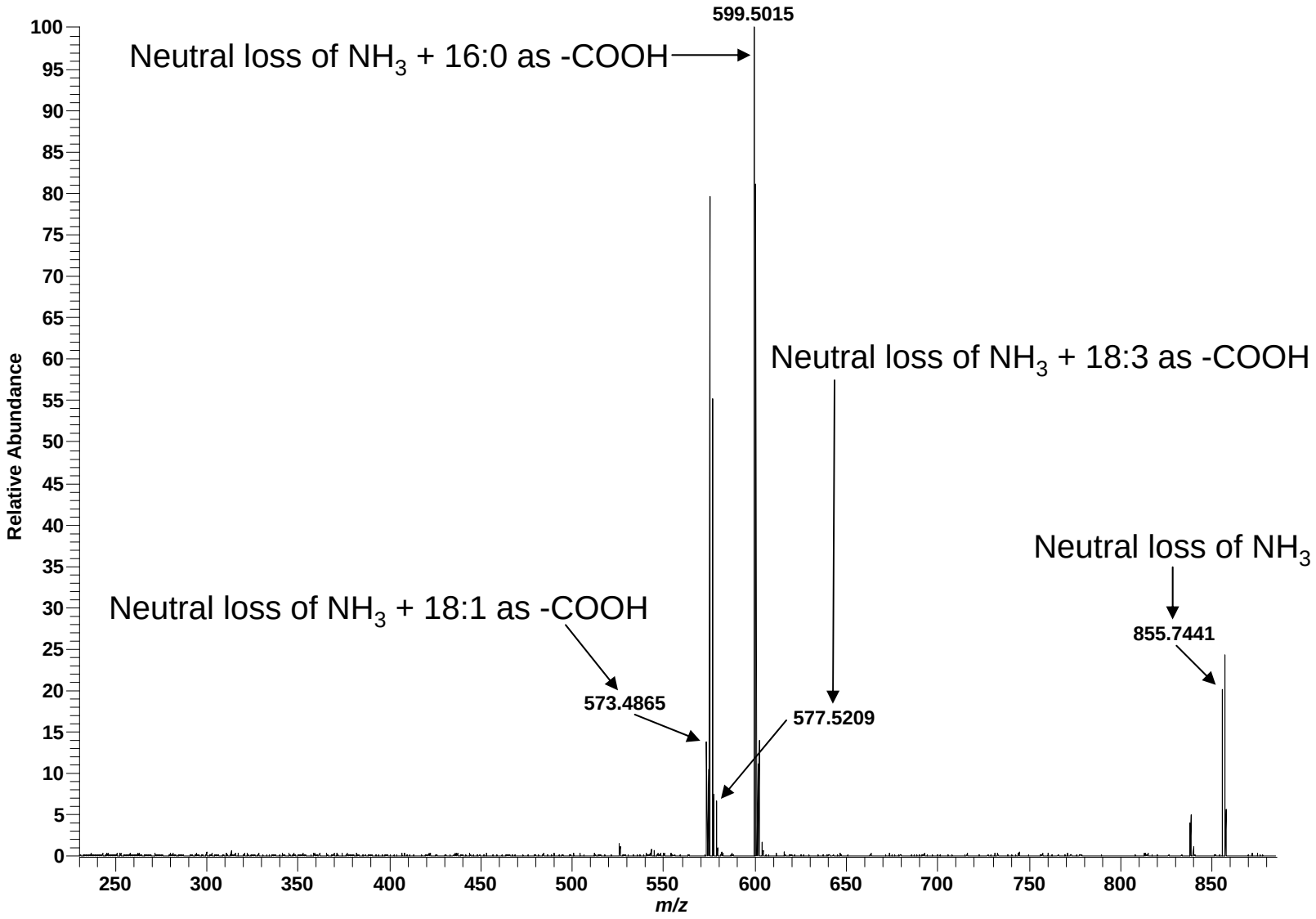

High mass measurement accuracy MS/MS utilizing LTQ-FT

Positive ESI: TAG (18:1,18:2,18:2); $C_{57}H_{100}O_6$; theoretical *m/z* 898.7864, $(M+NH_4)^+$

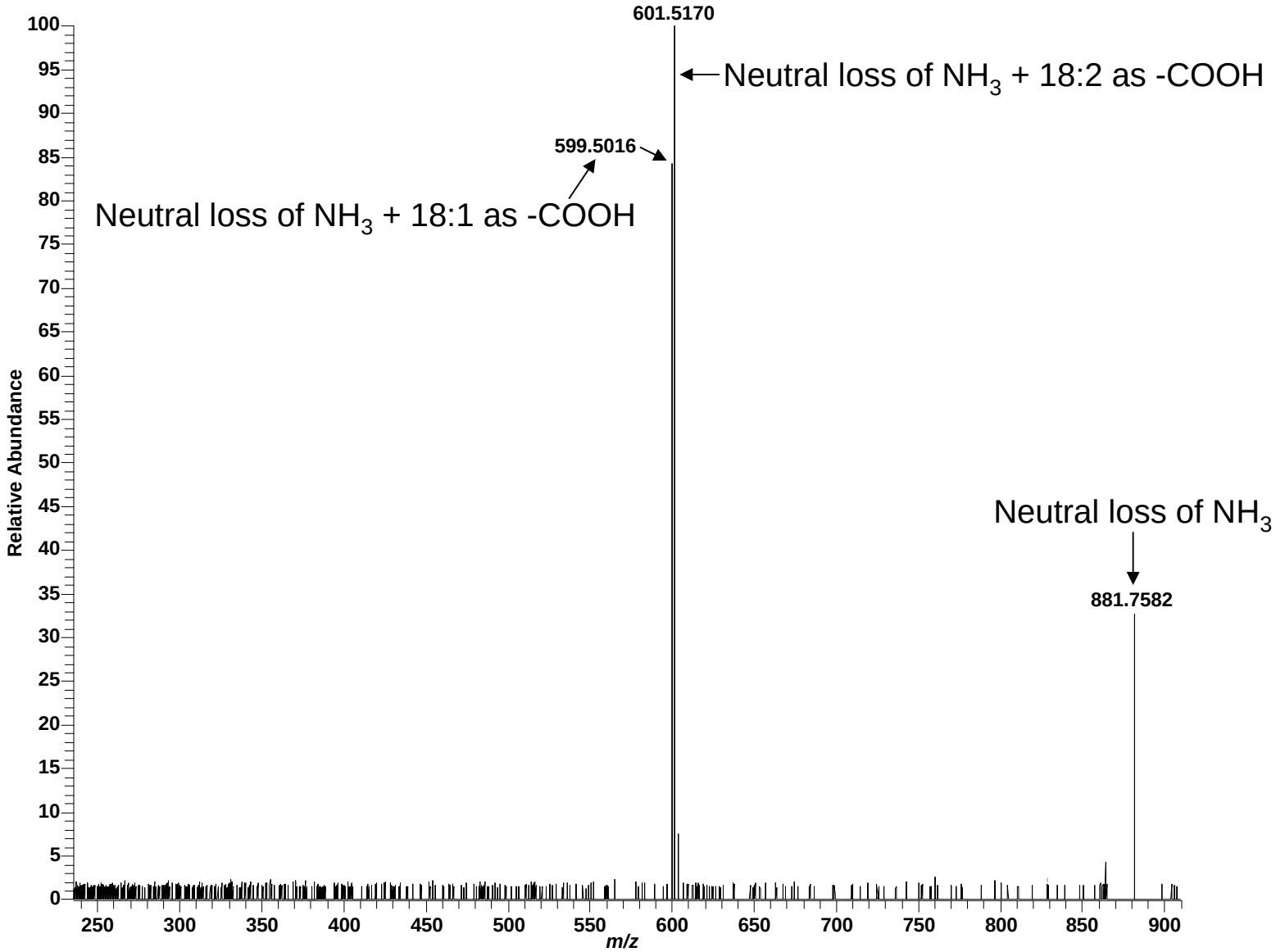

High mass measurement accuracy MS/MS utilizing LTQ-FT

Positive ESI: TAG (14:0,16:0,18:2); $C_{51}H_{94}O_6$; theoretical *m/z* 820.7394, $(M+NH_4)^+$

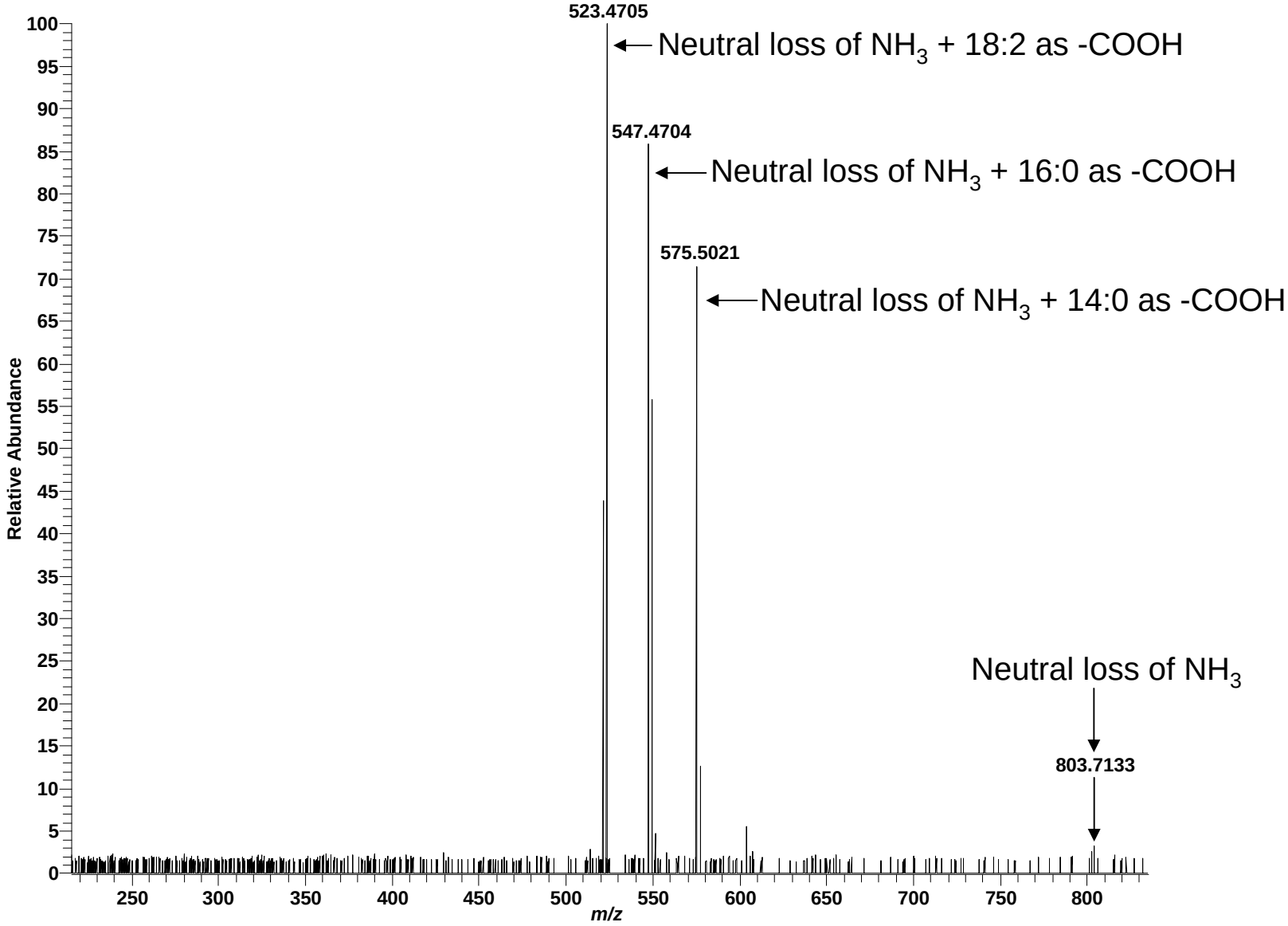

High mass measurement accuracy MS/MS utilizing LTQ-FT

Positive ESI: TAG (14:0,16:1,18:1); $C_{51}H_{94}O_6$; theoretical *m/z* 820.7394, $(M+NH_4)^+$

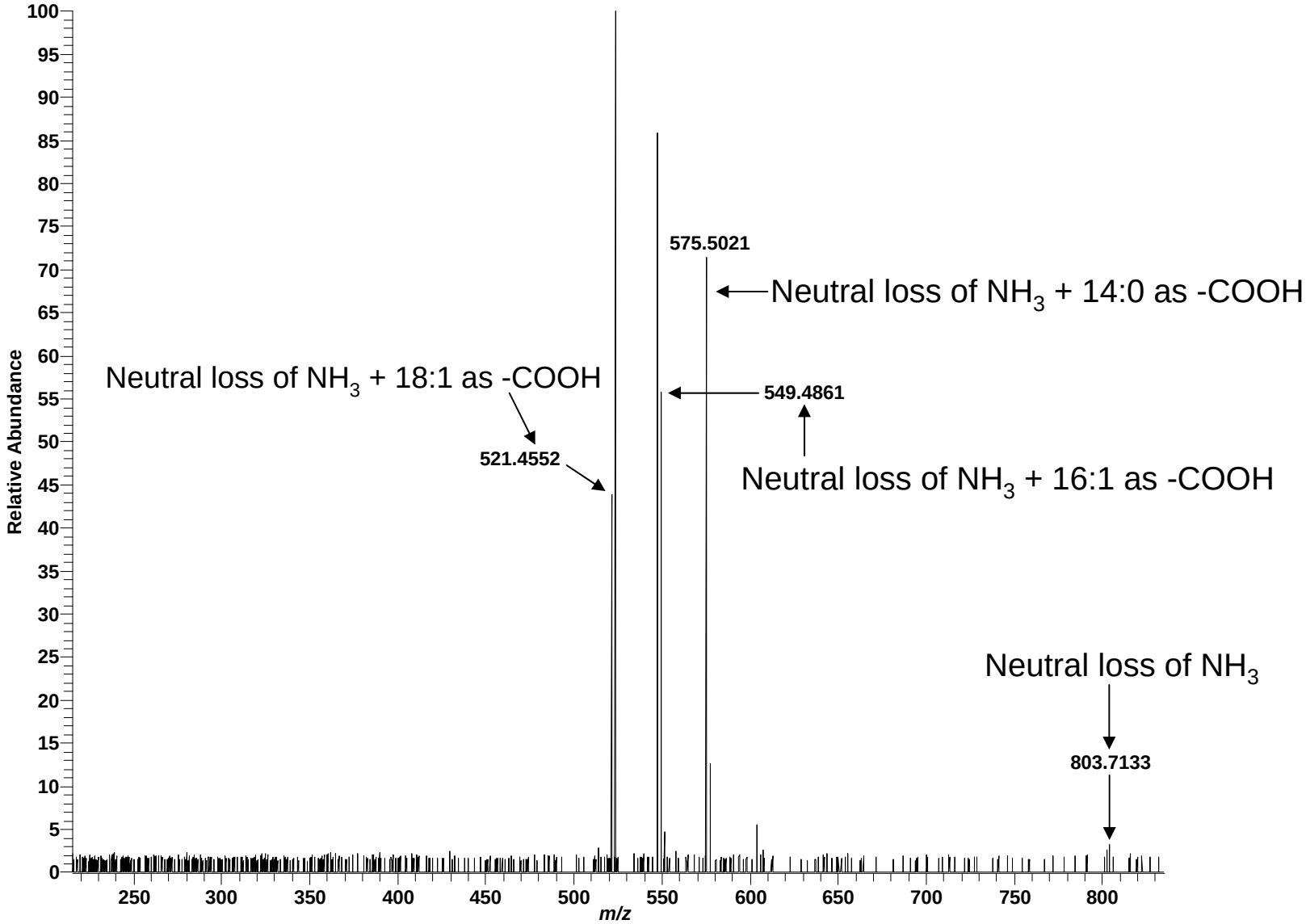

High mass measurement accuracy MS/MS utilizing LTQ-FT

Positive ESI: TAG (16:0,18:1,18:2); $C_{55}H_{100}O_6$; theoretical *m/z* 874.7864, $(M+NH_4)^+$

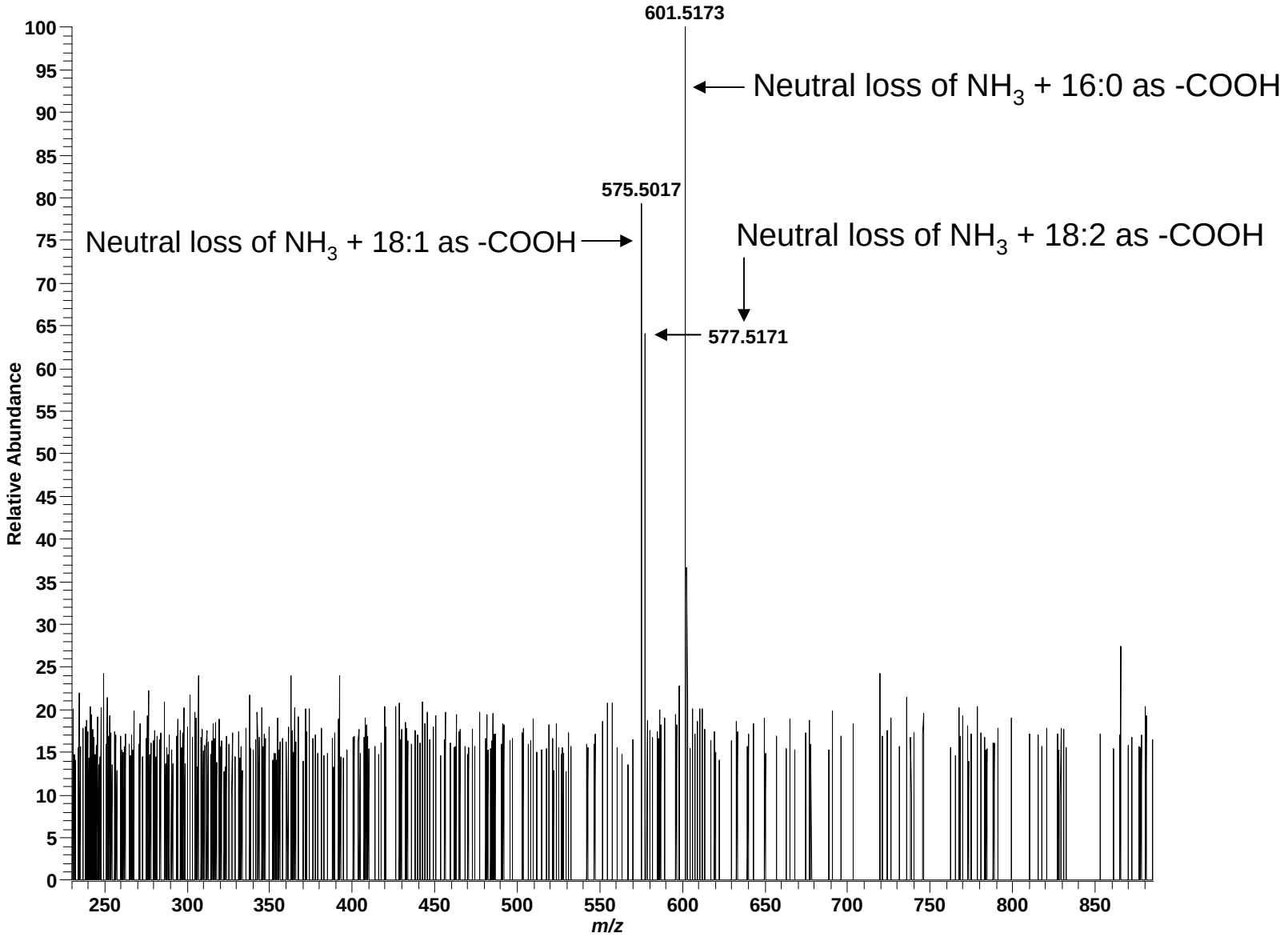

High mass measurement accuracy MS/MS utilizing LTQ-FT

Positive ESI: TAG (16:0,16:1,18:1); $C_{53}H_{98}O_6$; theoretical *m/z* 848.7707, $(M+NH_4)^+$

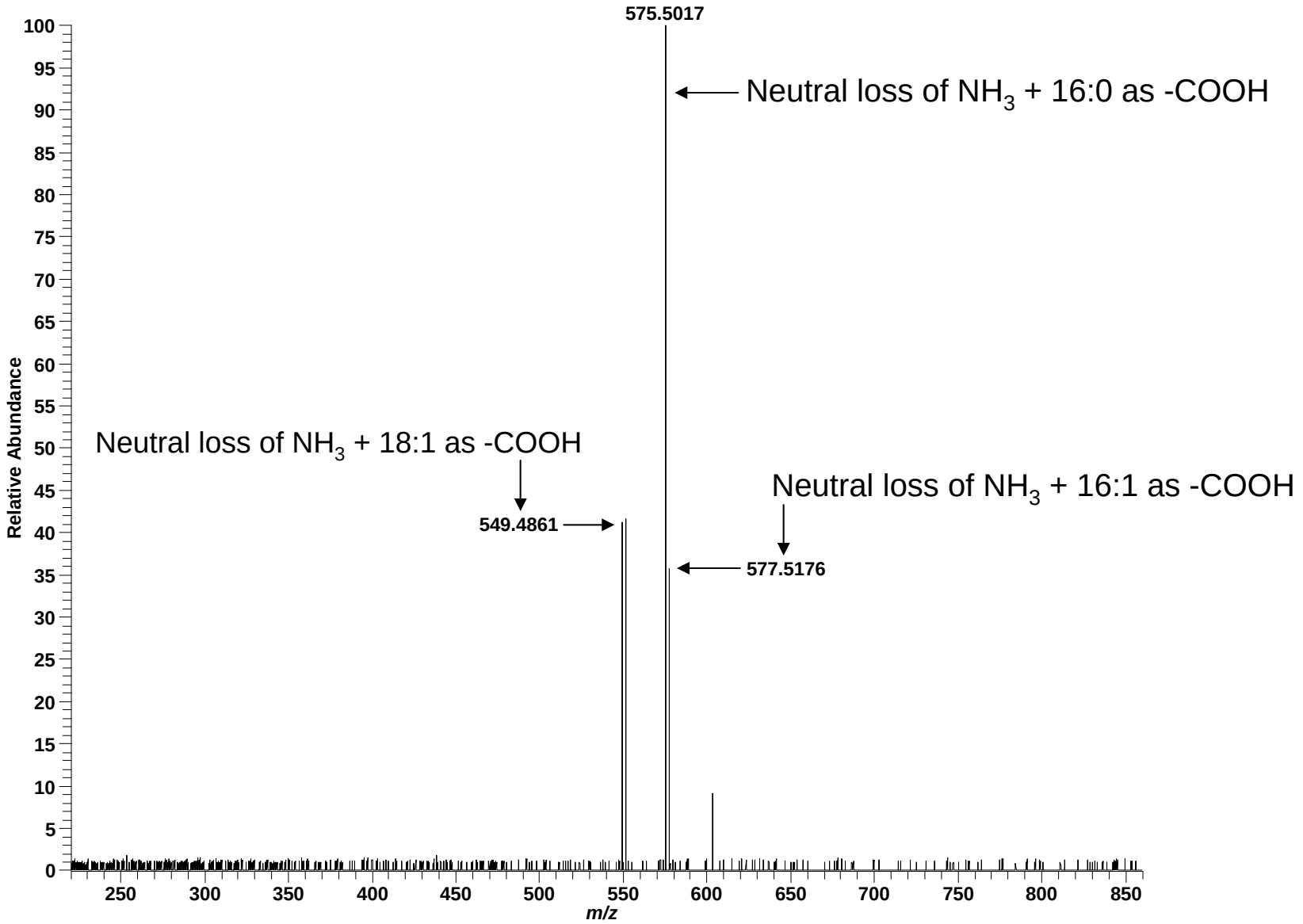

High mass measurement accuracy MS/MS utilizing LTQ-FT

Positive ESI: TAG (16:0,16:0,18:2); $C_{57}H_{102}O_6$; theoretical *m/z* 848.7707, $(M+NH_4)^+$

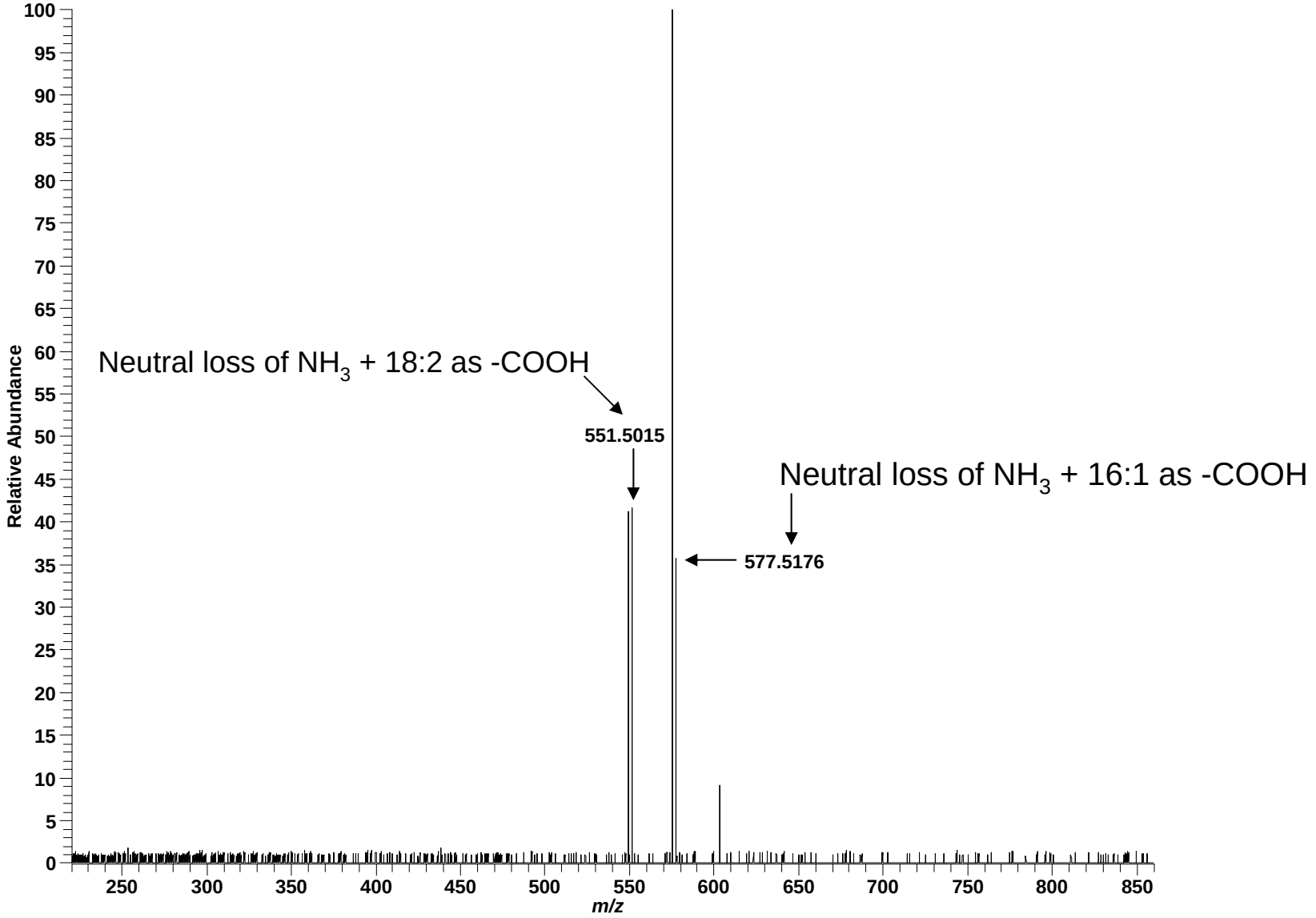

High mass measurement accuracy MS/MS utilizing LTQ-FT

Positive ESI: TAG (18:1,18:1,18:2); $C_{57}H_{102}O_6$; theoretical *m/z* 900.8020, $(M+NH_4)^+$

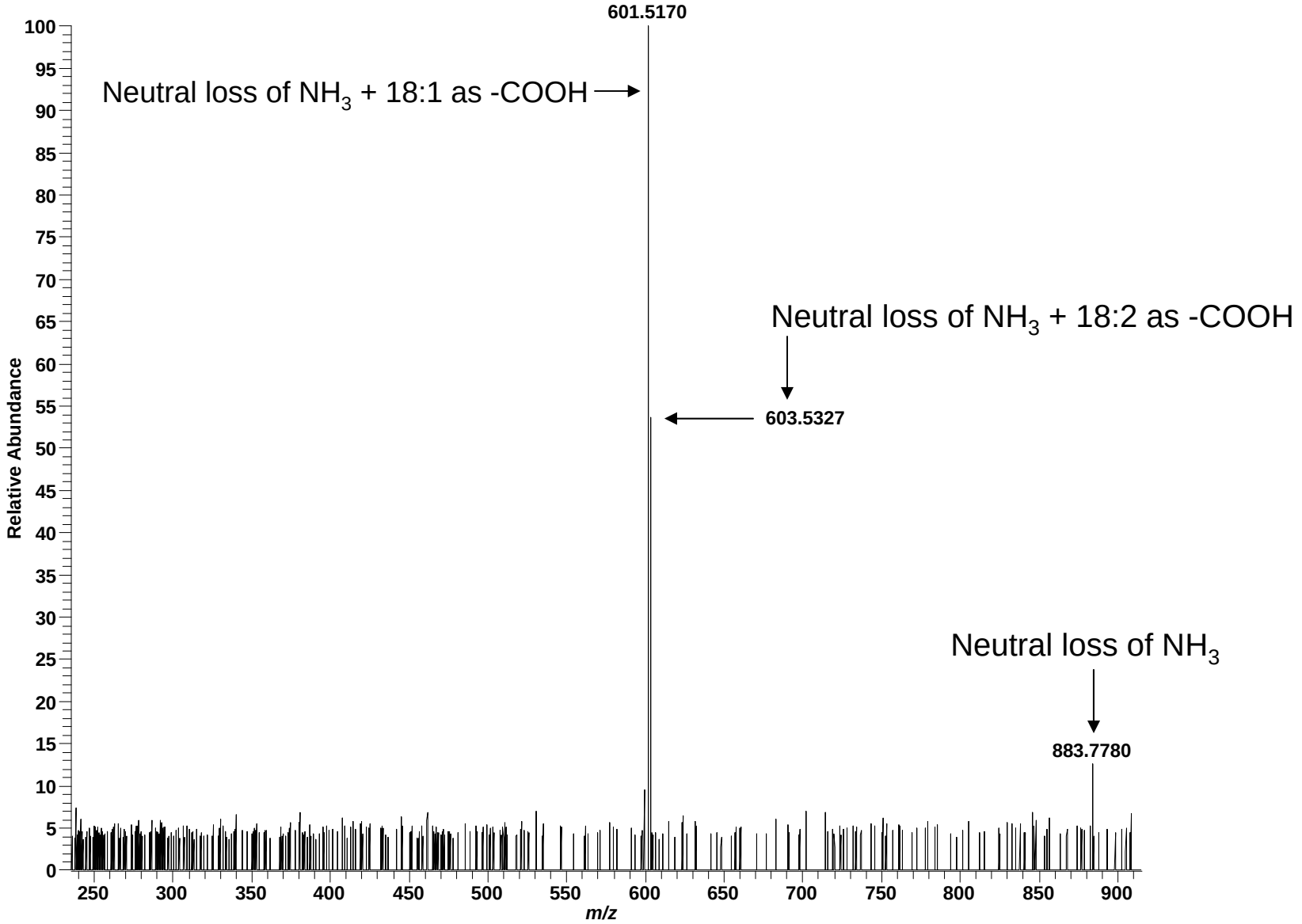

High mass measurement accuracy MS/MS utilizing LTQ-FT

Positive ESI: TAG (16:0,18:1,18:1); $C_{55}H_{102}O_6$; theoretical *m/z* 876.8020, $(M+NH_4)^+$

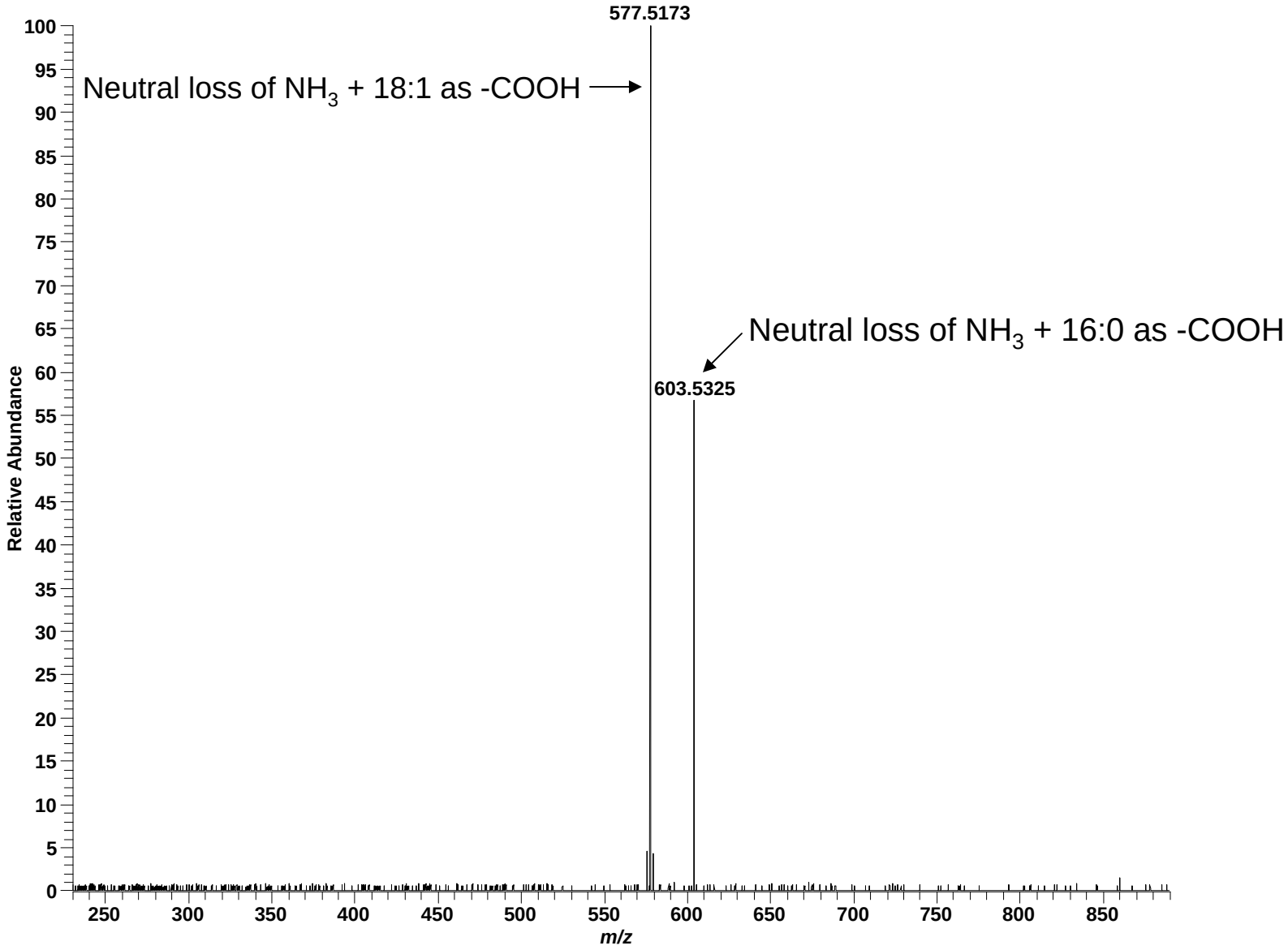

High mass measurement accuracy MS/MS utilizing LTQ-FT

Positive ESI: TAG (18:1,18:1,20:4); $C_{59}H_{102}O_6$; theoretical *m/z* 924.8020, $(M+NH_4)^+$

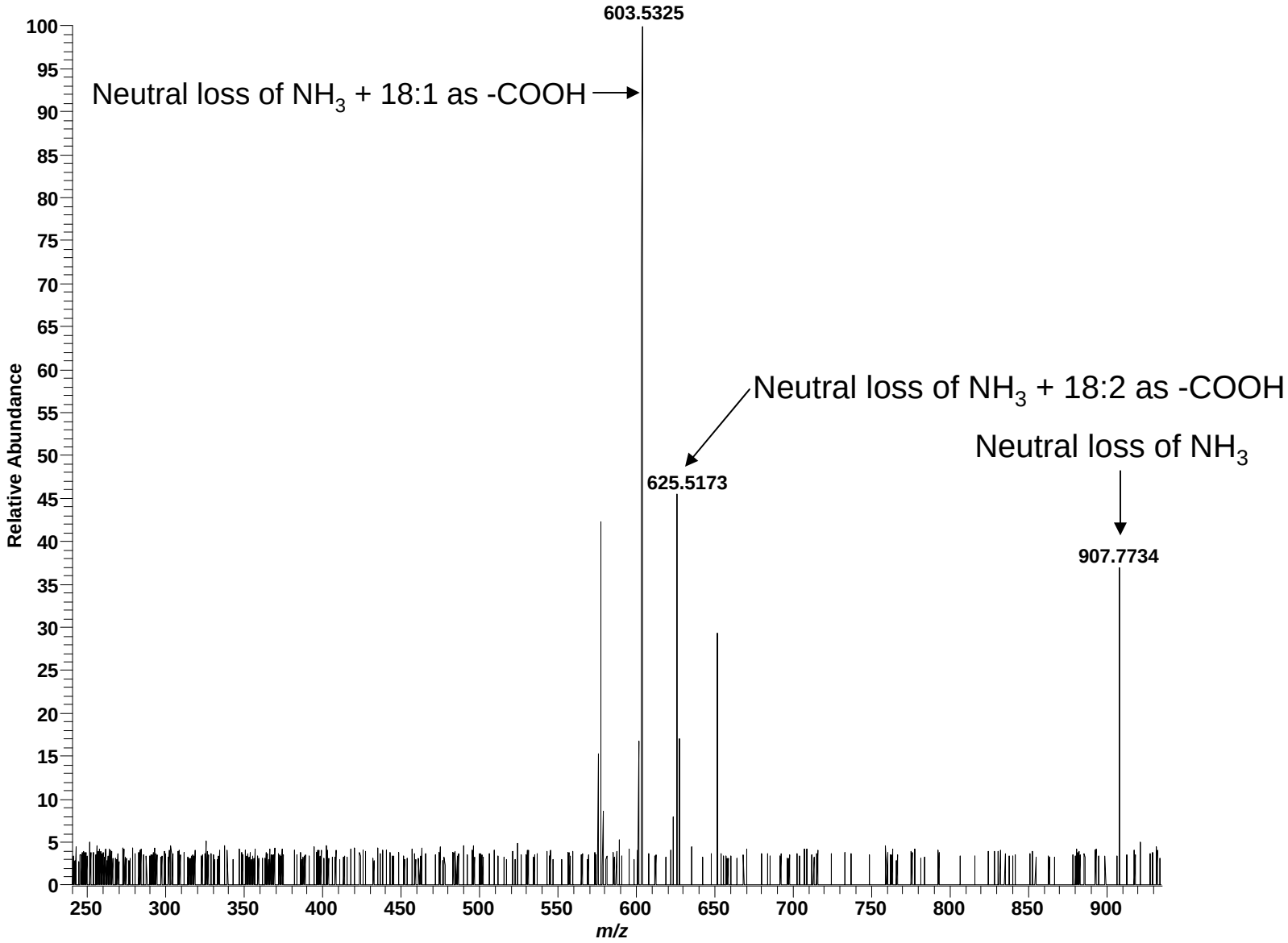

High mass measurement accuracy MS/MS utilizing LTQ-FT

Positive ESI: TAG (16:0,20:3,20:3); $C_{59}H_{102}O_6$; theoretical *m/z* 924.8020, $(M+NH_4)^+$

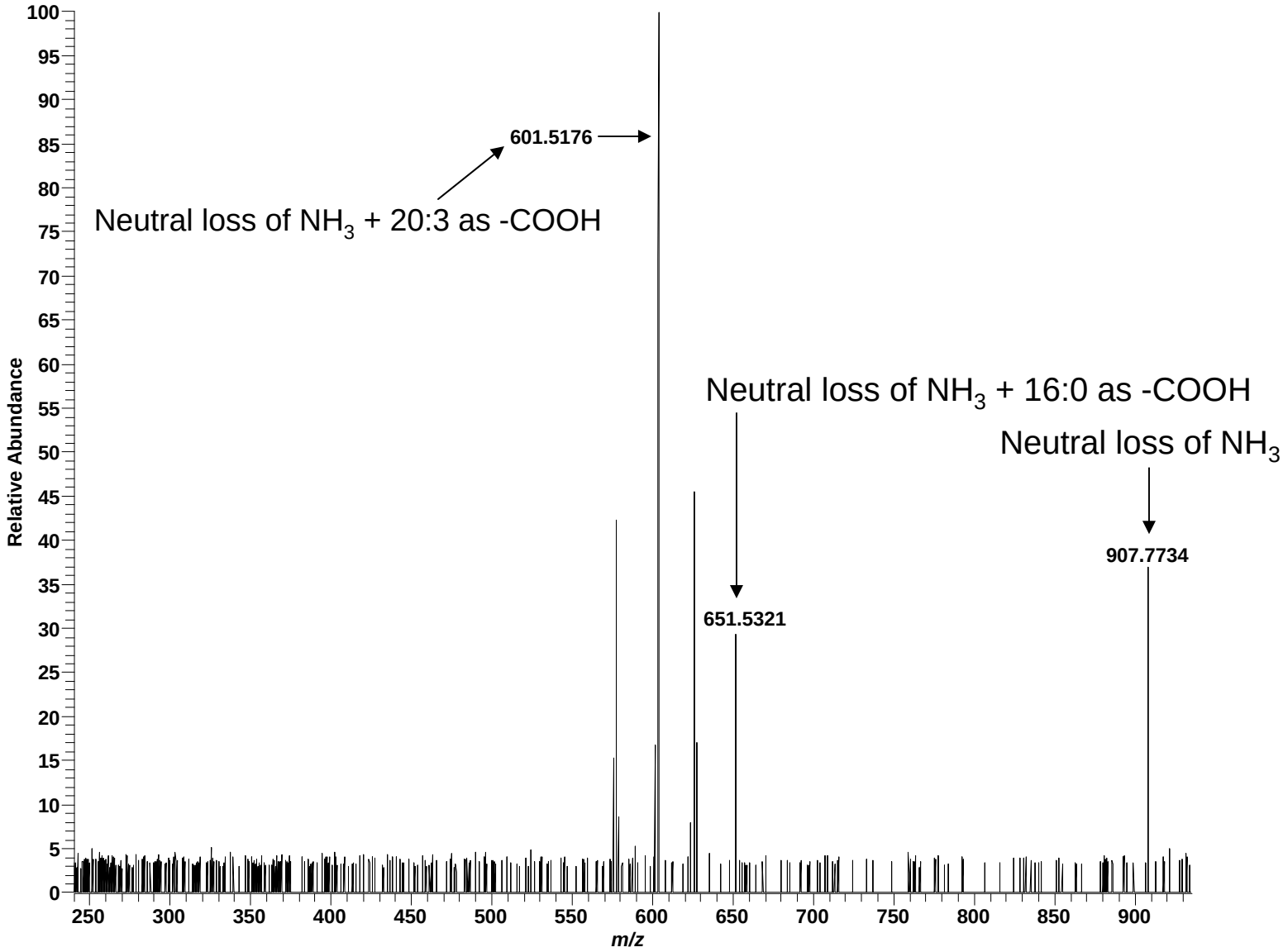

High mass measurement accuracy MS/MS utilizing LTQ-FT

Positive ESI: TAG (16:0,18:2,22:4); $C_{59}H_{102}O_6$; theoretical *m/z* 924.8020, $(M+NH_4)^+$

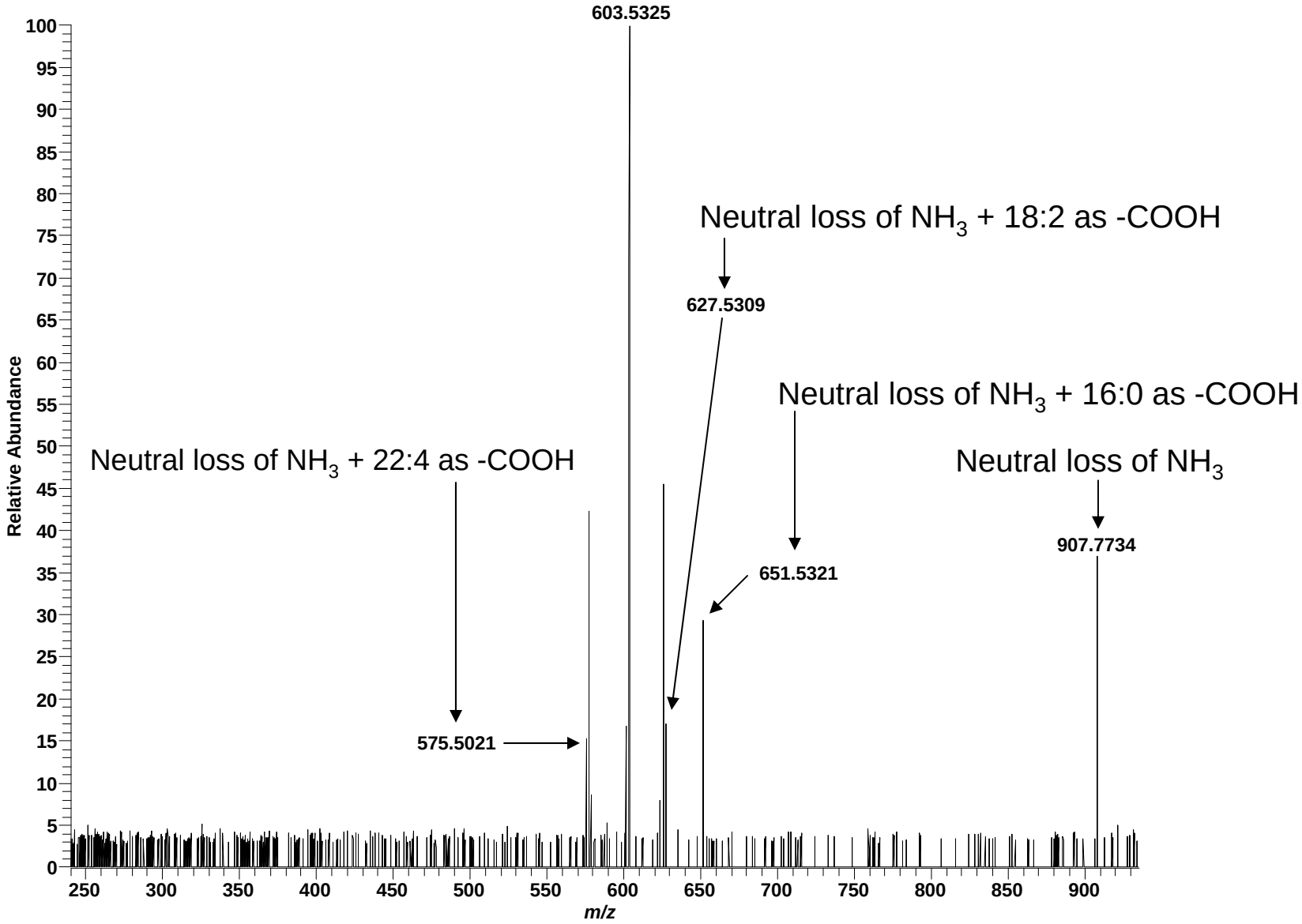

High mass measurement accuracy MS/MS utilizing LTQ-FT

Positive ESI: TAG (14:0,16:0,18:1); $C_{51}H_{96}O_6$; theoretical *m/z* 822.7550, $(M+NH_4)^+$

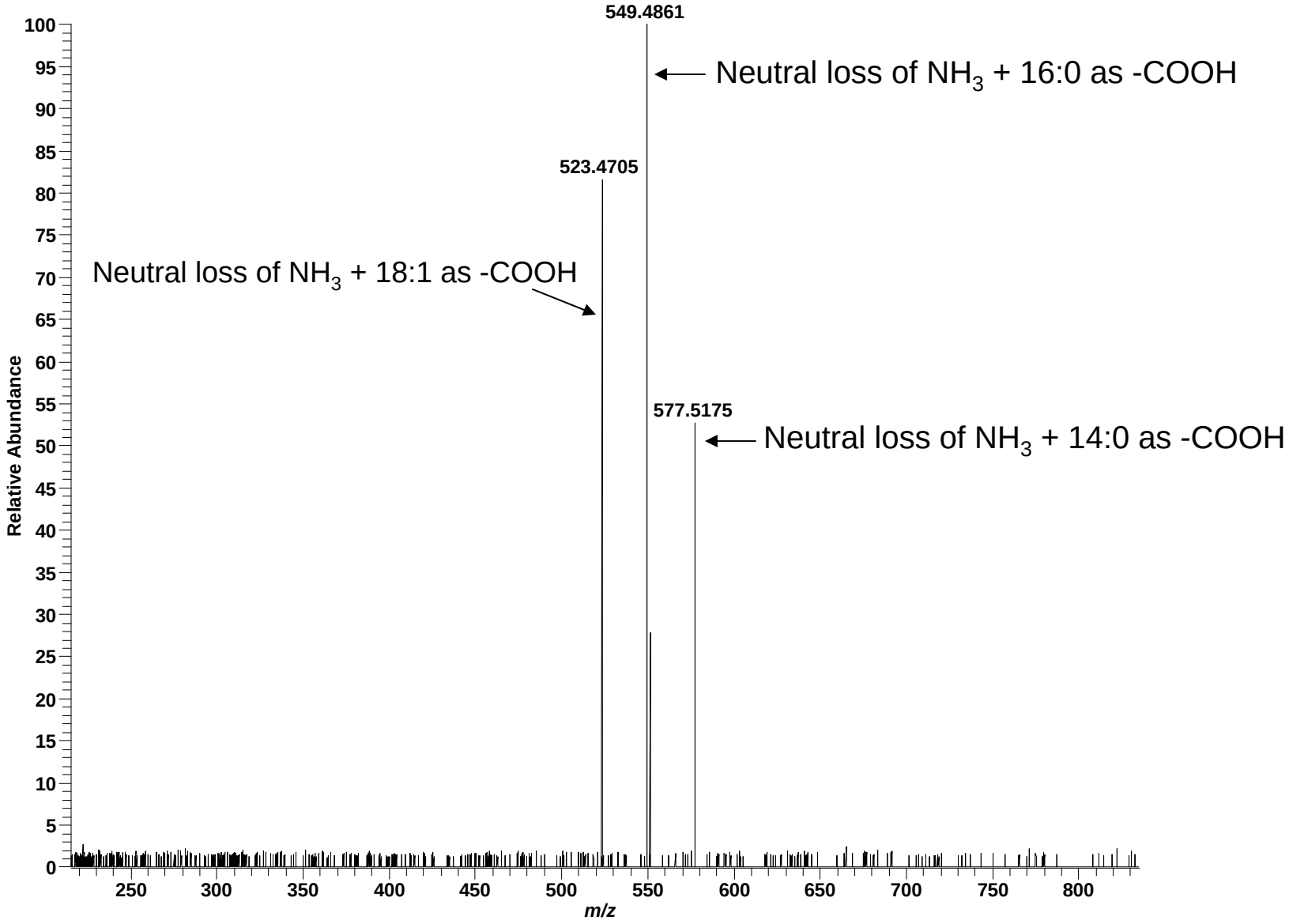

High mass measurement accuracy MS/MS utilizing LTQ-FT

Positive ESI: TAG (16:0,16:0,16:1); $C_{51}H_{96}O_6$; theoretical *m/z* 822.7550, $(M+NH_4)^+$

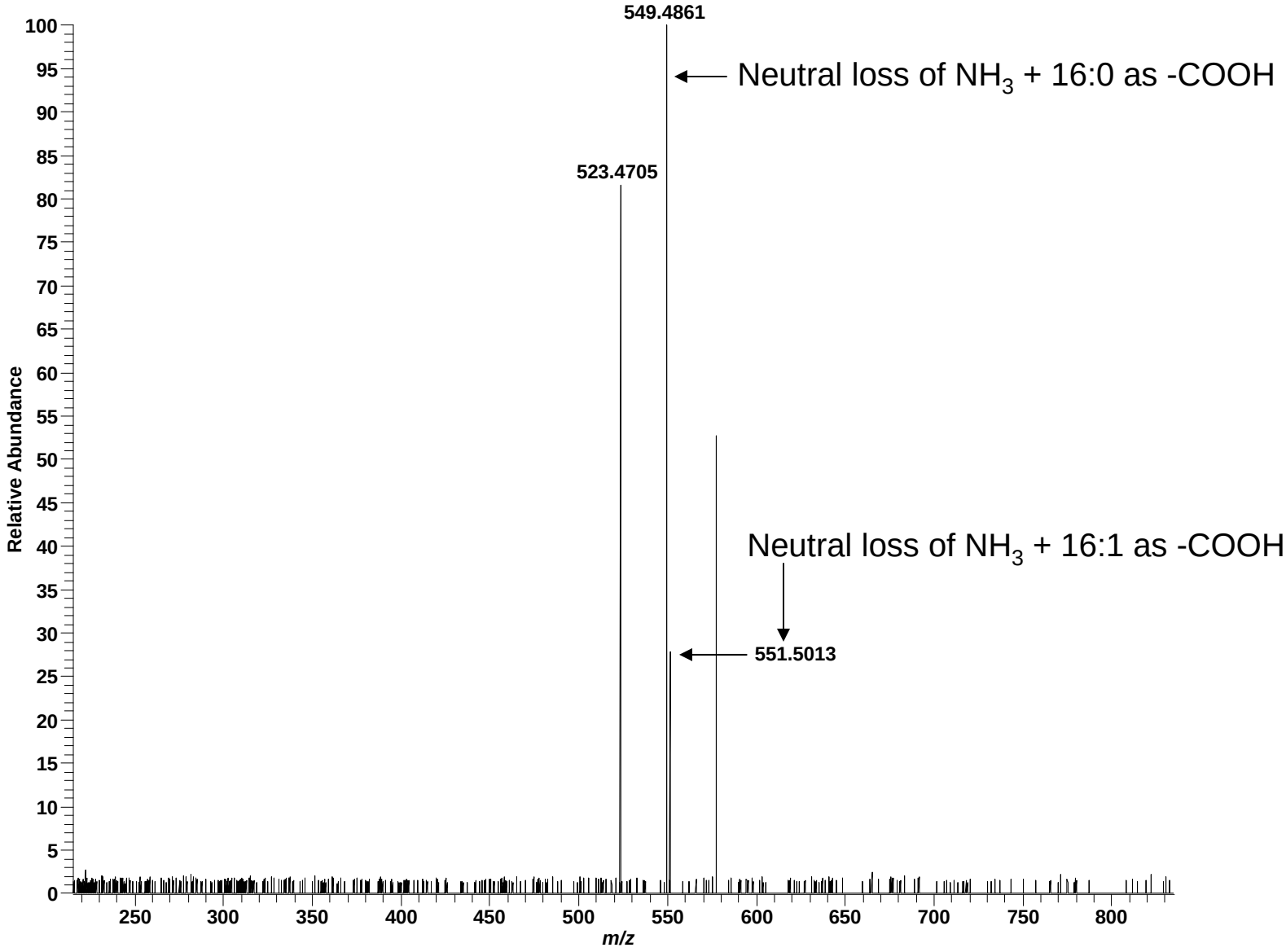

High mass measurement accuracy MS/MS utilizing LTQ-FT

Positive ESI: TAG (18:0,18:1,18:2); $C_{57}H_{104}O_6$; theoretical *m/z* 902.8177, $(M+NH_4)^+$

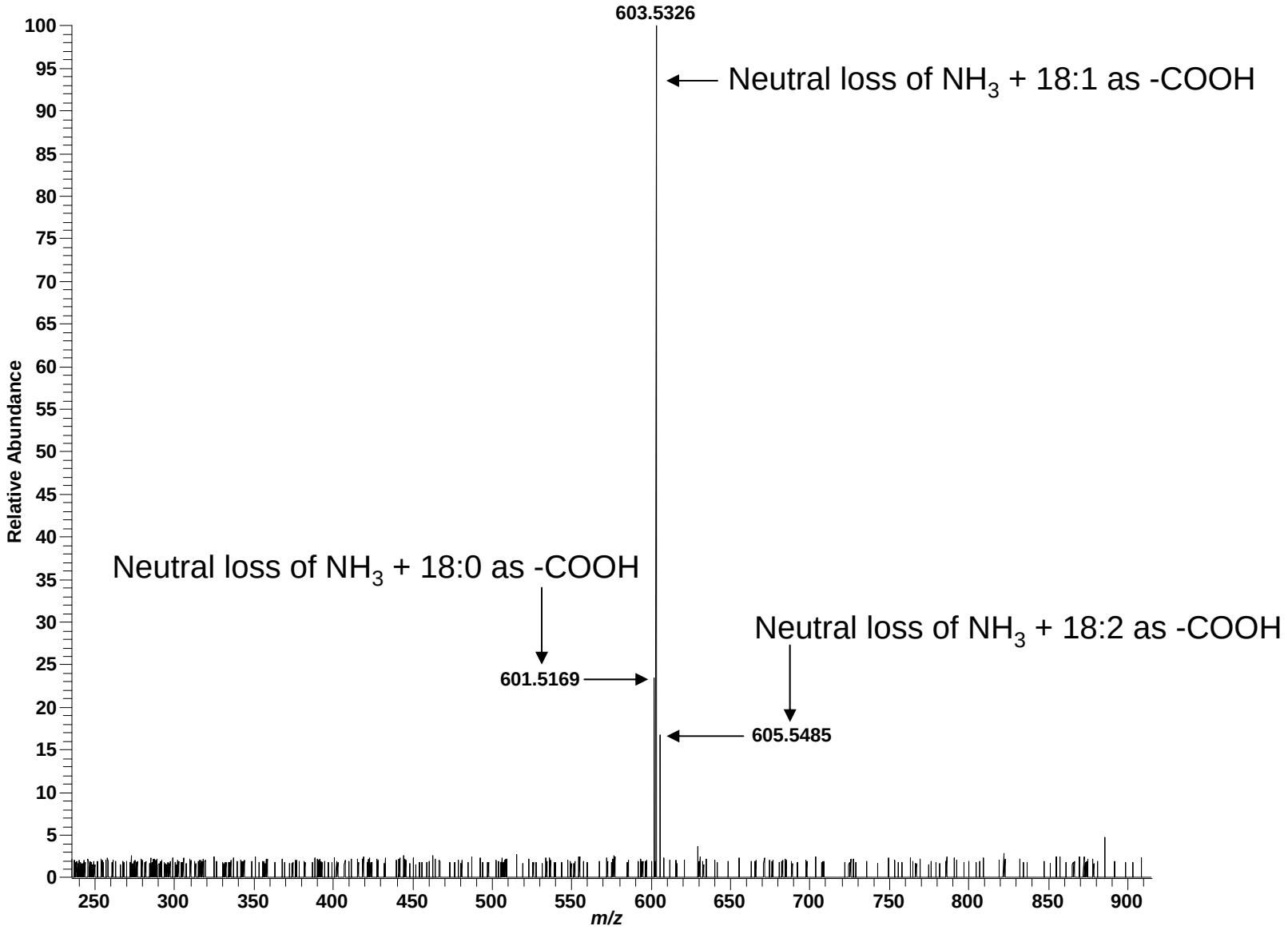

High mass measurement accuracy MS/MS utilizing LTQ-FT

Positive ESI: TAG (16:0,16:0,18:1); $C_{53}H_{100}O_6$; theoretical *m/z* 850.7864, $(M+NH_4)^+$